The Smart Water Meter

a new method to monitor fouling issue

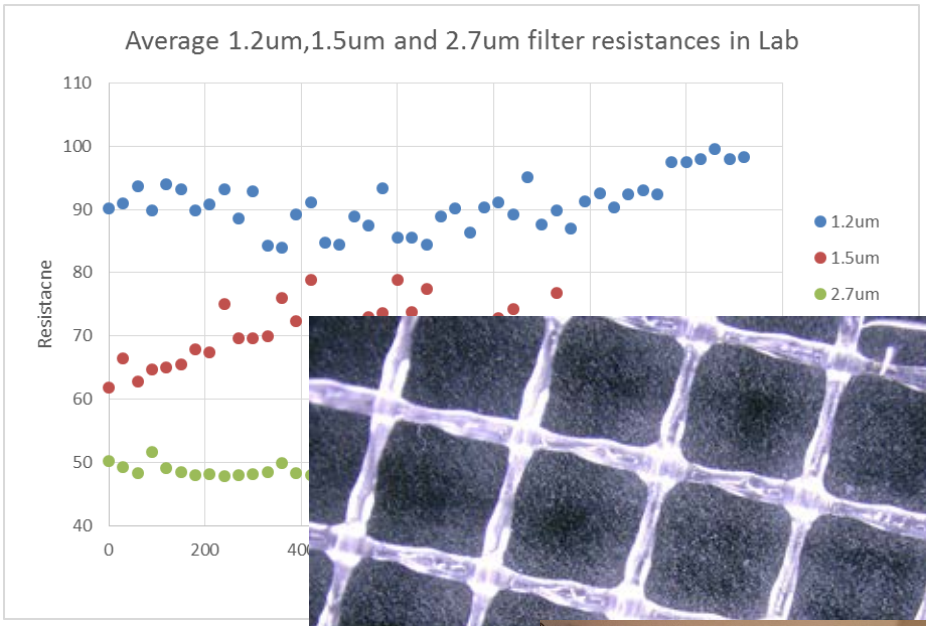

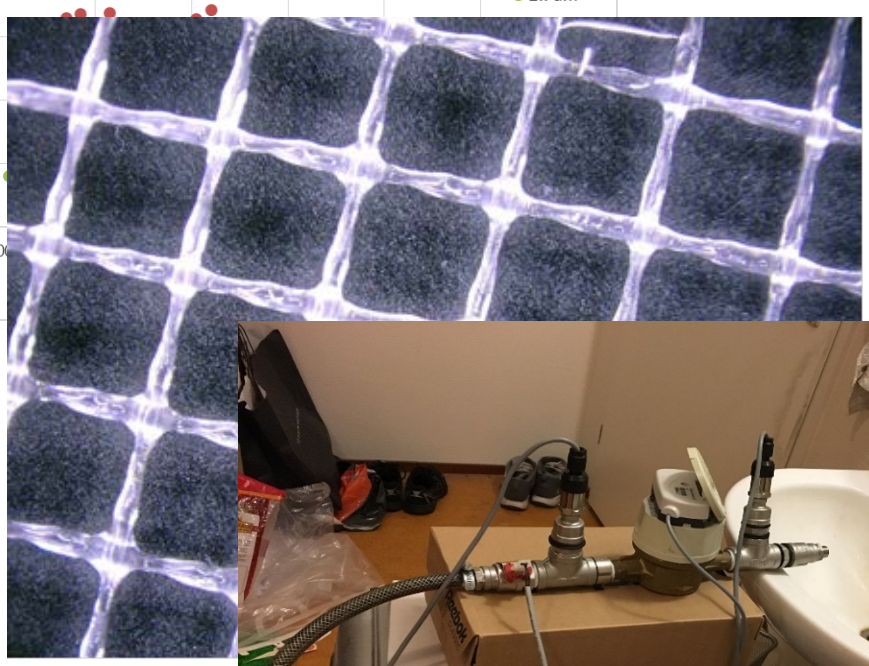

Zewei Chen

August 2016

Faculty of Civil Engineering and Geoscience

Delft University of Technology

The Smart Water Meter

A new method to monitor fouling issue

Zewei Chen

For the degree of:
Master of Science in Civil Engineering

Date of submission: 31.07.2016
Date of defense: 11.08.2016

Committee:

Prof. dr. ir. Walter van der Meer	Delft University of Technology Sanitary Engineering Section
Dr. ir. Gang Liu	Delft University of Technology Sanitary Engineering Section
Prof. dr. ir. G.J.Witkamp	Delft University of Technology Biotechnology Section

Sanitary Engineering, Department of Water Management
Faculty of Civil Engineering and Geosciences
Delft University of Technology

Preface

This is my final thesis as an MSc student from the Sanitary Engineering Section, Water Management Department at the Delft University of Technology, the Netherlands. During the entire one-year internship, the drinking water company Oasen has offered significant efforts in facilitating the whole research. Therefore I would like to express my sincere gratitude to these two administrations for the supervision and assistance they provided.

I would like to express my sincere thankfulness to my daily supervisor, Dr. Gang Liu, for his patience and professional guidance during my research. Without his help and suggestions, I cannot finish my research so smoothly. Further, I would like to thank Prof. Walter van der Meer, together with my colleagues from Oasen, including Harmen van der Laan, Xinwei He, Athina Chrysovergi, Timothy van Heeswijk and Nienke Ruepert, the generous assistance that you have offered me during my research in Oasen will never be forgotten.

This paper only presents the results that I achieved in the study of the last nine months, but the basis of this study, the knowledge I have leaned in the last two years in the university is far more than what shown in this paper. Here I would like to thank the Section of Sanitary Engineering of TU Delft, to those who lectured me, helped me, accompanied me during my study in Netherlands, especially Prof. Dr. G. J. Witkamp and those Chinese Post-Doc and Doctors including Ran Shang, Xuedong Zhang, Nan Jiang, Wei Wang, Wei Peng, Jingyi Hu, Feifei Wang, Cuijie Fen, Ying Bai, Hongxiao Guo, Fang Wei and Liangfu Wei, who has continuously help me and guided me in the last two years.

Finally, I would like to express my most sincere gratitude to my parents, the most influential persons in my life. Without their firm and constant love and support, it would be impossible for me to have such a precious opportunity to peruse and reach my achievement so far in my life. **谢谢爸爸妈妈，我爱你们！** Great appreciation also to my lovely girlfriend Weicheng Chen, for her kind encouragement and companion of my staying in Netherlands.

The objective of this research is to find a new method to monitor the water quality and potential water meter fouling during the drinking water distribution process. The knowledge it revealed is only a slight part. Hopefully, it can provide some useful information for those who want to provide even better quality drinking water for human beings all around the world.

Zewei Chen
July 2016

Abstract

The drinking water distribution network is a sealed and pressurized system which attached numerous biofilm and microorganism due to the long-time operation. In a foreseeable future, Oasen will adopt reverse osmosis to treat drinking water and thus the nutrient (biodegradable compounds) in drinking water will be slight. In that case, biofilms used to attach on pipelines may die and detach from pipes and these part of biofilm may clog consumers' water meter. To avoid the potentially clogged water meter issues, a new monitor method, the Smart Water Meter should be used to monitor the fouling issues during the distribution process. This research, supervised by TU Delft and Dutch drinking water company Oasen, is an attempt to verify the Smart Water Meter as a suitable method to monitor fouling issues and figure out what matters contribute to the water meter clogging issues.

Three objectives are included in this research:

- The first objective is to verify Smart Water Meter as a suitable method to monitor water quality and fouling issues during the distribution process. In this research, the pressure drop is the key factor to detect the fouling issue and two equipment, filtrated clogging potential (FCP) and crossflow clogging potential (CCP), are accepted to monitor the fouling issues both in a short term and long term.
- The second objective is to analyze what matters cause the pressure drop/filter resistance increase. This part analysis is to figure out the factors contribute to the potential fouling issues. Research can be divided into three parts, physical part, chemical part, and biological part. Physical part stress on explaining from pressure drop and filter resistance. Chemical part focus on determining the chemical compounds of fouling and biological part centralizes on ATP concentration. A better and comprehensive result could be obtained from the combining of analysis from these three aspects.
- The third objective is to investigate the characteristics of these matters, this part analysis is the extension of the second objective and this part research concentrate on the quantities of each matter. In physical part, microscope and particle counter are used to calculate the total clogging particle number. In chemical part, ICP-MS is adapted to detect the concentration of chemicals.

This research indicate that the Smart Water Meter is a suitable method to monitor fouling issues during the distribution process. In FCP experiment, filter resistance increased 15% in 16 hours operation time while in CCP experiment, the pressure drop grew from 0 to 10mbar in 27 days. Meanwhile, the clogging mechanisms of FCP and CCP are different; Particle clogging is the most important contributor for FCP while Biofouling plays a significant role in CCP. Therefore, FCP is more suitable to monitor the particles such as detached biofilm while CCP can detect the microorganism regrowth. Further, no relationship can be found between inorganic matters and clogging issues for both FCP and CCP experiments in this research, which indicate inorganic matter is not a primary contributor to fouling issues. Results also indicate that drinking water quality from consumers' tap is greatly influenced by the distribution process. Both the biofilm and hydraulic retention time will impact the water quality from consumer's tap.

List of Figures

List of Tables

List of Abbreviations

ATP	-	Adenosine triphosphate
CCP	-	Crossflow clogging potential
CV	-	Coefficient of variation
DOC	-	Dissolved organic carban
DWDS	-	Drinking water distribution system
FCP	-	Filtrated clogging potential
GFAAS	-	Graphite furnace atomic absorption sepectroscopy
ICP-MS	-	Inductively coupled plasma-mass spectrometry
MFI	-	Membrane fouling index
MFS	-	Membrane fouling simulation
RO	-	Reverse osmosis
SDI	-	Silt density index
TCC	-	Total cell counting

Content

1 Introduction

1.1 Background

Along with the increasing water pollution all over the world, providing safe and relatively cheap drinking water for public has become one of the most significant issues for drinking water companies. After treatment, drinking water travels through a distribution system to consumers. The distribution network which is commonly used the world widely is a large bioreactor in which biofilms and microorganism may thrive if adequate growth conditions are present(Payment et al. 1997). Therefore, although numerous water treatment processes are applied in drinking water treatment plants, well-treated drinking water may still be polluted during the long distribution process. There is a broad consensus that the final goal of water utilities is to offer good quality drinking water at the consumers' tap rather than only at the treatment plants (Liu, Verberk, et al. 2013).

In general, tap water has lower quality than the treated water at the treatment plant(Committee On Public Water Supply Distribution Systems: Assessing And Reducing Risks 2006). Many problems in drinking water distribution systems (DWDSs) are caused by microorganisms, such as biofilms growth (Camper 2004), nitrification(Regan et al. 2002), and bio-corrosion of pipe material(Beech & Sunner 2004). Completely understanding the microbiological ecology of the distribution system is significant for effective control strategies which will ensure the safe and high-quality drinking water at the end tap(Camper 2004).

1.2 Motivation: concern of Oasen on its changing of drinking water quality

Oasen is a Dutch drinking water company located in South-Holland (see Figure 1). The total supply area is 1200km^2, covering 750,000 inhabitants and 7,200 companies. Oasen has a potable water distribution network of about 4000km. The primary water source for all the treatment plants of Oasen is a combination of ground water and water through riverbank filtration from Rine River. Raw water is treated with conventional treatment processes including riverbank filtration, aeration, rapid sand filtration, pellet softening, granular activated carbon filtration and UV disinfection. Like all the drinking water companies in Netherlands, no chlorine is added in the whole process to avoid the production of disinfection by-products.

Figure 1: Distribution area of Oasen

Meanwhile, Oasen is also responsible for water reservoir protection, pumping station maintenance and pipelines cleaning in Gouda, covering around 115km^2 in total. The name of 'Oasen' in Dutch means bringer of life.

2 Literature review

2.1 Complexity of biological activities in drinking water distribution network

2.1.1 Introduction

A drinking water distribution system (DWDS) is the final and essential step to transfer safe and high-quality drinking water to customers(Liu, Verberk, et al. 2013). DWDS naturally contents the function of preventing bacterial intrusion. However, some biological processes, such as biofilm formation and detachment, microbial growth in bulk water, and the formation of loose deposits, may occur (see Figure 2). These processes will cause the deterioration of the water quality during the distribution process. In some extreme situation, pathogens may regrowth and cause a health risk to consumers(Liu, Verberk, et al. 2013). It is, therefore, necessary to develop an effective method to monitor the water quality during the distribution process.

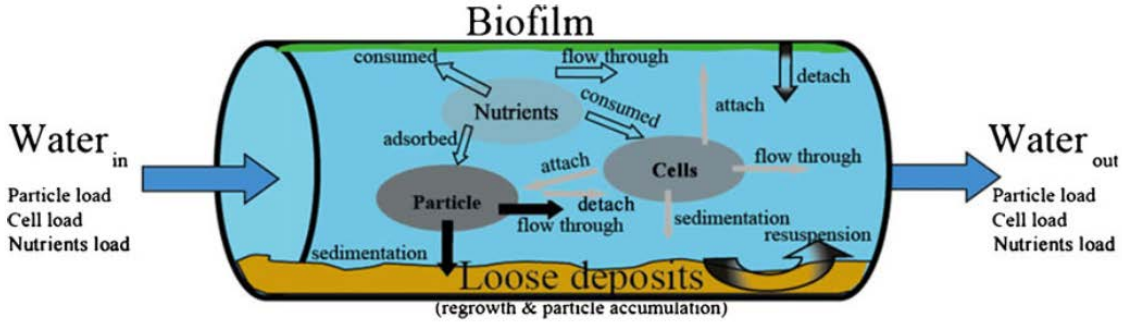

Figure 2: Processes related to microbial growth during drinking water distribution(Liu, Verberk, et al. 2013)

2.1.2 Quantification of microbial growth in DWDS

Microbial growth can be observed by the increase of biological activities during the distribution system. Brauns and O'Connor (Brauns et al. 2002) proposed a definition to represent the occurrence of blooms or high bacterial populations in the drinking water distribution system: "regrowth" and "after regrowth." regrowth refers to the recovery of the cells, which have entered pipelines from a water reservoir or treatment plants. After regrowth means the growth of microbes native to a water distribution system.

2.2 Modified Fouling Index (MFI)

2.2.1 Introduction

Modified Fouling Index (MFI) is a method to determine the fouling characteristic of membrane filtration feed water(Company 1980). The MFI is derived from the Silt Density Index (SDI). Similar like SDI, MFI method let water directly flow through filter/membrane to form a dead-end filtration. Compared with SDI, the advantage of MFI is this process can represent a linear relationship between the index and the concentration of colloidal and suspended particles. (Boerlage et al. 2002)

MFI is based on cake filtration, uses a 0.45 um microfiltration membrane to measure the particulate fouling potential of feed water with the dead-end flow at constant pressure. MFI is the most widely applied methods to measure the particulate fouling potential of feedwater.(Vrouwenvelder et al. 2006) Based on the Carman-Kozeny equation for specific cake resistance, in general, smaller particles present in the cake result in higher MFI values. Assuming cake filtration is the dominant mechanism in particulate fouling, the MFI can be used as a basis for the modeling influent decline in membrane system.(Brauns et al. 2002)

In general, there are two methods to measure MFI value, the original one, detecting under constant pressure condition and a new method to detecting under constant influent condition. Since these two approaches are both necessary for thesis, thus they will be discussed in next sections.

2.2.2 MFI calculation in constant pressure condition

For original MFI measurement, the following equation can be applied for calculating MFI value.

$$\frac{dV}{dt} = \frac{1}{\eta} \frac{\Delta p.A}{(R_m + R_k)} \tag{1}$$

In which,
R_m : resistance of the filter
R_k : resistance of the cake or gel per unit of area
A : surface of the filter
If there is no compression of the cake, then

$$R_k = \frac{V}{A} \times I \tag{2}$$

In which I is a membrane fouling potential of the water.
If Δp is constant and combine Equation (5) and Equation (6) and integrating from t=0 to t=t, then:

$$\frac{t}{V} = \frac{\eta R_m}{\Delta PA} + \frac{\eta VI}{2\Delta PA^2} \tag{3}$$

The value of $\frac{\eta R_m}{\Delta PA}$ depends on membrane material and pore size, which is constant. However, $\frac{\eta VI}{2\Delta PA^2}$ can act as an index to indicate the water fouling potential if ΔP , temperature, and A^2 are always computed to a fixed reference value(Company 1980). $\frac{\eta VI}{2\Delta PA^2}$ is the term indicated as the MFI.(Rheinheimer 2004)

In order to get a clear explanation of MFI, equation (7) can be rewritten as follows,

$$\frac{t}{V} = \frac{\eta R_m}{\Delta PA} + \frac{\eta VI}{2\Delta PA^2} = m + \tan\partial * V \tag{4}$$

In which,
m: $\frac{\eta R_m}{\Delta PA}$ (constant)
$\tan\partial : \frac{\eta I}{2\Delta PA^2}$

And based on Equation (8), a straight line can be drawn when $\frac{t}{V}$ being plotted against V. The slope ($\tan\partial$) of the straight line is then calculated. An example curve is shown in Figure 3

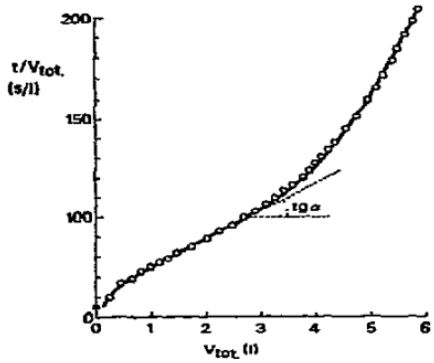

Figure 3: Ratio of filtration time and filtrate volume (V) as a function of total filtrate volume

2.2.3 MFI calculation in flow constant condition

The study concluded that a more accurate particulate following prediction would be obtained by determining the MFI in constant influent filtration(Vrouwenvelder et al. 2006). The existing Modified Fouling Index ($MFI_{0.45}$) test is based on cake filtration, which is defined by constant pressure filtration equation in the plot of t/V vs. V.

$$\frac{t}{V} = \frac{\eta R_m}{\Delta P A} + \frac{\eta I}{2\Delta P A^2} V \tag{5}$$

Where V is the filtrate volume, t is filtration time, ΔP is the pressure drop between two membranes, η is the water viscosity, R_m the membrane resistance, A the membrane surface area and I is the fouling index.

The MFI can also be determined in constant influent filtration. Taking the resistance is series model for filtration from equation (9) was derived, we obtain:

$$\frac{dV}{Adt} = \frac{\Delta P}{\eta(R_m + R_c)} \tag{6}$$

In which,
R_m: initial resistance to water
R_c: resistance due to particles deposit on the membrane surface as cake

$$R_c = \frac{V}{A} \times \alpha C_b = \frac{V}{A} \times I \tag{7}$$

In most cases, it is impossible to determine C_b. Therefore, in the MFI test the fouling index I is taken as the product of and as the signal for the fouling potential of the feedwater. Combining equation (1.3) and equation (1.4) gives,

$$J = \frac{\Delta P}{\eta(\frac{V}{A} I + R_m)} \tag{8}$$

Rewriting V/A as Jt and rearranging give the following equation:

$$\Delta P = J \eta R_m + J^2 \eta I t \tag{9}$$

The previous equation describes the pressure increase to maintain a constant influent with cake formed on the membrane. The MFI is calculated by the fouling index I as follow:

$$MFI = \frac{\eta_{20°C} I}{2\Delta P_o A_o^{\ 2}} \tag{10}$$

In which,

ΔP_o is 2 bar; $\eta_{20°C}$ is the viscosity of feedwater at 20°C and A_o is the surface area of the 0.45 um microfiltration test membrane of 13.8×10^{-4} m^2.

2.3 Membrane Fouling Stimulation (MFS)

2.3.1 Introduction

Membrane fouling stimulation is created by J.S. Vrouwenvelder. It is a relatively cheap and user-friendly tool to detect the fouling potential of feed water for RO process. MFS has a tiny dimension (0.07m×0.30m×0.04m), and the effective membrane length is 0.20m. Feed water will flow through the membrane during the operation, and the pressure drop could be obtained by measuring the pressures on two sides. After the operation, filters will be placed in an ultrasonic cleaning bath for detaching. Afterward received suspensions will be used to measure organic concentrations by measuring ATP.

Figure 4: Side view of MFS (Vrouwenvelder, J., et al., The Membrane Fouling Simulator: A practical tool for fouling prediction and control. Journal of Membrane Science, 2006. 281(1-2): p. 316-324.)

MFS meets all the requirements Vitens formulated for a (bio)fouling monitor. Firstly, the tool must be representative for spiral wound membrane element used in practice. Secondly, the obtained data must be accurate and reproducible. In this case, the database could be facilitated by interpretation of data collected at different locations and(or) under different conditions. Thirdly, the monitor must be able to track fouling quantitatively by: (1) operational parameters as the pressure drop, (2) in-situ, real-time and non-destructive observations (visual, microscopic and other methods) and (3) analysis of coupons taken from the monitor. (Vrouwenvelder et al. 2007)

MFS has two principal advantages compared with full-scale experiments; firstly, the small scale of MFS makes it easier to handle and operate in duplicate tests. Secondly, a real-time and nondestructive observation obtained from a transparent window.

2.3.2 MFS calculation

The total exchange area was calculated before the preussre drop calculation.

The total exchange area is calculated according to the geometry of the module and that of the hollow fibers. It is described by:

$$A = N\pi dL \tag{11}$$

Where N is the number of fibers, d is the fiber diameter and L is the efficient exchange length. The number of fibers is related to the diameter of the shell and that of the fibers by the expression:

$$PR\% = 100N(d_o / D)^2 = 100(1-\varepsilon) \tag{12}$$

Where PR% is the packing density, D is the shell internal diameter and is the overall porosity of the bundle. The specific membrane area is given by the type of fiber arrangement. This ratio is greatest for maximum compactness of the agreement.
The ultrafiltration modules of parallel hollow fibers present a global porosity
The pressure drop increase was related to the amount of accumulated biomass and the linear flow velocity. The relationship between pressure drop and velocity is shown in Equation 3.

$$\Delta p = \lambda \frac{\rho v^2}{2} \frac{L}{d_h} \tag{13}$$

In which

λ : friction coefficient
ρ : specific density
L: length of membrane
D_h: hydraulic diameter

2.3.3 Relationship between velocity and substrate concentration against pressure drop

There are extensive biofilm literature studies on the influence of factors such as and linear flow velocity and substrate load on the development of biofouling in membranes. (Radu et al. 2010)

Increasing the linear flow velocity may reduce the accumulation of microorganisms on the surface[1]. The effectiveness is because of the increased shear stress acting on the biofilm. It is suggested that increasing the linear flow velocity may be a suitable method to reduce biofouling in heat exchangers[2]. One possible way to increase the linear velocity is to increase the feedwater loading rate.

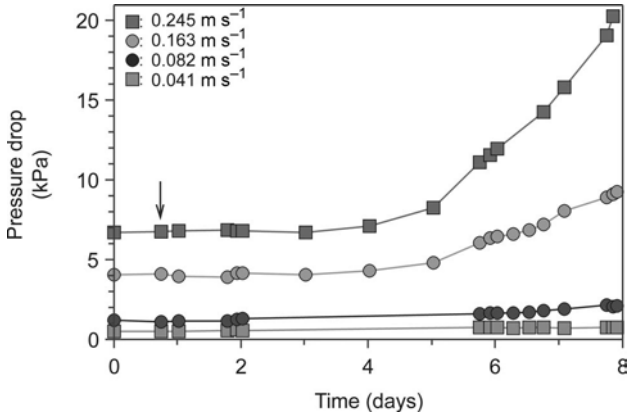

Figure 5: pressure drop with time over the monitor operated with different linear flow velocity and the same concentration of a biodegradable compound (200ug/l) in the feed water. The arrow indicates the starting time of the dosage.

Increasing the substrate concentration will increase the pressure drop increasing rate. As can be seen from Figure 4, after 14 days, the pressure drop of 400ug/l substrate concentration is ten times as much as the counterpart one of 0 ug/l. Visual observations indicated that more materials were stuck on the surface of the membrane when supplied with higher substrate concentrations.

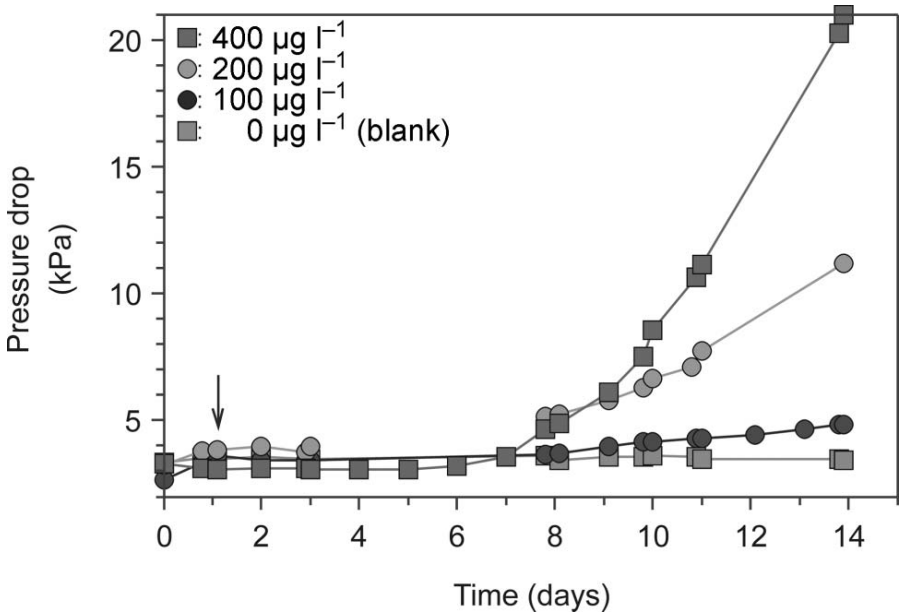

Figure 6: Pressure drop with time over the monitor with time over the monitor with and without dosage of different concentrations of a biodegradable compound to the feed water of the monitor. The arrow indicates the starting time of the dosage.

2.4 Hydraulic resistance and fouling

2.4.1 Introduction

It is important to understand some of the reasons why pressure drop increase while the water influent is constant. For dead-end filtration, the most important reason is fouling, this is a build of materials(Field 2010). Fouling may take the following forms:

- **Adsorption**: this occurs when specific interactions between the membrane and the solute or particle exist.
- **Pore blockage**: when filtering, pore blocking will occur, causing a reduction in influent due to the closure of pores.
- **Deposition**: a deposit of particles can grow layer by layer on the filter surface, leading to a significant additional hydraulic resistance.
- **Biofilm**: newly attached bacterial cells grow into biofilms and will cause an increase of hydraulic resistance.

In a simple term, fouling is about non-dissolved material that is either deposited on the membrane surface, or material deposited in the pore mouths or on walls, or indeed a mixture of both.(Field 2010)

2.4.2 Fouling overview

Fouling is the primary cause of the reduction in the active area of the membrane. The reduction of membrane contributes to a reduction in influent during pressure constant. Several parameters influence the fouling rate, for instance:

- Natural and concentration of solutes and solvents;
- Membrane/filter type;
- Pore-size distribution;
- Surface characteristics and material of filters

The size and type of undissolved materials have a strong influence on fouling issues. Foulants and fouling models were discussed in Table 1,

Table 1: Example of fouls and fouling model in membrane process(Scott 1998)

Undissolved materials	Fouling mode
Large suspended particles	Particle present in the original feed can block module channels as well as form a cake layer on the surface
Small colloidal particles	Colloidal particles can create a fouling layer
Macromolecules	Gel or cake formation on membrane
Small molecules	Some minor organic molecules tend to have strong interactions with membrane/filter surface
Biological	Growth of bacteria on the membrane surface

2.4.3 Modeling of fouling

For porous membranes, the active area of the membrane is the pores. Hence, most fouling mechanisms are related to them and the processes which lead to a reduction in the number of active pores. Based on this, four fouling mechanisms for porous membranes can be observed. As shown in Figure 7, these are:

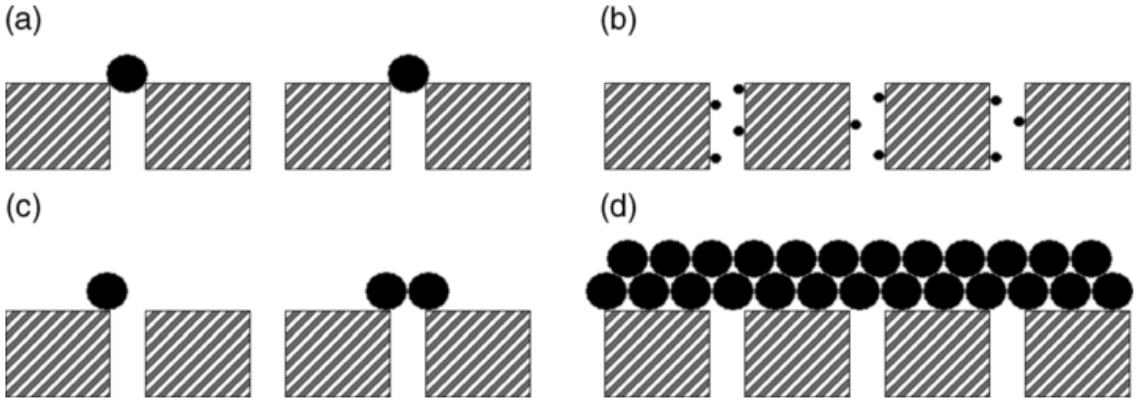

Figure 7: Fouling mechanisms of porous membranes. (a) Complete pore blocking; (b) internal pore blocking; (c) partial pore blocking; (d) cake filtration. (Field 2010)

1) Complete pore blocking,

2) Internal pore blocking,

3) Partial pore blocking,

4) Cake filtration

In Table 2 the background information concerned with each mode, their effect on the mass transport and the relevant transport equations are given. The equations are a reworking of Hermia's equation(Hermia 1982).

$$\frac{d^2t}{dV^2} = k\left(\frac{dt}{dV}\right)^n \tag{14}$$

Table 2: Fouling mechanisms, phenomenological background and transport equation (De Barros et al. 2003)

Fouling mechanism	n	Phenomenological background	Effect mass transport	Transport equation
Complete pore blocking	2	Particles massive than the pore size completely block pores	Reduction of the active membrane area. Depends on feed velocity	J=Jo. Kb.A.t
Internal pore blocking	1.5	Particles smaller than pore size enter the pores and get either adsorbed or deposited onto the flow	The increase in membrane resistance due to pore size reduction. Internal pore blocking is independent of feed velocity	J=Jo.(1+0.5 Ks (A.Jo)^0.5.t)^-2
Particle pore blocking	1	Particle reaching surface may seal a pore or bridge a pore or partially block it or adhere on inactive regions	Reduction of active membrane area. The effect is similar to pore blocking but not as serve	$J=J_o.\ (1+K_i\ .(A.J_o).t)^{-1}$
Cake filtration	0	Formation of cake on the membrane surface by particles which neither enter the pores nor seal the pores	The overall resistance becomes the resistance of the cake plus the resistance of the membrane	$J=J_o.(1+2K_c\ .(A.J_o)^2.t)^{-0.5}$

In the above equation, the phenomenological coefficients n and K depend on the fouling mechanism. The form of the equation for specific values of n is given in Table 2.

2.4.4 Biofouling

Biofouling in the membrane-based water system can lead to a significant decrease in influent under constant pressure condition(Radu et al. 2010). Newly attached microorganism grow into biofilms as long as nutrients are supplied by the water. Nutrients are the driving force for biofilm growth in membrane systems, and it is important to consider the concentration of organic carbon(Vrouwenvelder et al. 1998). Figure 8 shows the membrane samples taken from the monitors after the period of operation showed that fouling accumulated on the membrane surface and not on the pore size.

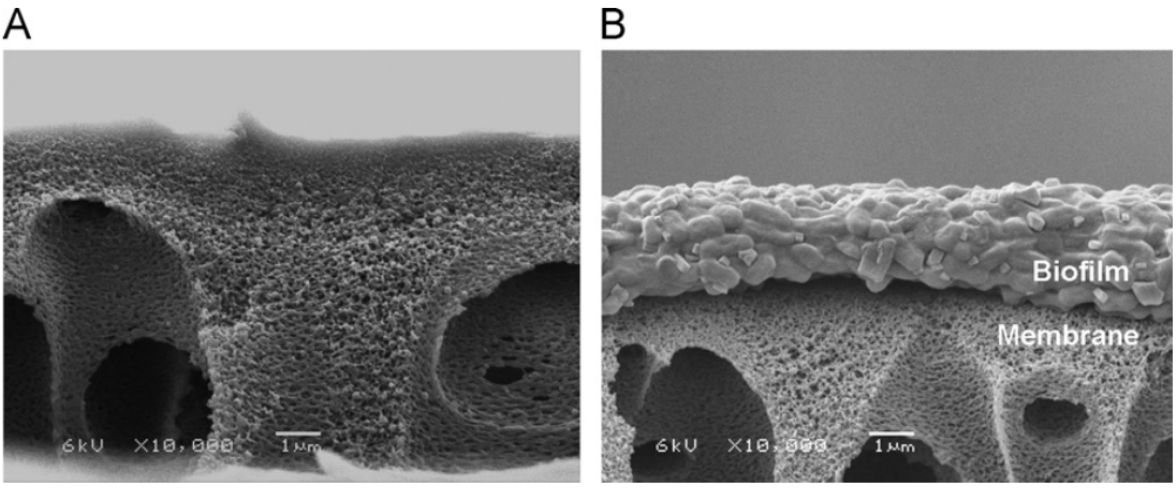

Figure 8: Scanning electron micrograph of a membrane cross section. (A) original membrane and (B) membrane with biofilm after four days of operation(Dreszer et al. 2013)

The influence of nutrient on biofouling is evident and crucial (Baker & Dudley 1998). The concentration of biodegradable substrate in the feed water significantly affect the biofilm growth. Another fact for biofouling is a higher influent caused more biofilm accumulation and thus a higher biofilm resistance(Dreszer et al. 2013).

2.5 Problem description

To provide even more safe water to the consumers, Oasen decides to use an innovated treatment, one-step reverse osmosis (one-step RO), to replace the conventional treatment in following years. One-step RO is to let the ground water directly go through RO membrane and nearly only water could pass through RO membrane. Therefore, drinking water from treatment plant is almost the pure water(Anon n.d.). On one hand, Using RO water can significantly improve the drinking water quality and also control the microbial growth during distribution process because biologically stable water can limit the growth of any kinds of bacteria by controlling the food source(Van der Oost et al. 2003). On the other hand, because the RO water is so pure and the nutrient concentration is almost zero, lots of biofilm and microorganisms attached on pipelines over the past decades may die because of the lacking of enough food and detach from pipelines. These detached biofilms and microorganisms present in water in pieces and may clog water meters. (See Figure 9 and 10).

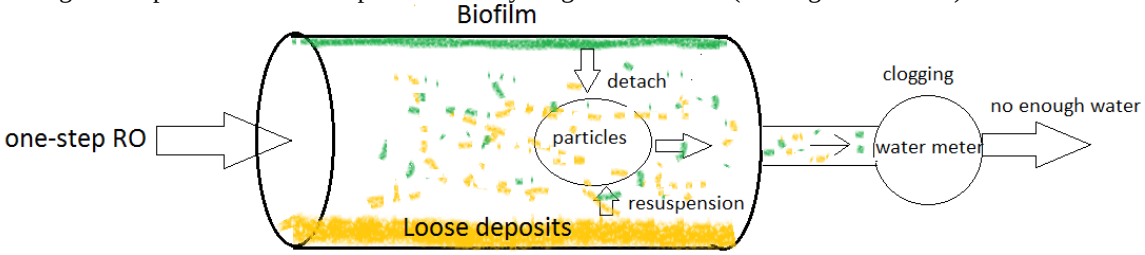

Figure 9: water meter fouling during distribution process

Figure 10: clogged water meter

To avoid the potentially clogged water meter issues, a new method, the Smart Water Meter is tested to monitor the fouling issues during the distribution process.

2.6 Smart Water Meter, a new method to monitor fouling issue/water quality

Smart Water Meter is a new concept from Oasen to track potential fouling issues during distribution network. In a foreseeable future, Oasen will use reverse osmosis to treat drinking water and thus the nutrient (biodegradable compounds) in drinking water will be slight. In that case, biofilms used to attach on pipelines may die and detach from pipes and these part of biofilm may clog consumers' water meter. The Smart Water Meter is a general concept can not only measure the water flow but also can monitor clogging potential by detecting the pressure drop increase and act as an early warning system, which let Oasen know and deal with clogging issues before complaints from consumers. The Smart Water Meter can detect the fouling issues by monitoring the pressure drop increase.

There are two concepts for Smart Water Meter: Filtrated clogging potential (FCP) and crossflow clogging potential (CCP). FCP is derived from Membrane fouling index (MFI), which leads water filtrate directly through the filter and CCP is original from membrane fouling simulation (MFS), which lets water crossflow the feed spacer.

In fact, At the beginning of the research, CCP was adapted as an only equipment for the Smart Water Meter. CCP can retain most of the particles and biofilms which larger than the corresponding pore size thus the pressure drop increase rate of CCP is high, which indicates the result of CCP can be obtained in a relatively short time. It is an efficient method to detect water fouling issues in short term but because of relativity short effective operation period of CCP, it is difficult to monitor the water fouling problems in a long term. Therefore, CCP was added as another part of Smart Water Meter for long-term water fouling potential monitoring.

2.7 The objective of this research

The literature that was mentioned in this chapter indicates that the microbiological activity in the drinking water distribution system cannot be ignored. Although nowadays what happened during the delivery process is still poorly understand(Liu, Verberk, et al. 2013), there is some method to detect biological activity. For instance, ATP measuring or total cell counting (TCC). However, these methods are relatively complex and cannot measure constantly. Therefore, the target of this research, along with other research that was done before in Oasen, was to verify the Smart Water Meter as a secure and reliable method to monitor water quality and fouling issues during distribution network.

The objective of this research include:

- Verify Smart Water Meter as a suitable method to monitor water quality and fouling issues during the distribution process.
- Investigate what matters cause the pressure drop/filter resistance increase.
- Analyze the characteristics of these matters.

3 Material and methods

3.1 Methodology

In this research, two experiments, FCP and CCP, were taken to investigate the potential fouling issues during the distribution network. The analysis process of the whole research is illustrated as a schematic drawing shown in Figure 11.

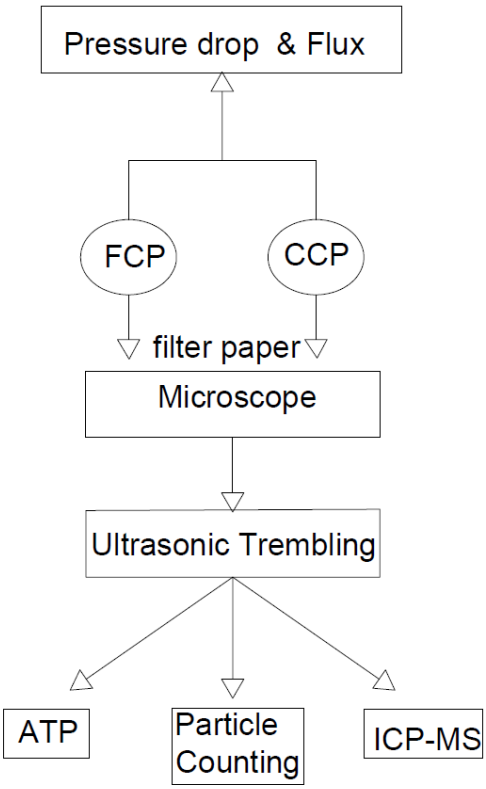

Figure 11: result in analysis process

The result of the experiment will be analyzed from three aspects: Physical part, Chemical part, and Biological part (see Figure 12). Physical part stress on explaining from pressure drop and filter resistance. Chemical part focus on determining the chemical compounds of fouling and biological part centralizes on ATP concentration. A better and comprehensive result could be obtained from the combining of analysis from these three aspects.

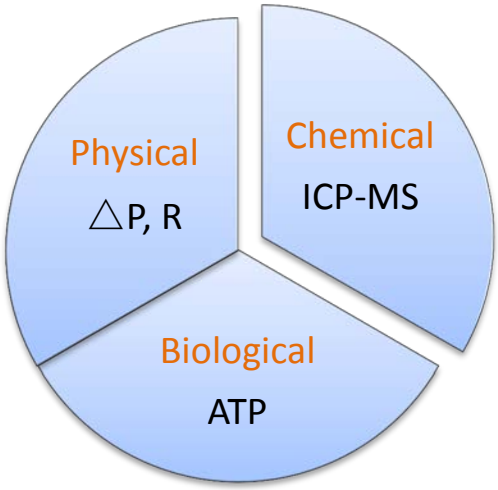

Figure 12: process analyze from physical, chemical and biological

3.2 Experiment setup and procedure

In general, there are two experiments designed for this research, filtrated clogging potential (FCP) and crossflow clogging potential(CCP). Details would be further explained in the following chapter.

3.2.1 Filtrated clogging potential (FCP)

FCP measuring in this study were carried out by use of micro glass fiber filters and polyvinylidence fluoride (PVDF) membranes. As shown in Figure 13**,** it is a dead-end microfiltration. There are two pressure sensors; one measures initial inflow pressure, the other measures the pressure after the filter and water meter. The pressure difference between two sensors is the pressure drop. The FCP equipment is shown in Figure 14.

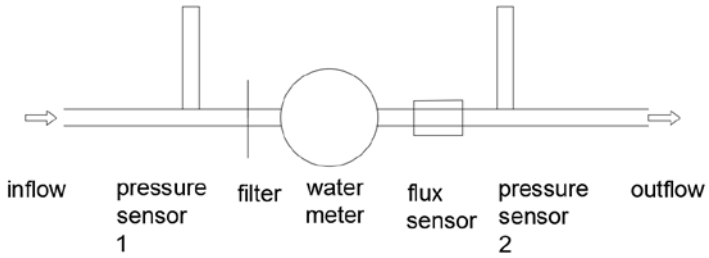

Figure 13: schematic diagram for FCP experiment

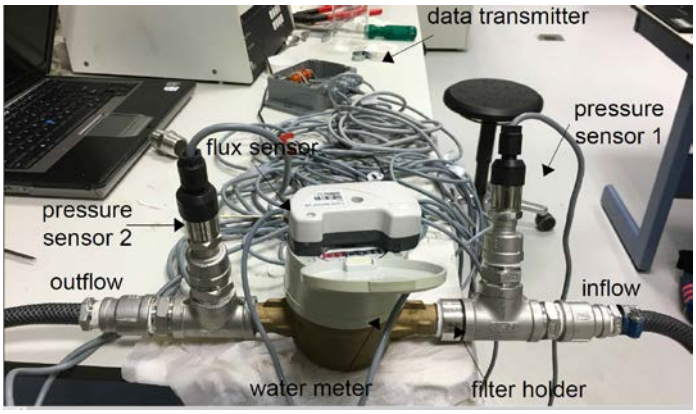

Figure: 14 FCP experiment in Lab

Unlike MFI, the prototype of FCP, the influent of FCP is inconstant because inflow is directly from drinking water tap and also the initial water pressure varied in a range which cannot be ignored. In this situation, Only water pressure drop cannot represent anything because both flux and initial water pressure are varied. Therefore, a new parameter should be applied to indicate the filter fouling issue. Fortunately, based on the convert Darcy's

law (see Equation 16 and 17), pressure drop could be transferred to filter resistance, which does not influenced by influent and initial pressure variation.

$$R_t = \frac{TMP}{J_t . u_t} \tag{15}$$

$$u_t = 1.784 - (0.575 \times T) + (0.0011 \times T^2) - (10^{-5} \times T^2) \tag{16}$$

in which,
R_t : membrane resistance
TMP : transmembrane pressure, in dead-end filtration is pressure drop
u_t : viscosity
J_t : influent
T: temperature

To test the flexibility of FCP, I operated the FCP in my apartment (see Figure 15). Because the water quality in the apartment is slightly different from the water in Laboratory, it is logical to expect a difference in two situation.

Figure 15: FCP experiment in apartment

3.2.1.1 Filtration material and influent area calculation

At the beginning of the experiment, three filters and two membranes were chosen. I choose filters with 1.2um, 1.5um, and 2.7um. These three pore sizes have been selected because 1.2um is the pore size used to measure suspended solids. 2.7um is chosen because 2.7um is the maximum pore size of glassfiber filter. 1.5um is a value between 1.2um and 2.7um. 0.45um and 0.2um membranes were chosen for this experiment. 0.45um was chosen because it is the size to measure dissolved organic carbon (DOC), and 0.2um is the size for DNA extracting.

Unfortunately, during the practical operations, drinking water can only filtrate through three filters, no water can pass the membrane. The main reason is the membrane pore sizes are too small thus the required pressure is higher than the maximum tap water pressure. Therefore, only three filters were chosen finally for FCP experiment.

Detailed information about filters and membranes is shown in Table 3 and Figure 16.

Table 3: types of filters and membranes for experiment

Type	Manufacture	CAT.number	Pore Size	Material
			um	
Filter	Whatman	1822-047	1.2	Glassfiber
Filter	Whatman	1827-070	1.5	Glassfiber
Filter	Millipore	APFD02500	2.7	Glassfiber
Membrane	GE	10600100	0.45	PVDF
Membrane	GE	10600102	0.2	PVDF

Figure 16: three different glass microfiber filters used in experiments

To prevent the filter from broken in water pressure condition, a unique order made filter holder was used in this experiment (see Figure 17A). This filter holder can support the filter evenly during operation time and can increase the effective operation time.

Filter holder can support the filter but at the same time, it also decreases the active filtration area. A new influent area needs to be calculated. By using the microscope, the surface area of a single hole is 1958294um^2 (see Figure 17B). The total hole number is 64, and the calculated total filtration area is 1.25cm^2.

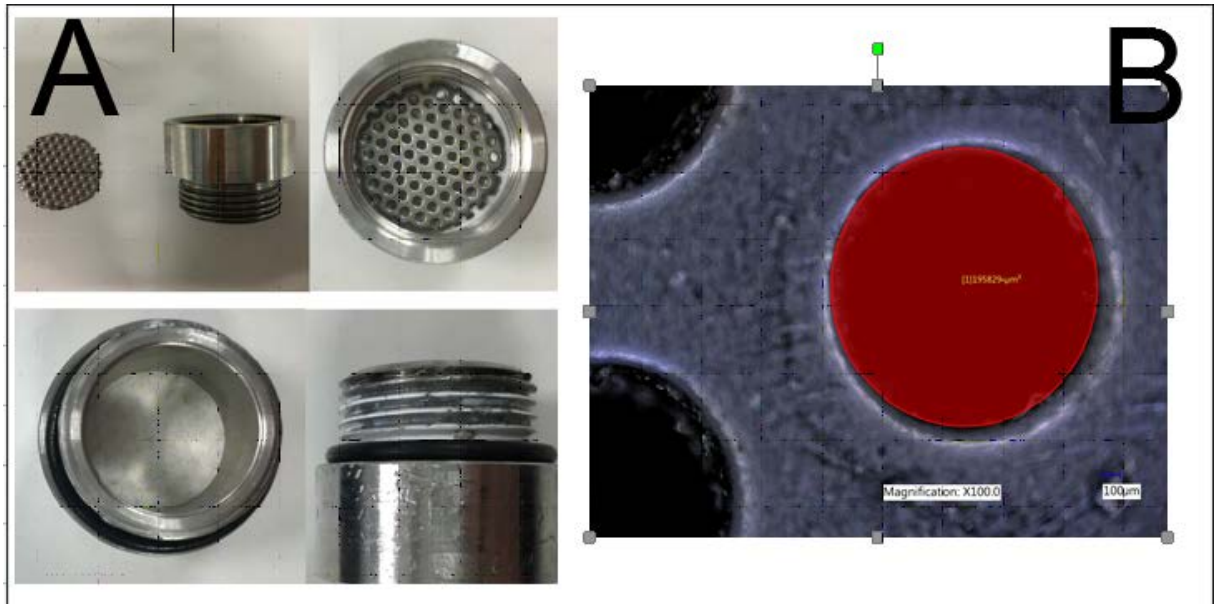

Figure: 17(A) side view of the filter holder (B) surface area of the single hole

3.2.2 Crossflow clogging potential (CCP)

CCP in this study was implemented by the same equipment from MFS. As can be seen from Figure 18 and 19, it is a crossflow filtration. There are two PVC slides and a feed spacer in between. All water pass the PVC surface and thus compared with FCP, the dead-end filtration, the pressure drop in CCP will be much lower.

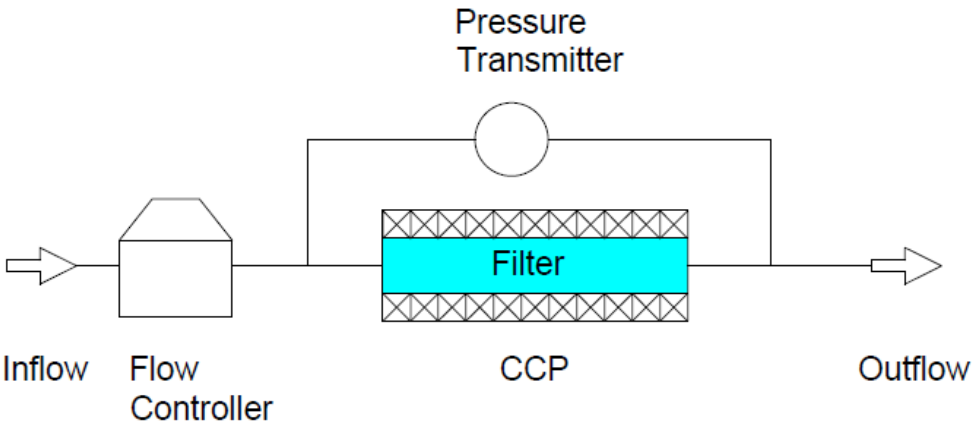

Figure: 18 Schematic diagram for CCP experiment

The duration of CCP experiment is expected to be longer than FCP experiment because there will be much less particle fouling issues in CCP examination during the same operation period. Biofouling issue is an essential element causes pressure drop increase in CCP test.

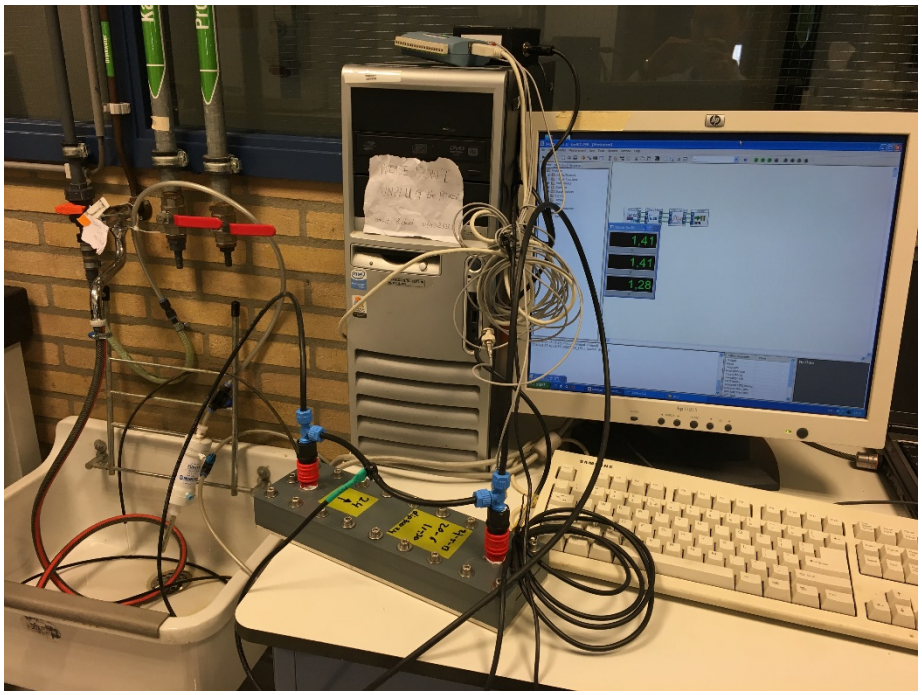

Figure: 19 CCP equipment

Like the MFS, there are two PVC and a feed spacer in CCP equipment (see Figure 20). During operation, feedwater will flow through the two PVC and the biomass accumulation in membrane and feed spacer will contribute to the pressure drop increase. The pressure drop in this experiment will be measured by the pressure sensor (see Figure 20) and will be transferred to the computer for further analysis.

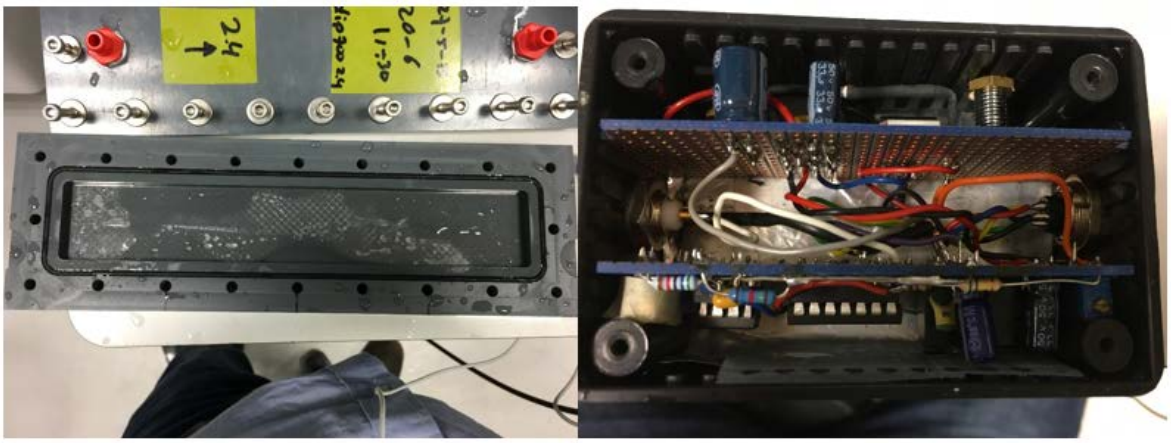

Figure 20: CCP equipment inside (left), pressure sensor (right)

3.3 Measurement

Measurements in this research are supposed to meet the requirement from Chapter 3.1. Further explanation would be discussed in the following section.

3.3.1 Pressure drop and influent

Pressure drop and influent are the most important parameters for this research because based on these two parameters, we can have a brief idea whether there is a fouling issue or not. For FCP and CCP measuring, all pressure drop and influent are digital data, but there is still a little bit difference.

For FCP measuring, during operation, two pressure sensors measure pressures every 5 to 7 seconds. Measured data will transfer to a control panel (see Figure 21 left) and then will upload to the Internet. At the starting point of the experiment, this control panel didn't work as expectation. Sometimes the control panel did not upload any data and sometimes when it started to upload data; the uploaded data was random numbers that did not make any sensor. After numerous calibrations with colleges from IT department, this control panel finally work. When I started the experiment, I will connect my laptop to "Oasen-monitor" (Figure 21 right upper). Then I can access to real-time data from http://192.168.1.1/data/ (Figure 21 right lower).

The influent sensor acted like a digital water meter and can only measure entirely water flow go through the water meter, to get instantaneous flow velocity, I need to calculate the ratio between the total water flow increasing and the lasting period.

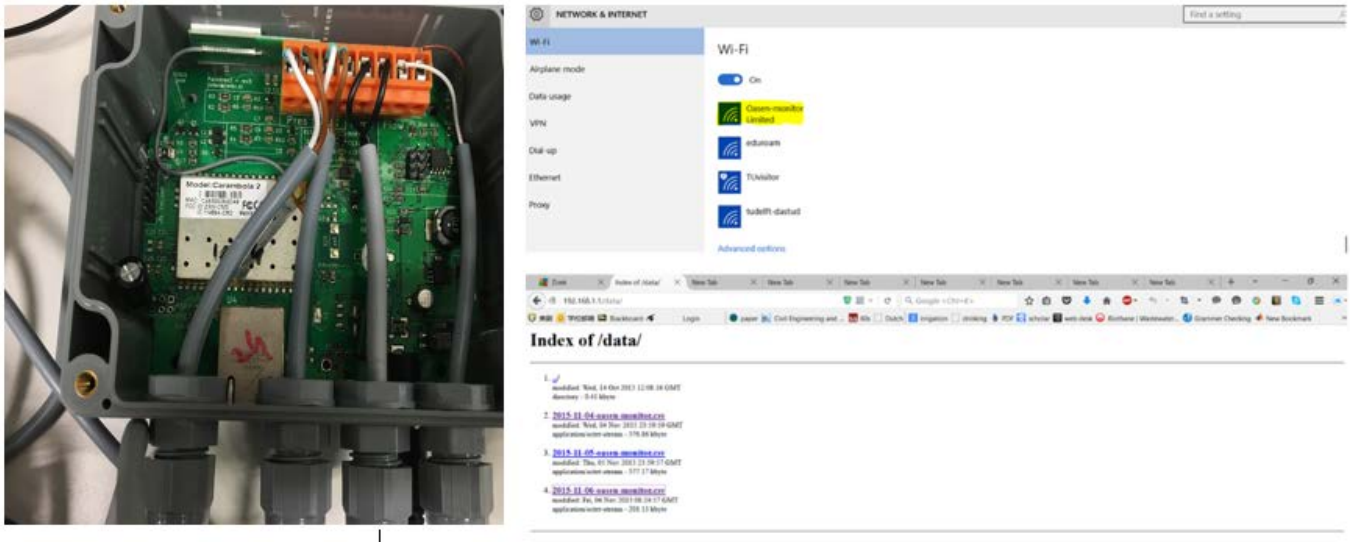

Figure 21: Control panel for FCP (left), Oasen monitor (right upper), real-time data (right lower)

For CCP measuring, during operation, pressure sensor will measure pressure drop and transfer to the computer by USB link. The data analyze software for CCP is *DASYlab 13.0* (see Figure 22). All the data (pressure drop along the operation time) will be documented by this software and all the data will be further analyzed by Excel.

Figure 22: CCP data analyze software

3.3.2 Filter observation by High-resolution digital microscope

For a further understanding of the fouling issue in filters, a high-resolution digital microscope was applied (see Figure 23). The maximum magnification is 1000 times the original size. The minimum resolution is about 1um which is limited by the resolving power of this optical instrument.

Compared with other digital microscopes, there are three significant advantages. The first one is the live depth composition eliminates the need for manual focus adjustment; the second one is the high-resolution HDR can increase the resolution limit which can allow more details in very high magnification condition. The last one is this microscope can compose 3D picture automatically, and this 3-D image can let us better understand the fouling issue.

Based on VHX-5000's advantages, three primary functions of this microscope for my research are as follows;

- Observe and analyze the filter after operation period under high resolution.
- Measure the massive particle clogging number and area (larger than 1um) in filter after operation period
- Compose 3D photo of the filter.

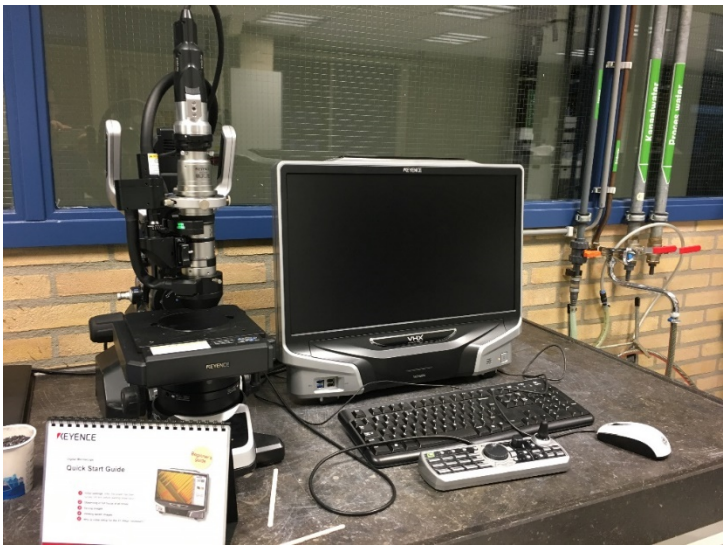

Figure 23: Keyence VHX-5000 digital microscope

To obtain an accurate measuring result, for each measurement, five points were chosen randomly from the filter, and the final result for each measurement is the average of the selected five points.

Since VHX-5000 is optical microscope and the minimum resolution is 1um, it is evident that this lens cannot capture particles smaller than 1um thus the total particle accumulation in the filter is obtained from particle counting equipment. Further detail would be explained in Section 3.3.5.

3.3.3 Ultrasonic trembling

For further analyzing the physical, biological and chemical parts of matters stuck in the filter, we need to detach matters from filters into suspensions. After a literature review, low-energy ultrasonic trembling was chosen. (see Figure 24) Because of the non-destructive, rapid and reproducible removal of biofilm from the filter(Oulahal-Lagsir et al. 2000). Based on N.Oulahal-lagsir's research, the variability of the result was constant, +/-24%, and this variability is acceptable for my research.

The trembling process is as follows,
1) A sample filter and 15mL demi water add to a plastic bottle.
2) Trembling in a water bath for three times, for two minutes each.(Liu et al. 2016)
3) Obtaining the suspension for further research.

Figure 24: 40 kHz low energy Ultrasonic water bath

3.3.4 ATP measuring

3.3.4.1 Introduction

The ATP analysis in this research was conducted according to 2nd generation ATP test kits from Aqua-tools Company. The advantage of this ATP measuring is unlike other traditional microbiological test requiring days for feedback; Aqua-tools can get result in minutes(Modified & Kit 2010). The theory of this method can be explained with the following formula:

$$ATP + O_2 + luciferin \xrightarrow{Mg^+ + luciferase} AMP + PPi + oxyluciferin + light \quad (17)$$

Aqua-tools ATP test is based on firefly luciferase, where a sample containing ATP is introduced to a solution containing the enzyme Luciferase, which naturally occurs in the tails of fireflies, to produce light. The light is detected in a Luminometer as Relative Light Units (RLU)(Modified & Kit 2010) (See Figure 25).

cATP was measured in this research. cATP represents ATP from living microorganisms in suspension in a fluid and therefore is a direct indication of the biomass concentration.

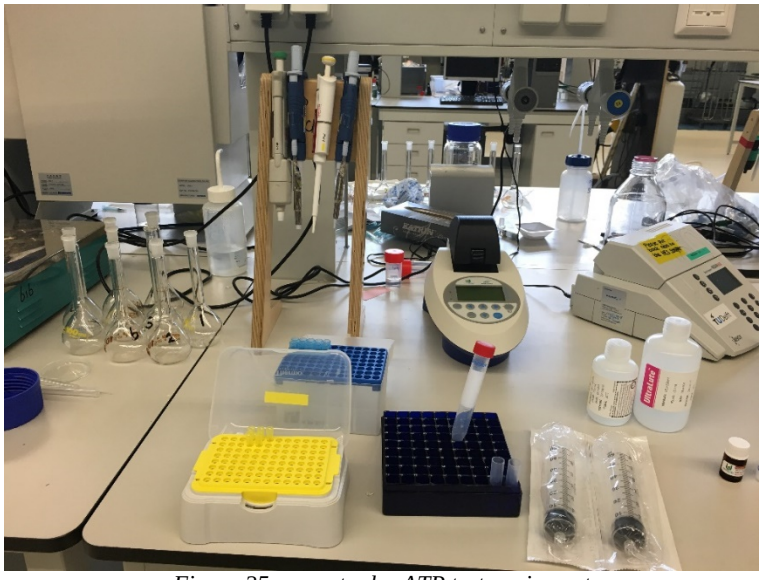

Figure 25: aqua-tools cATP test equipment

3.3.4.2 Test process

The brief introduction of the ATP measuring is using UltraCheck to convert luminometer RLU values into actual ATP concentration. Suspension from ultrasonic trembling was used as sample water. Detail procedure was shown as follows,

a. Add 2 drops of UltraCheck 1 and 2 drops Luminase to a test tube, swirl gently five times and then insert into the luminometer. Record $RLUuc_1$ for final calibration.
b. Slowly push the entire sample volume through the filter by syringe, record the sample volume.
c. Add 1mL of UltraLyse 7 through the filter and add 9mL of UltraLute into the Tube.
d. Using micropipette transfer 100uL of diluted extraction tube and add 100uL of Luminase, swirl gently five times and insert into the Luminometer. Record RLU_{cATP} for final calculations.

The final calculation is to convert RLU values to ATP concentrations using the following equation.

$$cATP(pg\_ATP/mL) = \frac{RLU_{cATP}}{RLU_{UC1}} \times \frac{10,000(pg\_ATP)}{V_{Sample}(mL)} \tag{18}$$

Cellular ATP (cATP) represents the amount of ATP contained within living cells and is a direct indication of total living biomass quality(Modified & Kit 2010).

Based on the measured cATP concentration and the sample volume, three parameters related to ATP could be calculated, total cATP of the filter (pg); concentration of cATP on the filter (pg/cm^2) and cATP captured by filter per liter water (pg/L). The equations were shown as follows,

$$total\_cATP(pg) = cATP\_con.(\text{pg/ mL}) \times 15mL \tag{19}$$

$$cATP\_con.\text{filter}(\text{pg/ cm}^2) = \frac{total\_cATP(pg)}{filter\_area(cm^2)} \tag{20}$$

$$cATP\_per\_liter(pg/L) = \frac{total\_cATP(pg)}{filtrated\_volume(\text{L})} \tag{21}$$

3.3.5 Particle counter

The particle count gives an indication of the amount and size of suspended particles retained on the filters during the operation period. The type of the particle counter that was used for this research was HIAC Royco 9703 (see Figure 26). Half of suspension from ultrasonic trembling was used for particle counting (the other half for ATP testing). This particle counter can provide particle distribution range from 0.1um to 4 mm. Combine this data with the result from the microscope; we can better understand the particle clogging distribution situation on the filter.

Figure 26: HIAC Royco liquid particle counting system, model 9703

3.3.6 ICP-MS

Inductively Coupled Plasma Mass Spectrometry (ICP-MS) is an analytical technique used for elemental determinations. It is capable of detecting metals and several non-metals at concentrations as low as one part in 10^{15} (part per quadrillion, ppq) on non-interfered low-background isotopes. The ICP-MS has many advantages over other elemental analysis techniques such as atomic absorption and optical emission spectrometry;

- Detection limits for most elements equal to or better than those obtained by graphite furnace atomic absorption spectroscopy (GFAAS)
- The ability to handle both simple and complex matrices with a minimum of matrix interferences due to the high-temperature of the ICP source.
- Superior detection capability to ICP-AES with the same sample throughput
- The ability to obtain isotopic information

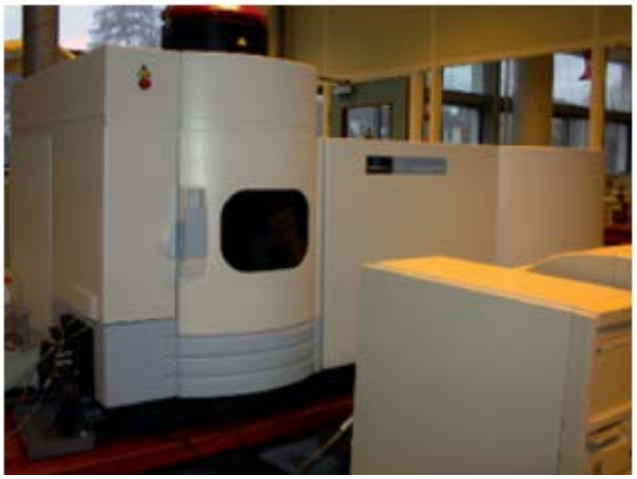

Figure 27: ICP-MS machine

The ICP-MS allows determination of elements with atomic mass ranges 7 to 250 (Li to U), and sometimes even higher. Some masses are prohibited such as 40 due to the abundance of argon in the sample. Unlike atomic absorption spectroscopy, which can only measure a single element at a time, ICP-MS has the capability to scan for all elements simultaneously. This allows rapid sample processing. A simultaneous ICP-MS can record the entire analytical spectrum from lithium to uranium in every analysis.

The ICP used in this experiment is ICP optical emission spectrometer PerkinElmer Optima 5300DV from Chemical department. The measured quantity of this equipment is over 70 elements in solution. Sample volume is 1.5-2.5ml/min and 2-5 min/sample. The main applications are composition analysis, and most elements are detectable at very low concentration.

4 Result and discussion

4.1 Introduction

In this chapter, all results and analyses are explained from two main parts. Filtrated Clogging Potential (FCP) and Crossflow Clogging Potential (CCP). In each part, detail results will be discussed from three different aspects: physical, biology and chemical (Yiantsios & Karabelas 1998). By analyzing the results from these three aspects, an overall understanding of filter fouling and water quality could be obtained.

Meanwhile, three research objectives could be achieved by these three research aspects. Study 1 could be answered by physical aspect research including resistances in different water quality and different filter pore size. Study 2 and Study 3 could be measured by biological aspect and chemical parts such as ATP and ICP-MS.

To make sure all experiments are reliable and reproducible, all experiments and measuring are taken at least three parallels(Filippini et al. 1990).

The methodology for this research has been explained in Chapter 3.1, thus will not repeat here.

4.2 FCP result and discussion

4.2.1 Physical part

4.2.1.1 Introduction

In general, physical aspect analyzes for FCP including resistance measuring, digital microscope measuring and particle counting. Resistance measuring is the most important result of this research because resistance increasing along operation time give a visible evidence for filter fouling. High-resolution digital microscope observation gives clear pictures for filter details after filtration. Moreover, the microscope can even measure the fouling area ratio and particle clogging diameter and number, which can help the comparisons in different operation situation. Particle counter can also show the clogging particle diameter and number. The measuring result of particle counter is more accurate compared with the counterpart one in the microscope.

4.2.1.2 Resistance

At the beginning of the experiment, the pressure drop was used to represent filter fouling issues. It was expected that pressure drop would increase along with the operation period because of the fouling issues(Boerlage et al. 2004). However, unlike all the previous experiments operated by other researchers, either initial pressure or influent was constant during the experiment, in my experiment, both initial pressure and influent are inconstant(Boerlage et al. 2004; Park et al. 2006). The main reason is that FCP experiment is to measure the drinking water quality directly from tap water thus the initial water pressure varied together with pressure variation in the pipelines. Meanwhile, the original water pressure variation contributes to the inconstant influent. Therefore, since the influent was inconstant, the pressure drop cannot directly use as an indicator for filter fouling issue.

In this situation, filter resistance was adapted as a new parameter to represent filter fouling issue. Based on the convert Darcy's law **Equation 16** and **Equation 17** in Section 3.2.1, filter resistance could be calculated by pressure drop and influent and the filter resistance is not influenced by the initial pressure and influent variation. The resistance results of different pore size filters under different operation conditions will be discussed as follows.

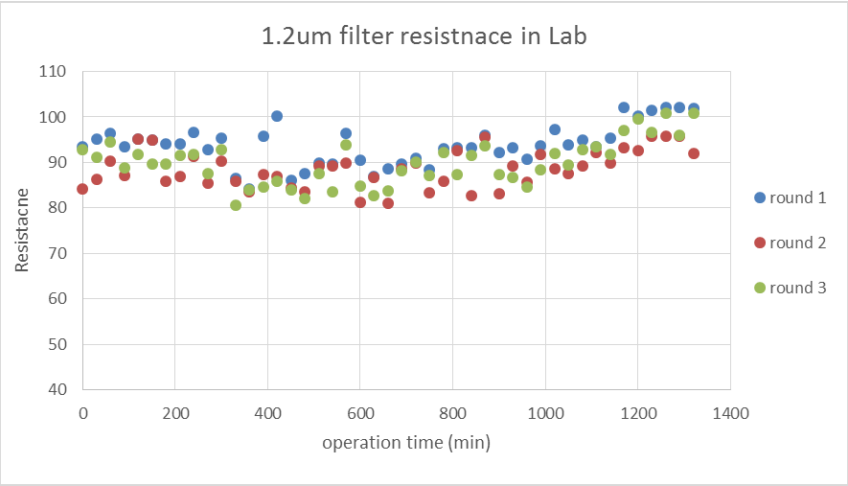

Figure 28: 1.2um filter resistance result operated in Lab

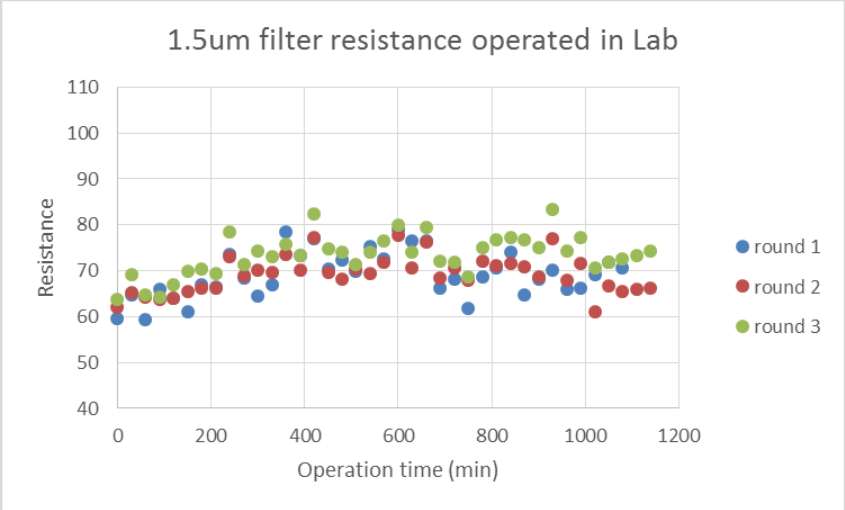

Figure 29: 1.5um filter resistance result operated in Lab

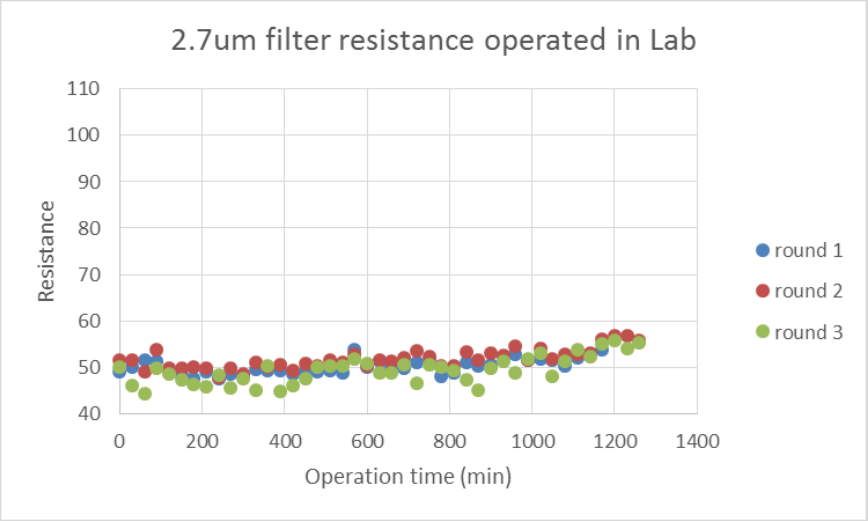

Figure 30: 2.7um filter resistance result operated in Lab

Previous three figures demonstrate the relationship between filter resistance and process time in Lab condition. For each pore size filter, three parallel experiments are taken to reduce systematic error. As can be seen from these figures, although there is some fluctuates during the whole operation period, resistance trend lines of these three filters are increased and the resistance tends to remain stable at the end of the operation period. Meanwhile, the results of three parallel experiments for same pore size filter are almost the same, which indicates the accuracy and reproduce of the experiments.

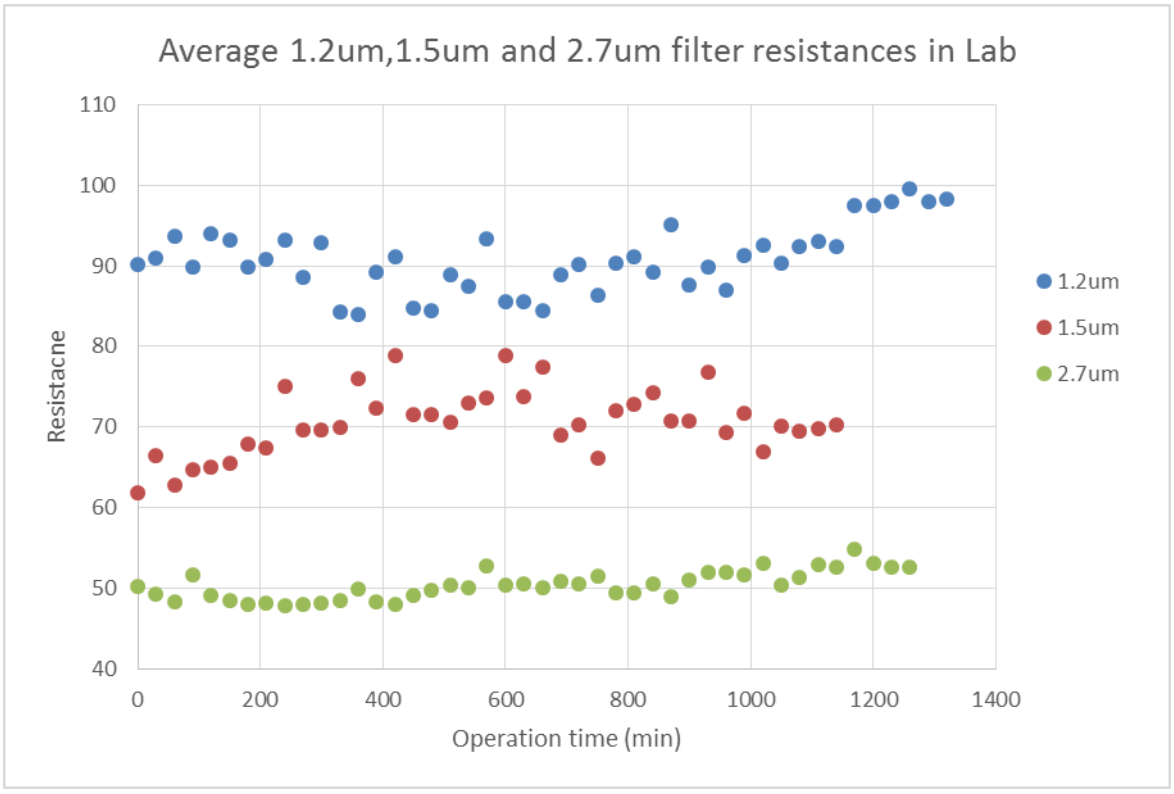

Figure 31: Average 1.2um, 1.5um and 2.7um filter resistance result in Lab

For better comparing the filter resistance under different pore size conditions, the average filter resistance of three parallel measuring was shown in Figure 31. As can be seen from this figure, the initial resistance of 2.7um is 50, which is the lowest among three filters. The initial resistance of 1.5um is 61, and the highest initial resistance is 90 from 1.2um filter. Furthermore, the final resistance of 2.7um is 52.5, and the resistance growth rate is only 5%. However, the last resistances of 1.5um and 1.2um are 70 and 98.5 respectively, which corresponding to 14.5% and 12% resistance growth rate.

It is logical to explain 2.7um filter having the lowest initial resistance and the least resistance growth rate because the larger the pore size, the smaller the filter resistance will be(Boerlage et al. 1997).The resistance growth rate represents the fouling condition during the operation period because the more particle is clogged on filters, the higher the resistance will be(Boerlage et al. 1998). Therefore, since the 2.7um filter has the largest pore size, fewer particles are clogging during the same operation condition, and thus, the resistance growth rate is the least among these three filters(Choi et al. 2009).

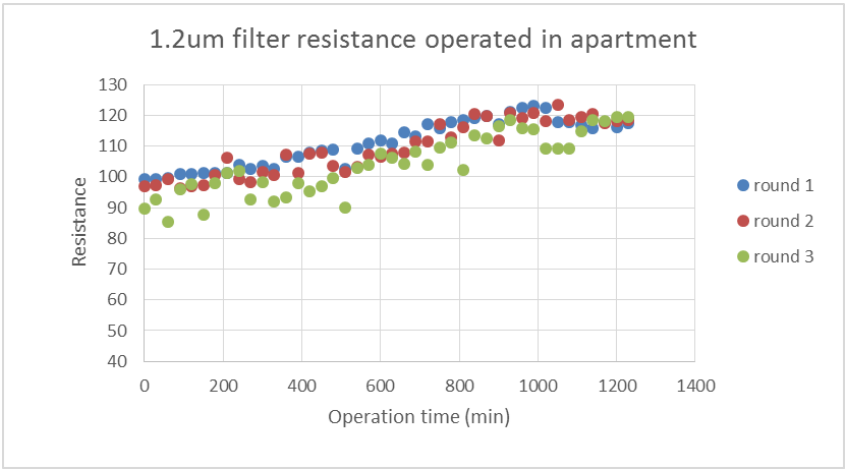

Figure 32: 1.2um filter resistance result operated in Lab

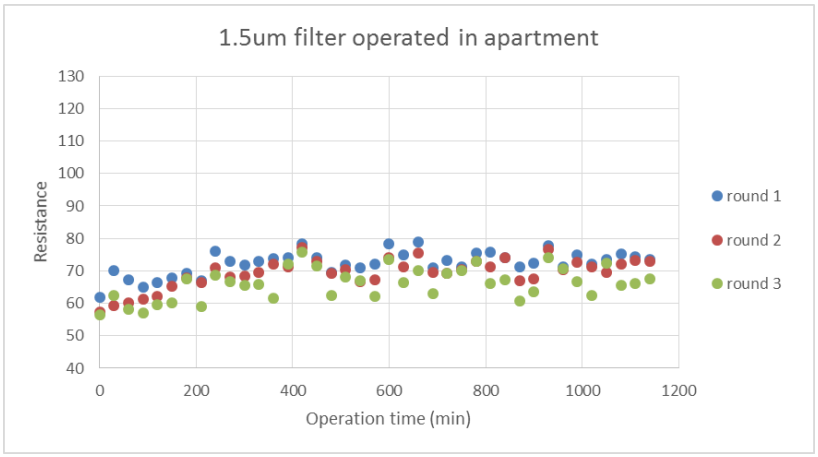

Figure 33: 1.5um filter resistance result operated in Lab

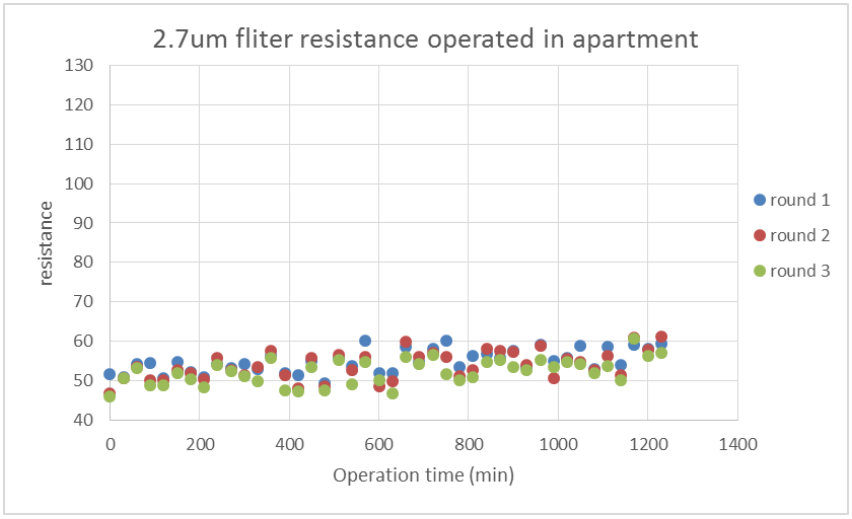

Figure 34: 2.7um filter resistance result operated in Lab

Previous three figures demonstrate filter resistances variations of three filters in apartment states. As the operation in lab condition, three replicates were taken for each pore size filter. The resistance trend lines of these three filters are all growing, and the resistance tends to reach a peak and remain stable at the end of the operation period. Also, the results of three parallels in each pore size filter are almost the same, which indicates the accuracy and reproduce of the experiments.

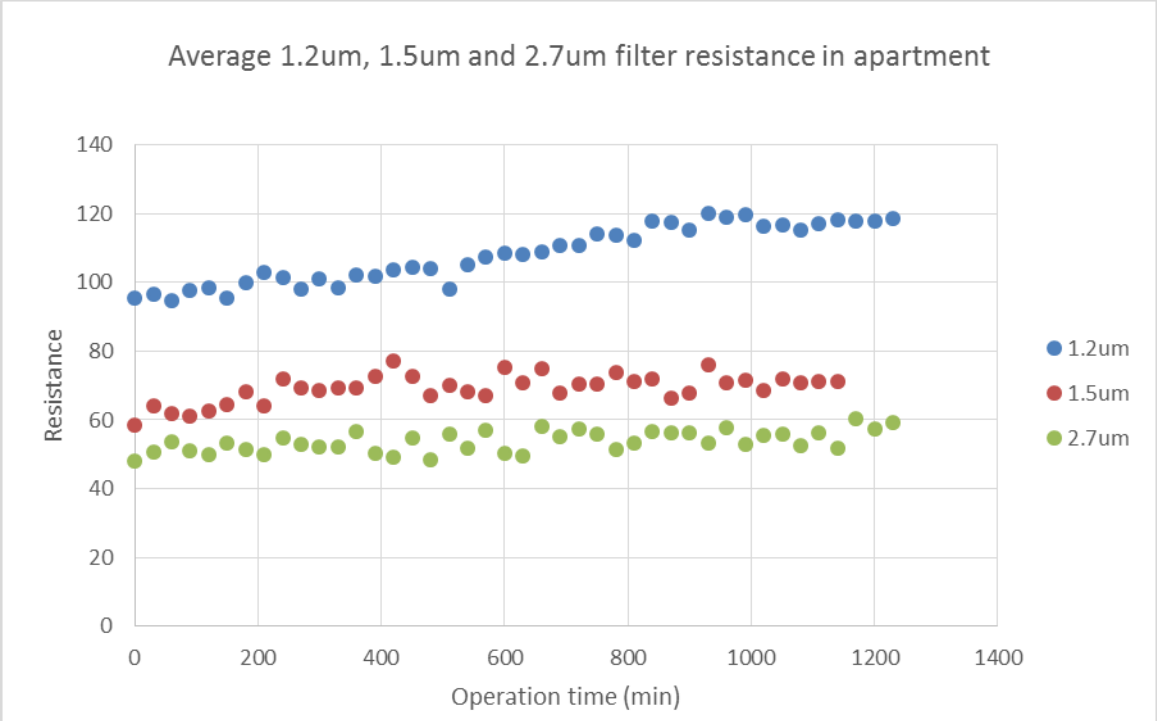

Figure 35: Average 1.2um, 1.5um, and 2.7um filter resistance operated in apartment condition

The results of average filter resistances of three different pore sizes run in apartment conditions were compared in Figure 35. As can be seen from this figure, the initial resistance of 2.7um is 48, which is the lowest among three filters. The initial resistance of 1.5um is 59, and the highest initial resistance is 95 from 1.2um filter. Moreover, the final resistance of 2.7um is 59, and the resistance growth rate is 23%. The final resistances of 1.5um and 1.2um are 71 and 118 respectively, which corresponding to 20% and 24% resistance growth rate.

Compared with the average filter resistance increasing in Lab condition (see Figure 28-30), the filter resistance growth rates in apartment state are higher than the counterpart ones in Lab condition. To explain this difference, a hypothesis is water in an apartment may contain more particles thus causing a more severe fouling issue during the same operation period(Liu, Lut, et al. 2013). This hypothesis will be discussed later from different aspects.

For better comparison of the different pore size filter resistances in various operation conditions, the result of different pore size filter resistances was shown separately in the following figures.

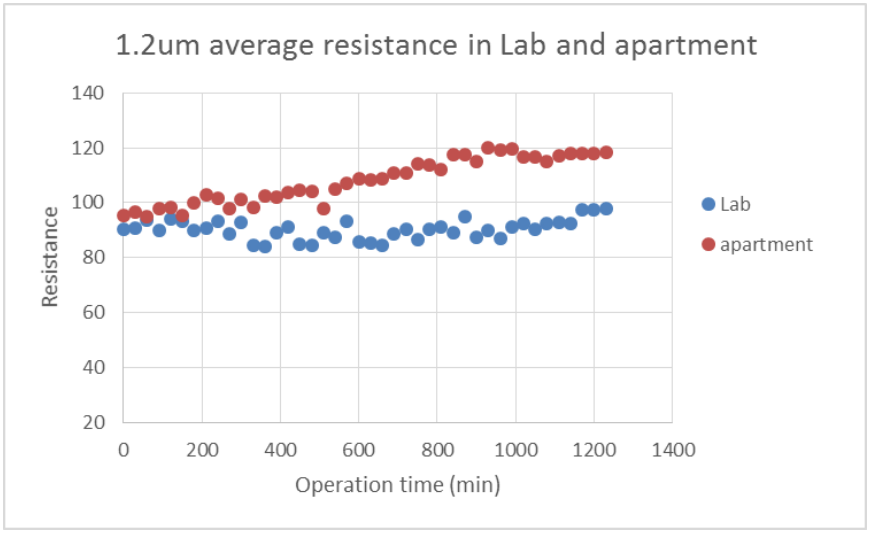

Figure 36: Average 1.2um filter resistance operated in Lab and apartment condition

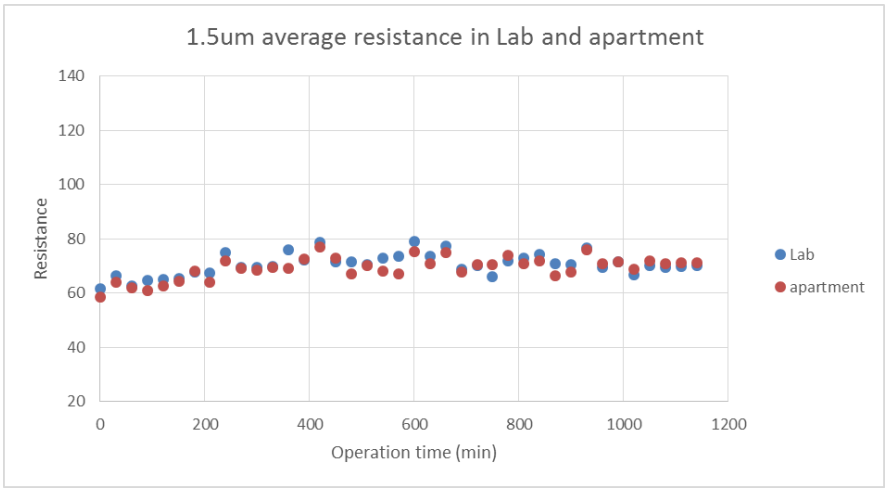

Figure 37: Average 1.5um filter resistance operated in Lab and apartment condition

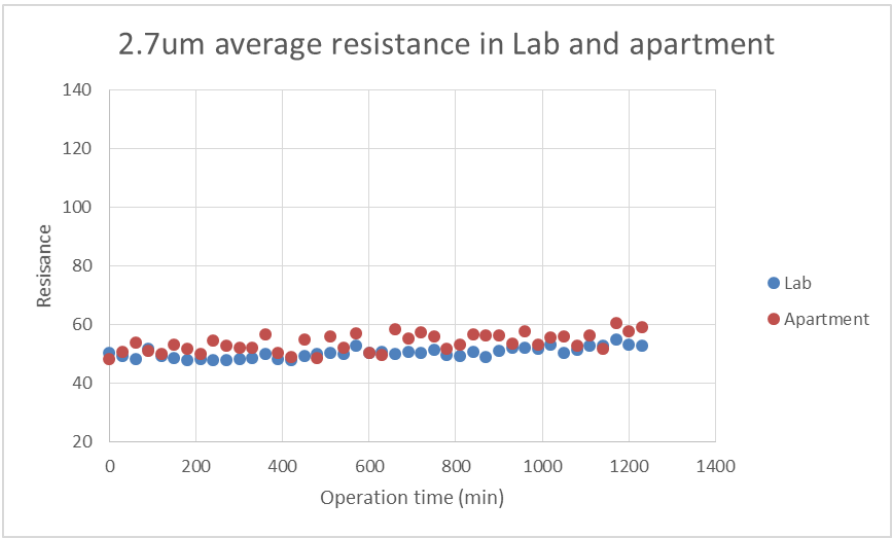

Figure 38: Average 2.7um filter resistance operated in Lab and apartment condition

Previous three figures show different pore size filter resistances increasing in various operation conditions separately. As shown in Figure 36, in 1.2um filter, there is a noticeable difference between two process conditions. The initial resistance of 1.2um in apartment state is 96, which is slightly higher than 90, the initial resistance in Lab condition. The resistance increasing slope in apartment state is steeper compared with Lab condition. Also, the final resistance of apartment condition remain stable at 120 and the final resistance in Lab condition is only 100.

There is no clear difference can be observed in 1.5um filter resistance under different operation conditions (see Figure 37). The initial resistances in Lab and apartment are almost the same, about 60. Furthermore, the resistance increasing trend of these two conditions are similar, and the final resistances are still almost the same, about 71.

Figure 38 shows the apparent difference in 2.7um filter resistance under two different operation conditions. Although the initial filter resistance were the almost the same, about 50, the resistance growth trend of apartment state is higher than the counterpart one of Lab condition thus the apartment final resistance is 60, which is 8 more than the final resistance of Lab condition.

In general, the comparisons between different operation conditions indicate that more particles are clogged in apartment state than Lab condition. The biggest difference appeared in 1.2um filter. A reasonable explanation is the 1.2um filter has the smallest pore size thus this filter is the most sensitive to particle concentration variation during the same operation period. Another possible explanation is that there are more particles in 1-2um range thus more particle clogging in 1.2um filter under apartment operation condition(Wang et al. 2007; Liu, Ling, et al. 2013).

4.2.1.2.1 Resistance results discussion

As can be seen from Figure 36 and Figure 37, the resistance growing rate of 1.5um filter is much lower compared with 1.2um filter. This result is unreasonable because the pore size difference between two filters is only 0.3um. Further discussion is needed to explain this unexpected result.

The possible explanation is the porosity difference between two filters. It is possible the porosity of the 1.5um filter is higher than the counterpart one of 1.2um. Therefore, for 1.2um filter, it is easier to have clogging issue thus the resistance growing rate will also be higher. Unfortunately, there is no porosity information for these two filters. However, another information about these two filters is shown in the following the table.

Table 4: filters data information

	1.2um	1.5um
Manufacturer	Whatman	Whatman
Grade	Grade GF/C	Grade 934-AH
Filtration speed	Medium to fast	Fast
Air flow rate	6.7s/100ml/in^2	3.7s/100ml/in^2
typical thickness	260um	435um
basis weight	53g/m^2	64g/m^2
material	Borosilicate glass	Borosilicate glass

As shown in Table 4, there are two distinct differences in two filters. The first is the theoretical filtration speed of 1.2um is from medium to fast while the counterpart one for 1.5um filter is fast. Meanwhile, to filtrate the same amount of air, the required time of 1.2um filter is almost twice as much as the 1.5um filter. Based on this information, we can assume the porosity of 1.5um filter is larger than 1.2um filter even though there is no direct porosity data.

4.2.1.3 High Digital Microscope

High-resolution digital microscope gives clear pictures of the filter details after filtration. By observing images from different pore size filters operated in various conditions, we can a have straight and clear comprehension of the filter fouling issues.

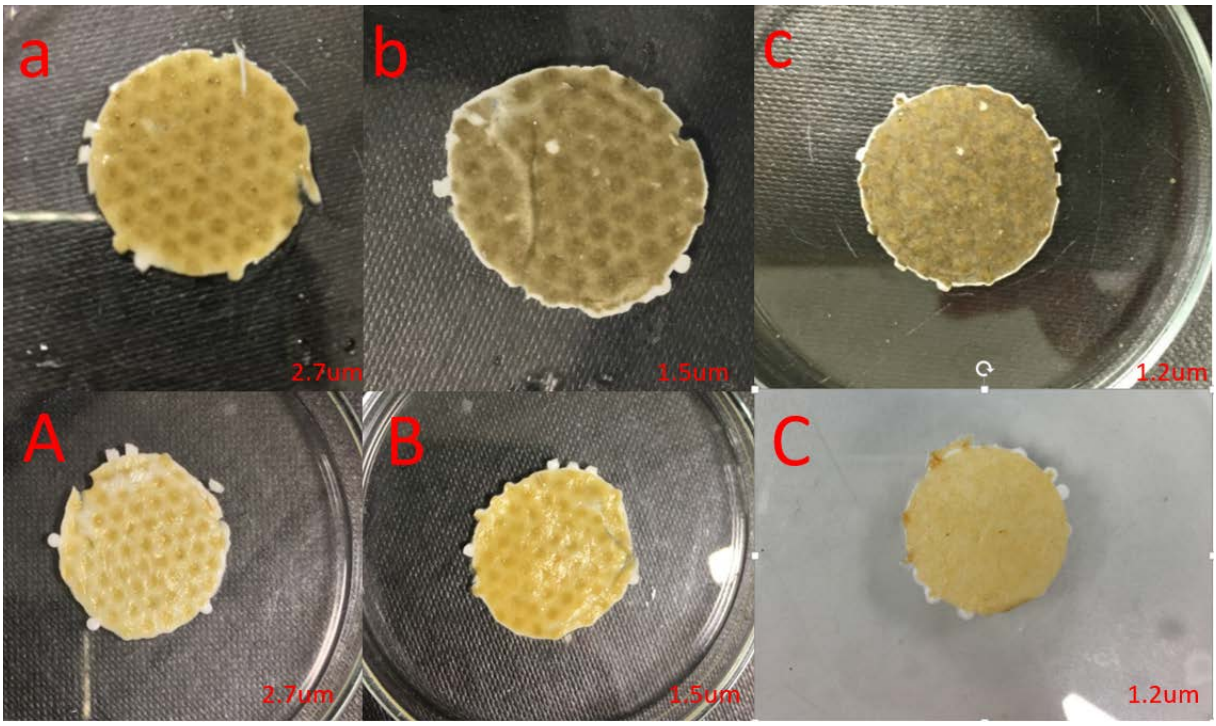

Figure 39: different pore size filters operated under different conditions a) 2.7um filter in apartment b) 1.5um filter in apartment c) 1.2um filter in apartment A) 2.7um filter in Lab B) 1.5um filter in Lab C) 1.2um filter in Lab

Figure 39 demonstrates pictures of different pore size filters operated under two separate conditions. These pictures were taken by phone camera. Two results can be obtained from these pictures. The first one is under the same operation condition, the smaller the pore size, the darker the filter would be (see a comparison between Figure 39 a,b,c, and A, B,C). It is logical to explain the filter color changes because smaller pore size means more particles would be retained in the filter and thus the filter becomes more "dirty." Another indication is that the filter color of apartment condition is black while counterpart one operated in Lab condition is yellow when the pore sizes are the same (see a comparison between Figure 39 a and A, b and B, c and C). A possible hypothesis is the apartment water composition is slightly different from the water in Lab. The Fe concentration in the apartment could be higher thus more Fe clogged on the filter and thus, the filter looks more black. Meanwhile, the humus concentration in Lab condition could be higher and thus more organic matters clogged on the filter which contributes to the yellow color of the filter. More results will be shown in the following ATP measuring and ICP-MS measuring sections to support this hypothesis.

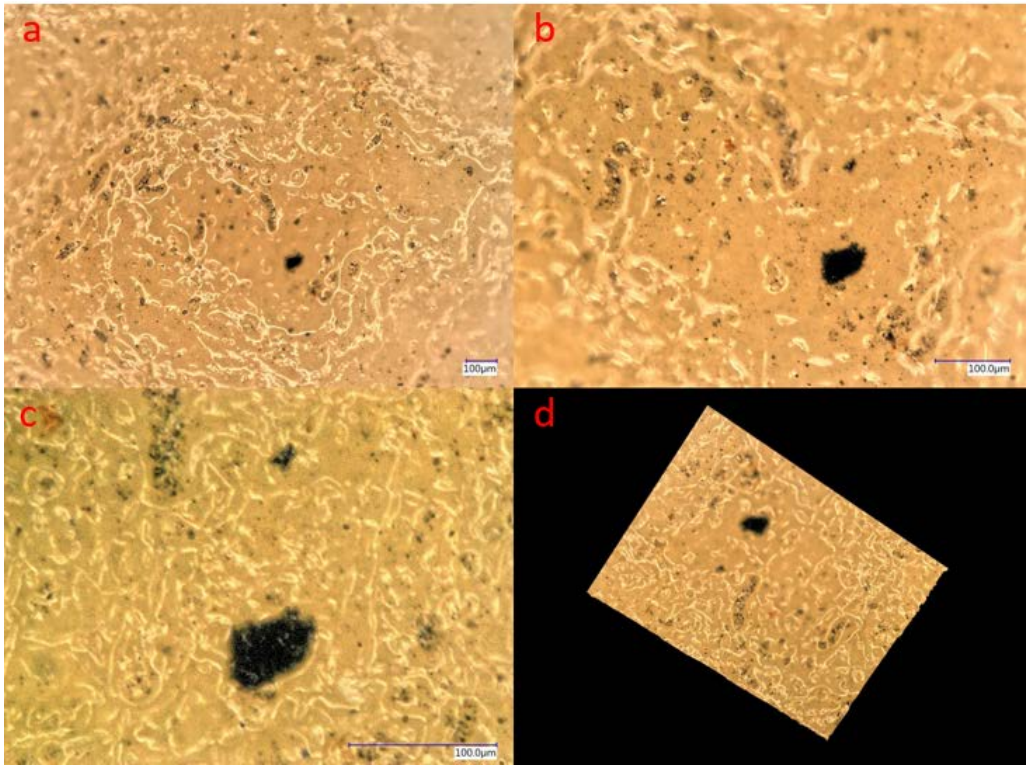

Figure 40: 1.2um filter operated under Lab condition a) 100X microscope b) 500X microscope c) 1000X microscope d) 3D filter picture

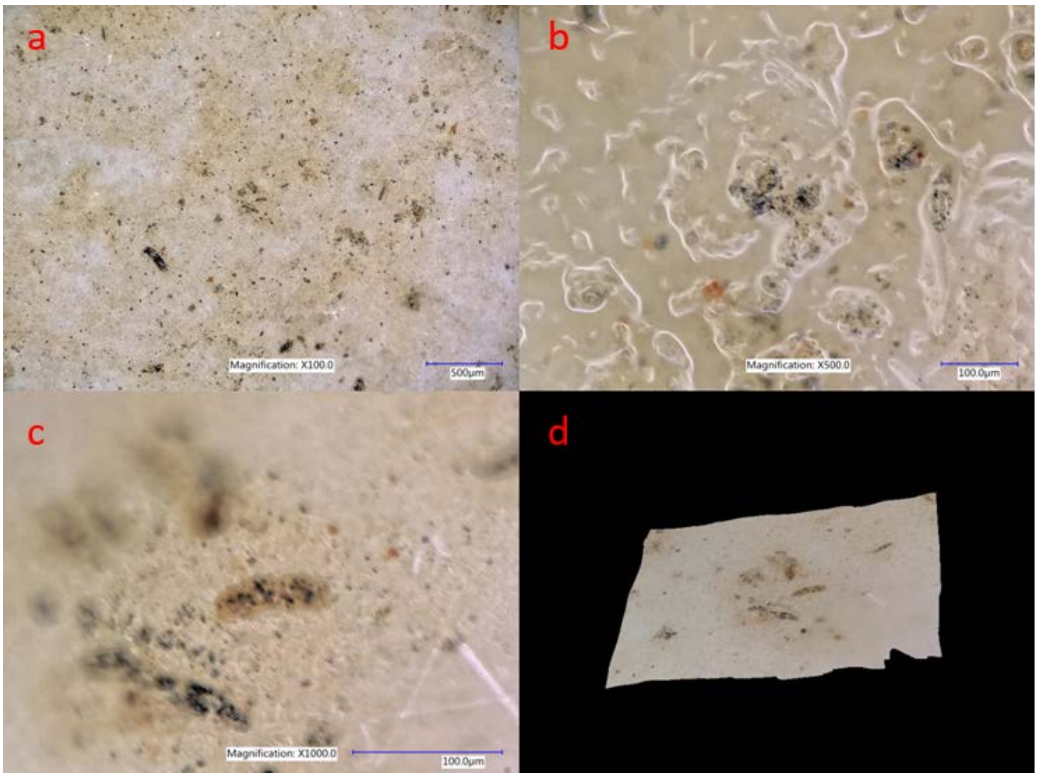

Figure 41: 1.5um filter operated under Lab condition a) 100X microscope b) 500X microscope c) 1000X microscope d) 3D filter picture

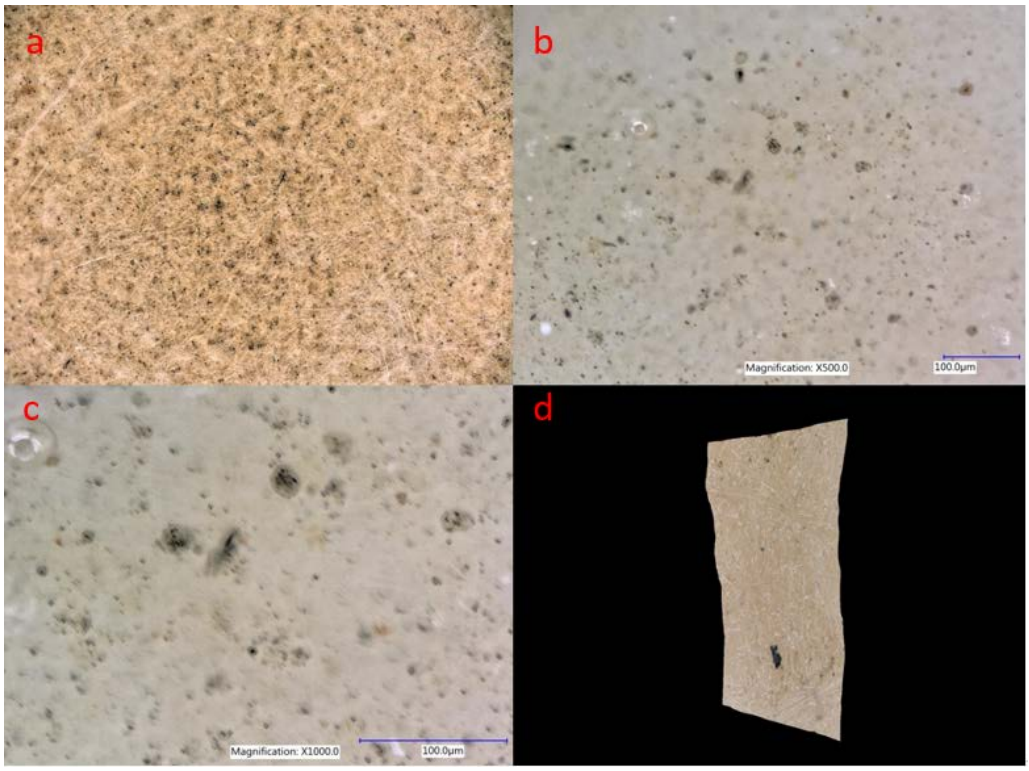

Figure 42: 2.7um filter operated under Lab condition a) 100X microscope b) 500X microscope c) 1000X microscope d) 3D filter picture

Previous three figures demonstrate high digital microscope pictures from three filters operated in Lab conditions. For each pore size filter, four images with100X, 500X, 1000X and a 3D filter image were shown. These four photos together can represent an overall physical condition of the filter after operation period.

As can be seen from these three figures, no clear difference could be obtained from different filters. The main reason is that there are too many particles clogged on filters, and thus it is tough to tell the difference by naked eyes. Furthermore, because of the resolution of this optical microscope is limited by light diffraction, pictures under high magnification are not very distinct, which also increases the identification difficulty.

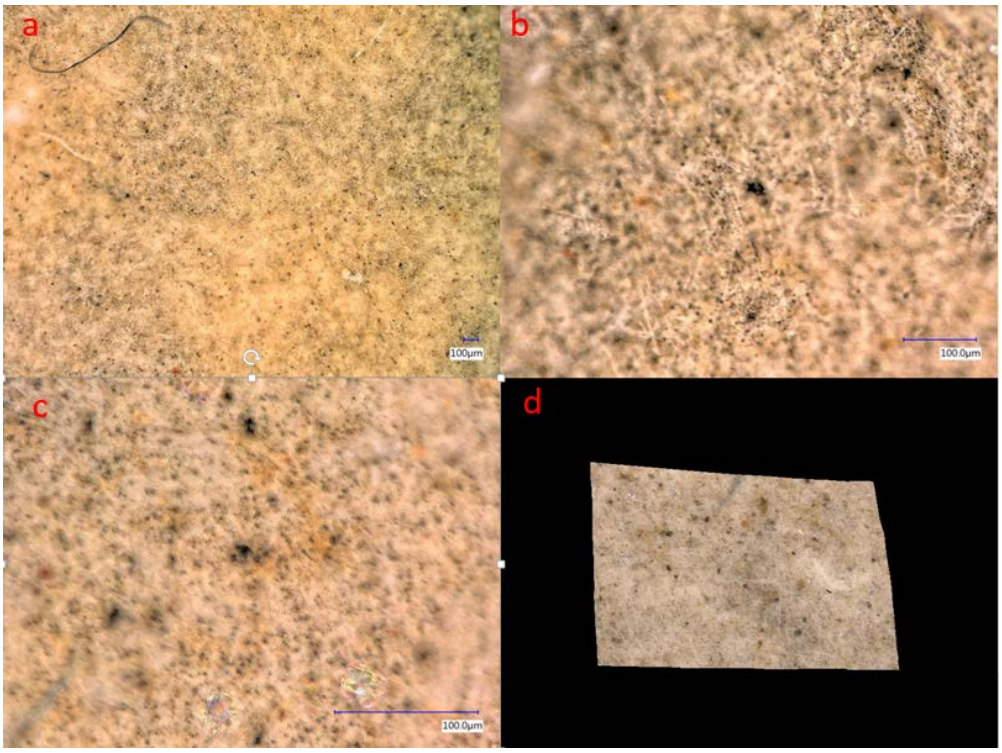

Figure 43: 1.2um filter operated under apartment condition a) 100X microscope b) 500X microscope c) 1000X microscope d) 3D filter picture

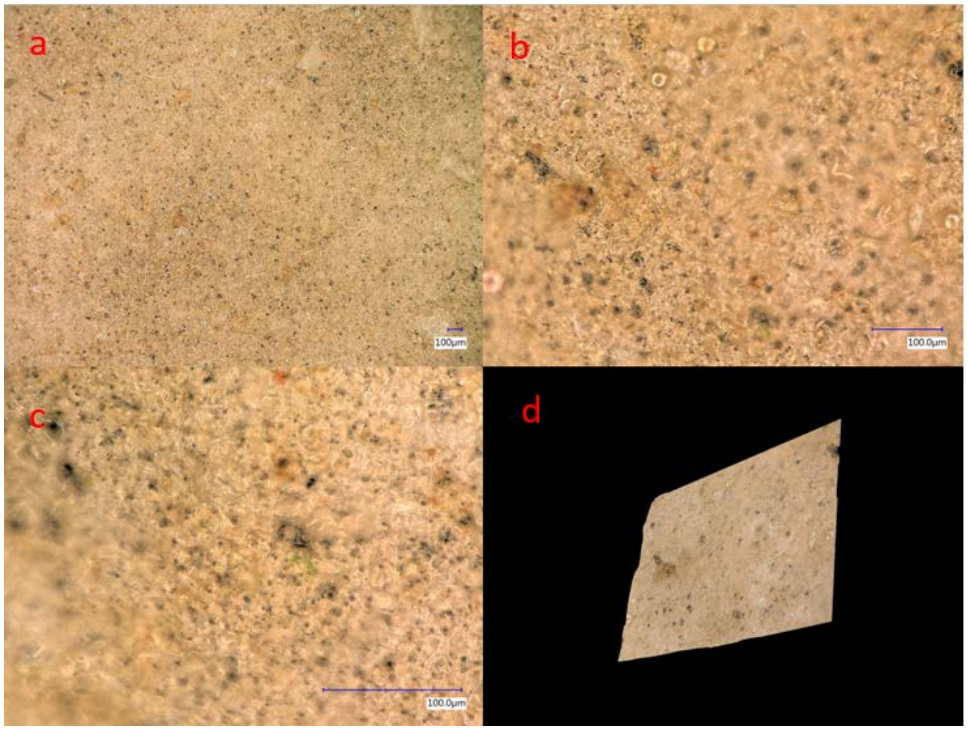

Figure 44: 1.5um filter operated under apartment condition a) 100X microscope b) 500X microscope c) 1000X microscope d) 3D filter picture

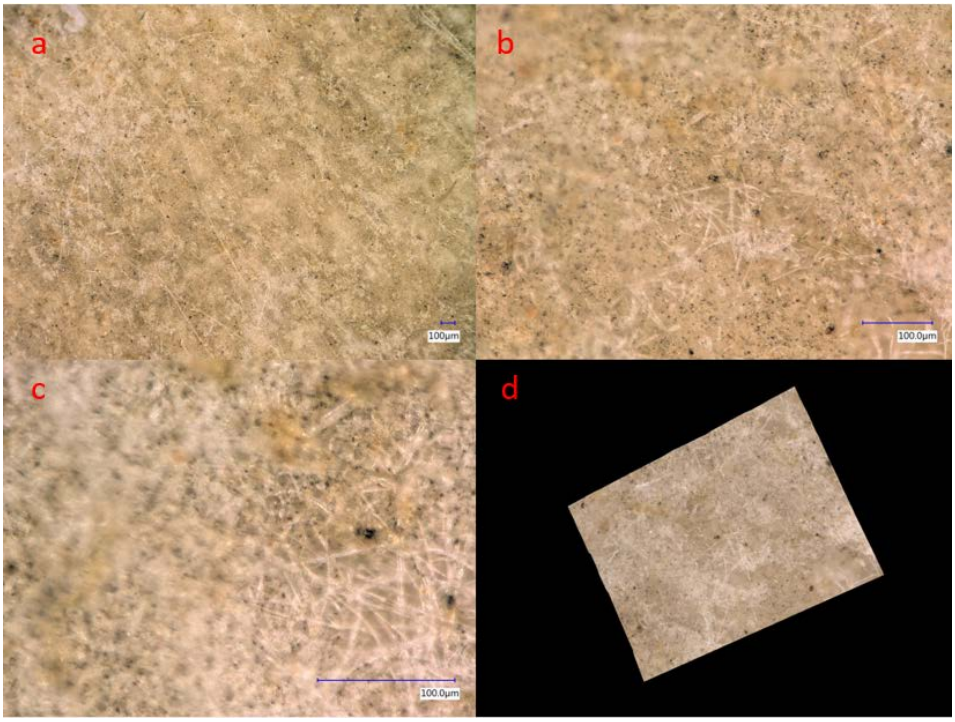

Figure 45: 2.7um filter operated under apartment condition a) 100X microscope b) 500X microscope c) 1000X microscope d) 3D filter picture

Previous three figures demonstrate microscope images from three pore size filters operated in apartment condition. Unlike filters performed in Lab condition, the filter differences in apartment state are evident. Particles retained on the 1.2um filter are the most while the 2.7um filter has least clogged particles.

Also, by comparing same filters operated in different operation conditions, it is a clear distinction about particle clogging situations (see Figure 40 and Figure 43, Figure 41 and Figure 44, Figure 42, and Figure 45). There are bigger black dots in apartment pictures compared with Lab condition, which means more particles clogged in apartment situation. This result matches the previous indication in Section 4.2.1.2.

Even though the picture difference between different operation conditions is evident and can be distinguished by naked eyes, for better and more reliable analyzing, particle counting would be used to calculate the amount and dimension of particles(Liu, Ling, et al. 2013).

4.2.1.4 Particle counting

Particle counting is used to determine particle size and number. The number and size distribution of particle indicate the filter fouling issues. In this research, two particle counting methods were adopted, microscope particle counting measurement and particle counter. The first one is to use the particle analysis function of the microscope. Theory of this analysis is to use the color difference of microscope pictures to determine the size and number of particles (see Figure 46). The advantage of this method is microscope can give direct and visible images to present filter fouling. The disadvantage of microscope particle counting is the result may not be so reliable because the resolution of this optical microscope is 1um thus no particle smaller than 1um could be observed(Gibson et al. 2001). Furthermore, sometimes particles may accumulate together, and the microscope may consider these collected particles as a massive particle, which will also cause the inaccuracy of microscope particle counting.

To mitigate the drawback of microscope particle counting, particle counter was used at the same time. Particle counter is to measure the suspension from the ultrasonic water bath. The result of particle counter has the particle size range from 0.4um to 4mm and the result is more accurate compared with microscope particle counting.

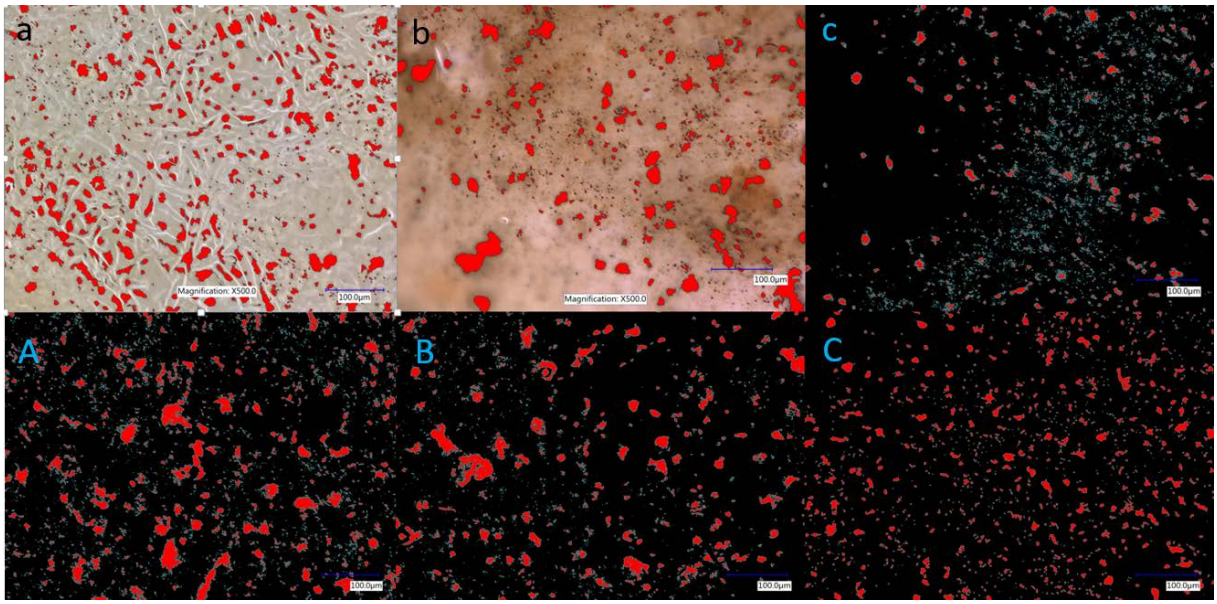

Figure 46: particle counting by microscope for different pore size filters a) 1.2um in Lab b) 1.5um in Lab c) 2.7um in Lab A) 1.2um in apartment B) 1.5um in apartment C) 2.7um in apartment

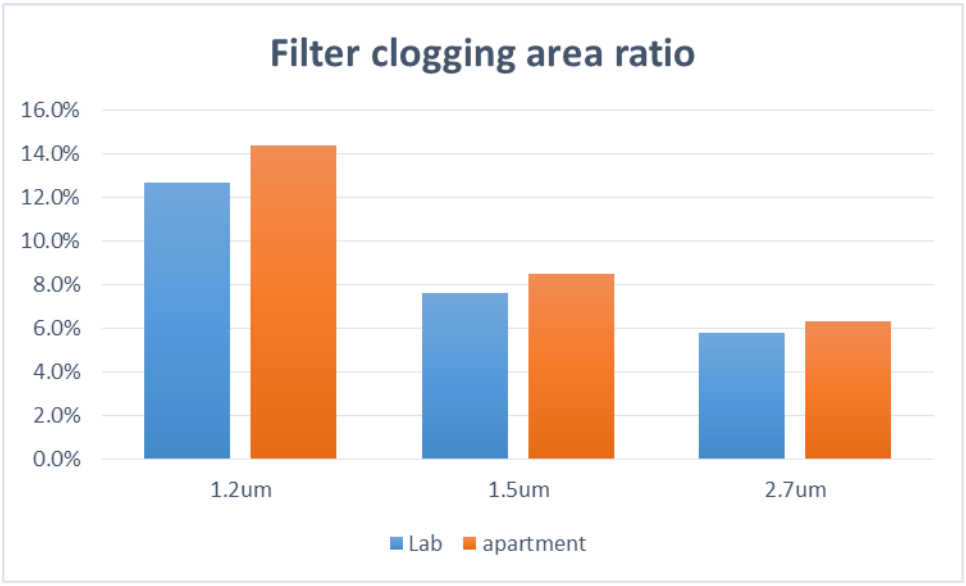

Figure 47: filters clogging area ratio for different pore size filter operated under Lab and apartment condition

Figure 46 and Figure 47 present the microscope particle counting pictures for different pore sizes operated under Lab and apartment conditions. The result here is the same as previous researchers(Siddiqui et al. 2016; Bucs et al. 2014). As shown these two figures, in the same operation condition, smaller pore size filter retains more particles and thus filter clogging area ratio are larger than filters with bigger pore size. Meanwhile, same pore size filters operated in apartment condition intercepted more particles and had larger clogging ratio comparing with the one operated in Lab conditions.

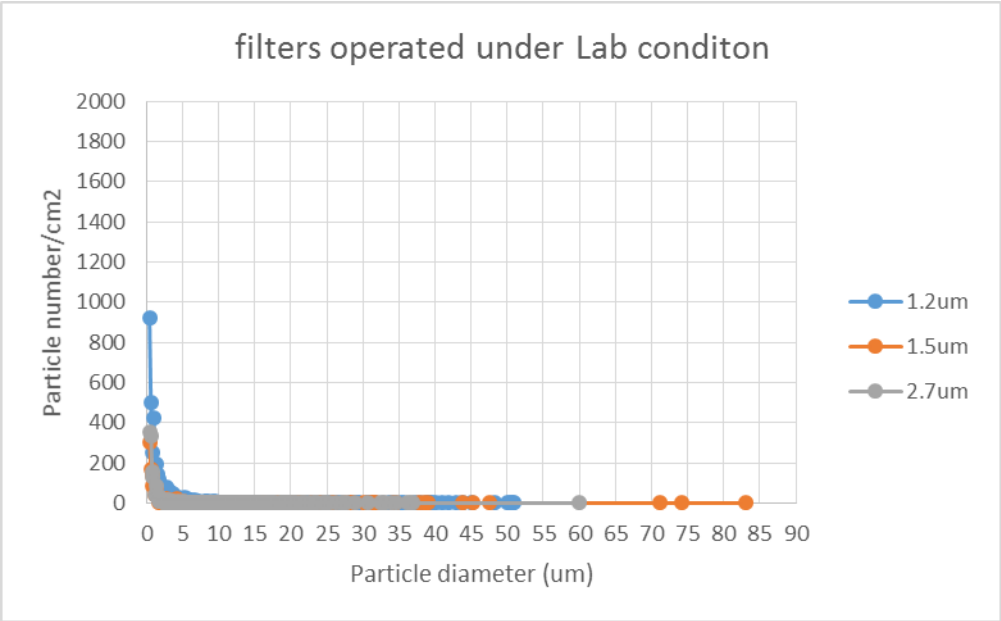

Figure 48: particle counting by microscope for filters operated under Lab condition

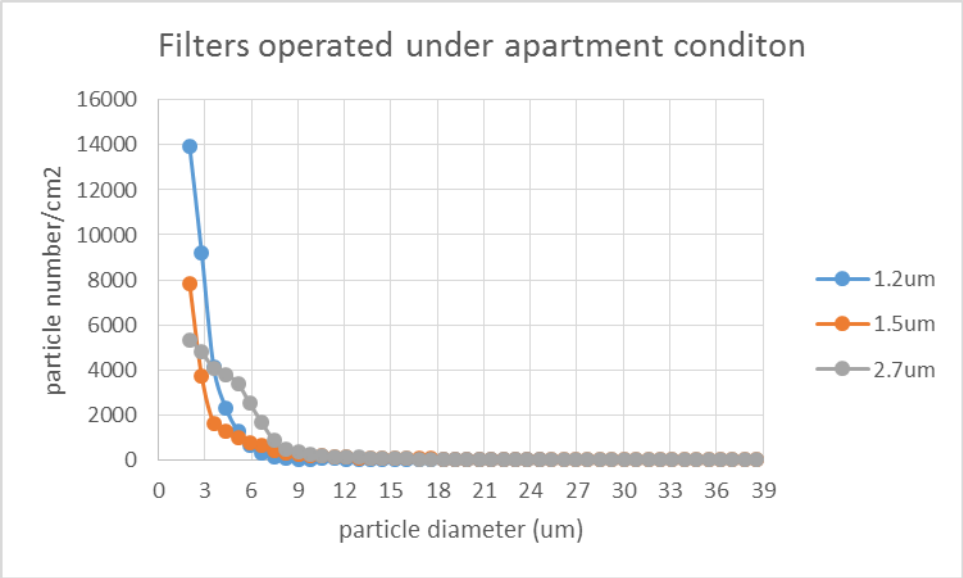

Figure 49: particle counting by microscope for filters operated under apartment condition

Previous two figures present the relationships between particle size and particle number for different pore size filters operated under different conditions. Results of these two figures are from the microscope particle measurement. It can be seen that most of the particle blocking on filters range from 0 to 5um. This result is logical because most particles in drinking water are below 5um(Vrouwenvelder et al. 1998).

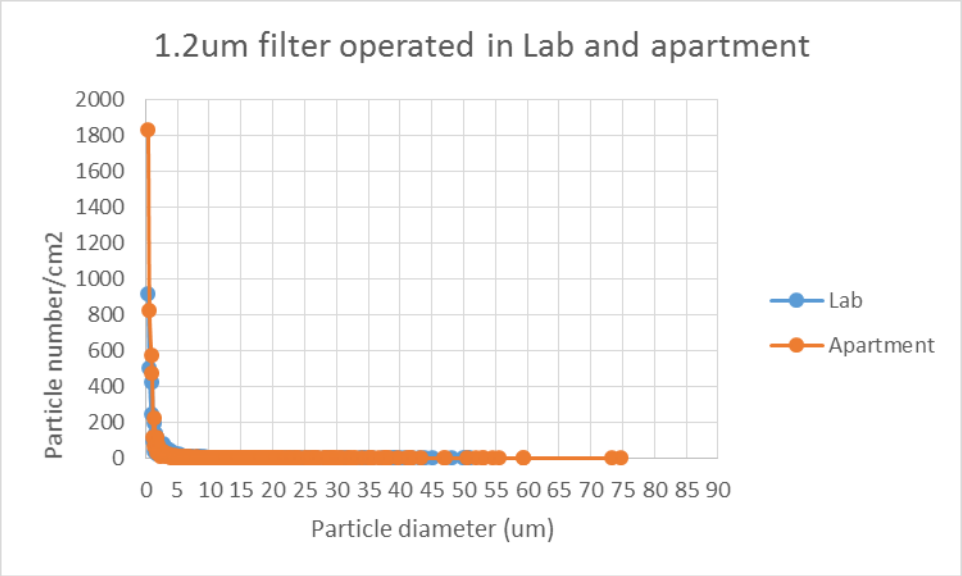

Figure 50: Particle counting by microscope for 1.2um filter operated in different condition

The 1.2um filter was selected as an example for comparing the fouling issues in different operation situations. 1.2um filter particle counting in different operation situations was shown in Figure 50. Most of the particles are accumulated from 0 o 5um and the detail particle distribution data was shown in Appendix 1. We observed the maximum particle number in apartment condition is about 1800, almost twice as many as the maximum particle number in Lab condition. This result also supports the conclusion that more particles were clogging under apartment condition because of the water quality difference.

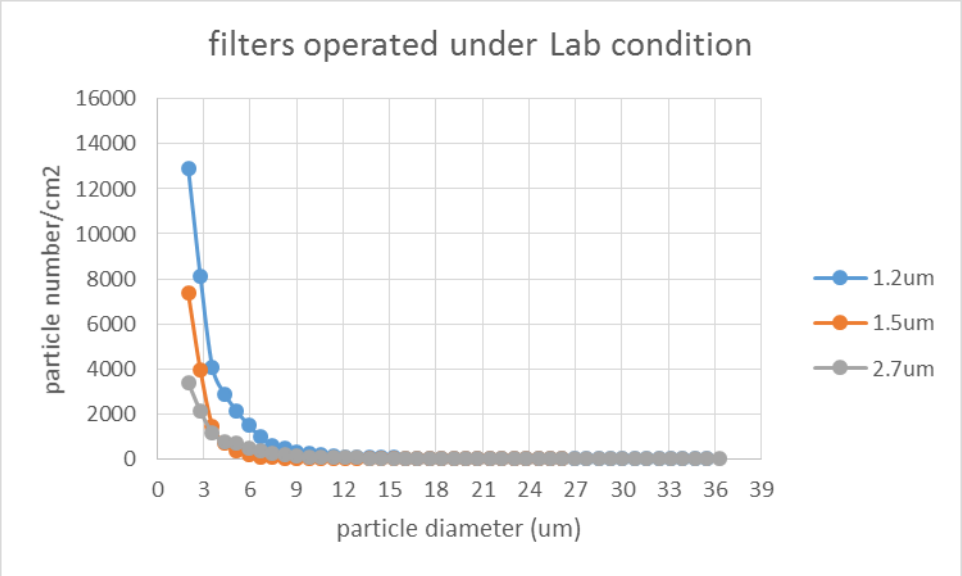

Figure 51: particle counting by particle counter for filters operated under Lab condition

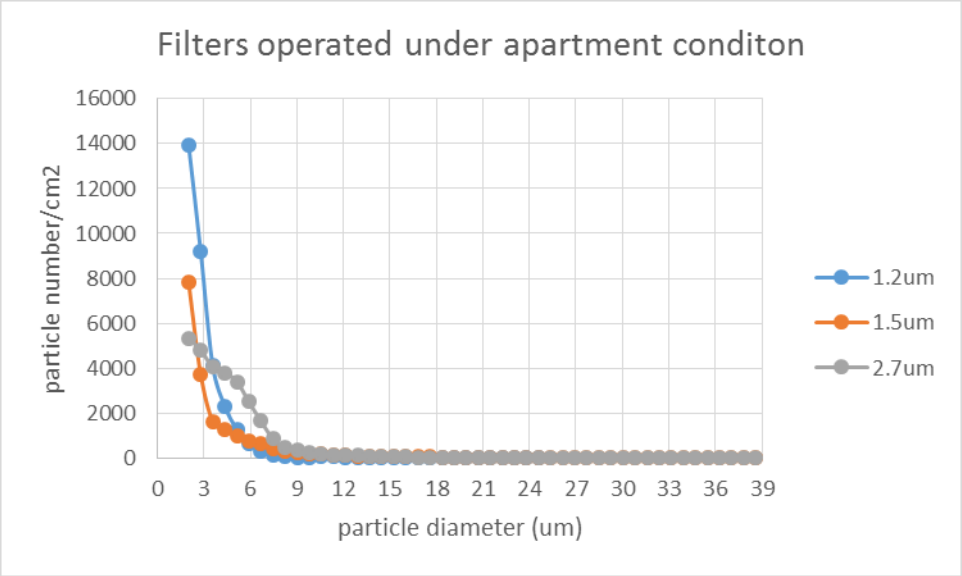

Figure 52: particle counting by particle counter for filters operated under apartment condition

Figure 51 and Figure 52 present the results from particle counter. 10mL suspensions from ultrasonic trembling were used for this analysis. Results show most of the particle sizes range from 0 to 6um. Meanwhile, this result is almost the same as the microscope result.

By comparing the results between microscope particle counting and a particle counter, it is easy to notice that the particle number measured by particle counter is much higher than the microscope one (see Figure 48-52). The possible explanations are as follows. On one hand, the particle detecting range for this particle counter is from 0.4um to 4mm while the theatrical minimum detecting size for the microscope is 1um(Hell & Wichman 1994). Thus, numerous of particles smaller than 1um could not be measured by microscope and this contributes to the particle number underestimated. On the other hand, as mentioned in the previous discussion, there are some particles accumulated together on filters, and thus, the microscope would consider the collected particles as a single large particle(Gibson et al. 2001). In this case, the particle number would decrease while the particle size would increase. As shown in previous figures, the maximum particle size in microscope measuring is 85um while the maximum particle diameter in particle counter measuring is the only 39um, which also supports the explanation.

Even though the results from two particle counting methods have some differences, both results support the previous hypothesis and indicate the Smart Water Meter can act as a suitable method to monitor water quality.

4.2.2 Biological part

4.2.2.1 Introduction

The biological component analysis in this research is to present biofouling issue. ATP concentration is the primary parameter to indicate the biofouling for the filtrated clogging potential(Hammes et al. 2010). ATP measuring is divided into two parts, one is the total amount of ATP on filters, and the other is the ATP/influent, which represent how much ATP was retained with 1-liter feedwater.

4.2.2.2 ATP measuring

ATP measuring in this research has a variation between 15% to 25%(Oulahal-Lagsir et al. 2000; Hammes et al. 2010). To make results are reliable and reproducible, four parallel experiments were taken for each condition. The results are shown in following two figures.

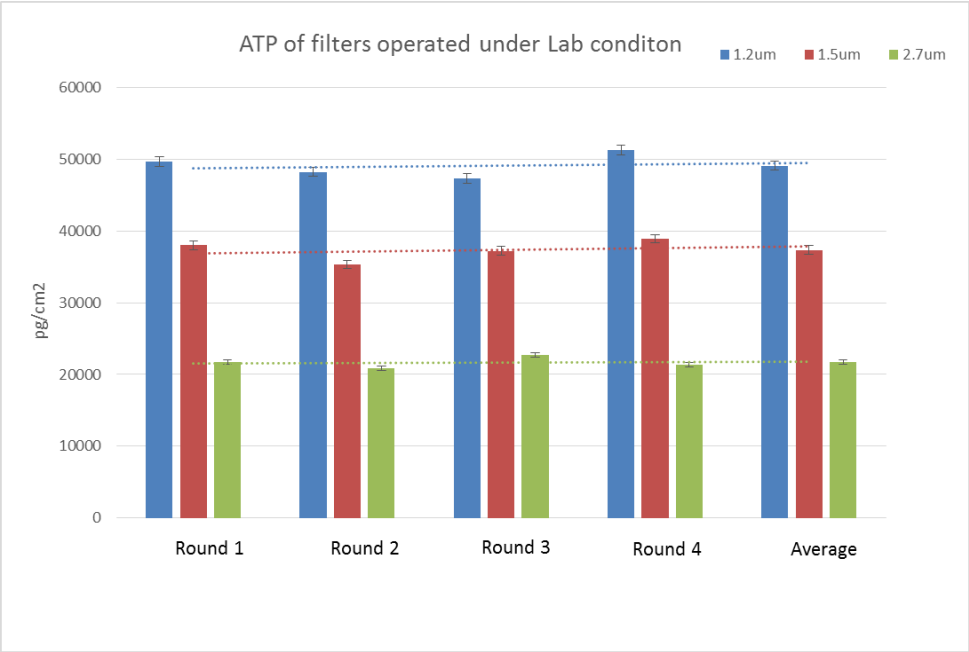

Figure 53: ATP measuring for filters operated under Lab condition

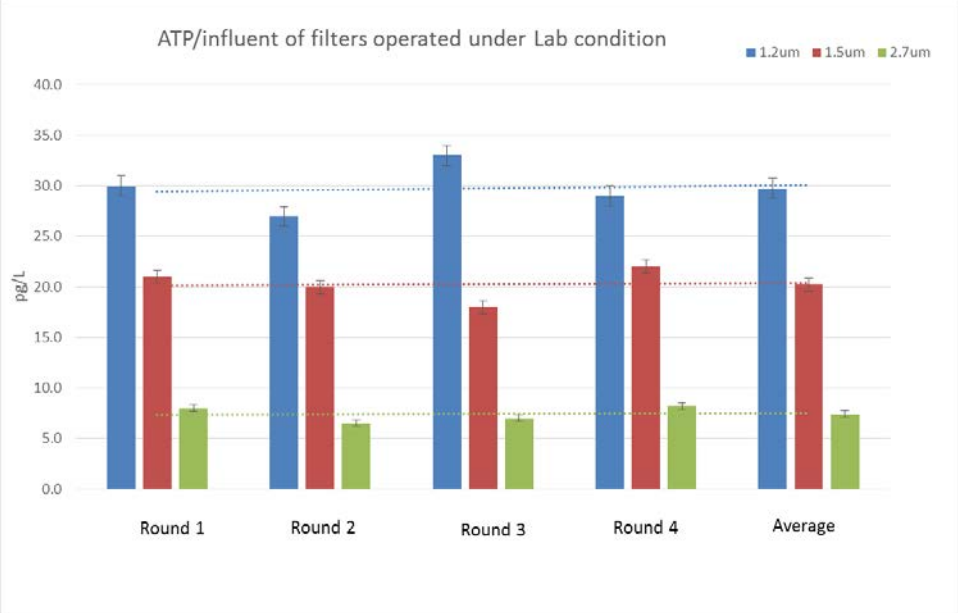

Figure 54: ATP/influent measuring for filters operated under Lab condition

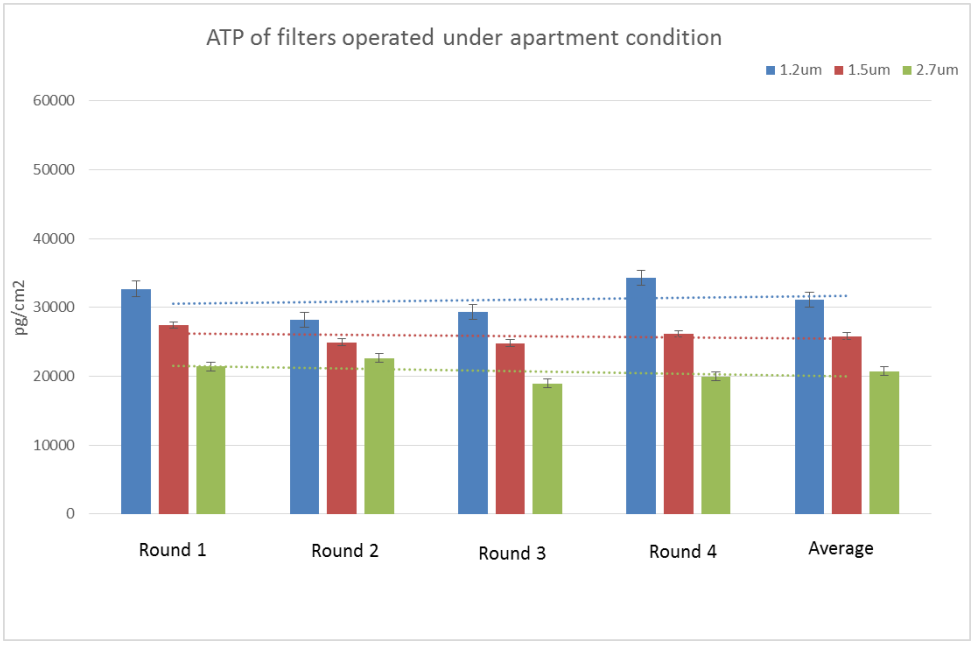

Figure 55: ATP measuring for filters operated under apartment condition

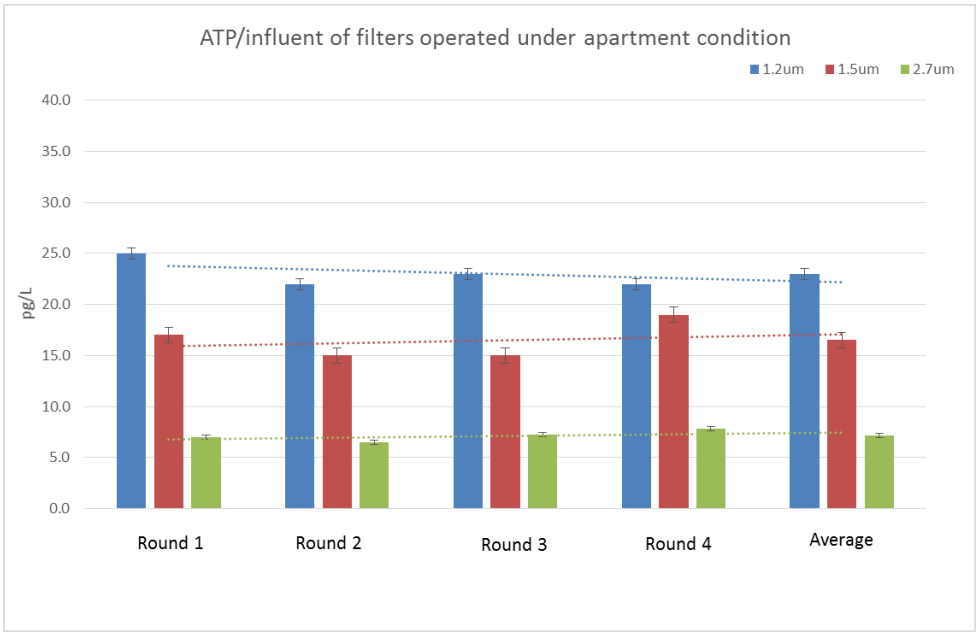

Figure 56: ATP/influent measuring for filters operated under apartment condition

Previous four figures illustrate ATP measurement for filters operated in different conditions. Filters with smaller pore size can retain more ATP both in total ATP and ATP/influent.

Furthermore, fortunately, the coefficient of variation (CV) for total ATP on the filter is only 4% while the CV for ATP/influent is slightly higher, 9% (See Appendix 2). This range of variation is acceptable and does not influence the analysis(Oulahal-Lagsir et al. 2000).

Comparison between filters operated under Lab and apartment conditions will be discussed as follows.

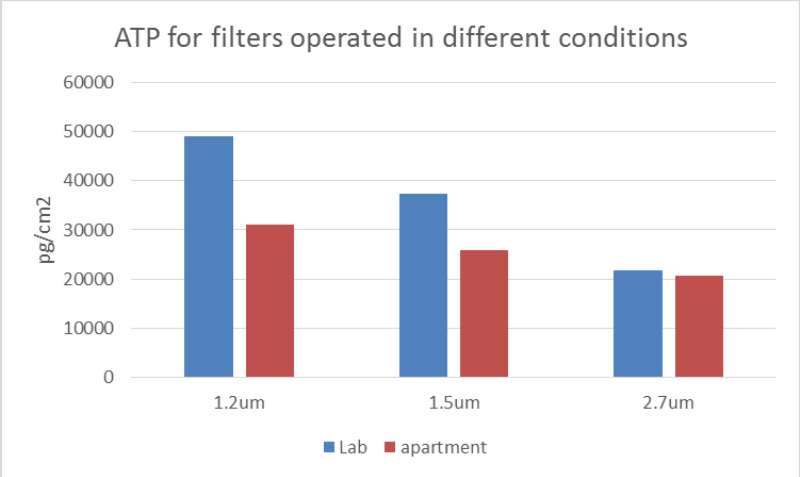

Figure 57: Average ATP for filters operated in Lab and apartment conditions

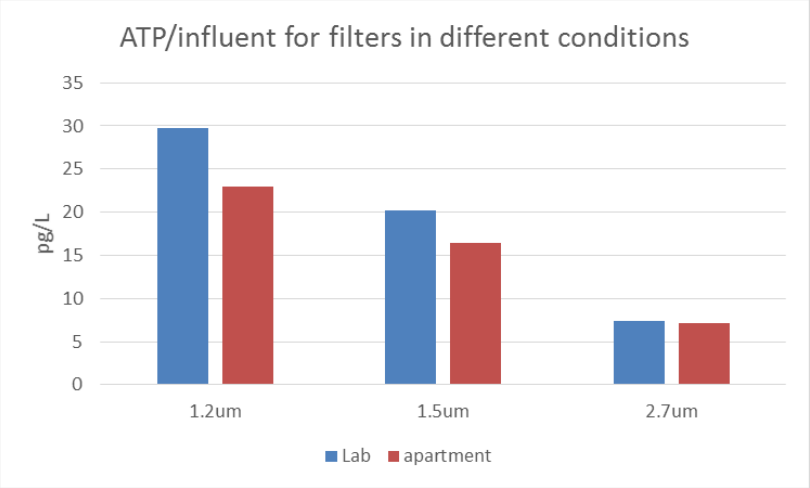

Figure 58: Average ATP/influent for filters operated in Lab and apartment conditions

Comparison between two operation conditions was presented in Figure 57 and Figure 58. Unlike previous results, all ATP concentrations in Lab condition are higher than the counterpart ones in apartment state. This result indicates there are more biofilms clogged in Lab condition. This result supports the Figure 39, in which filters from Lab condition appeared to be yellow (more microorganism attached) compared with the counterparts from apartment condition.

4.2.3 Chemical part

4.2.3.1 Introduction

The aim of chemical analysis in this research is to figure out the inorganic matters clogged on filters. Based on the constitution of drinking water, the expected inorganic elements are iron and calcium. However, since the size of Fe and Ca ions are much smaller than the filter pore size (see Figure 59), the expected Fe and Ca retaining rate is very limited.

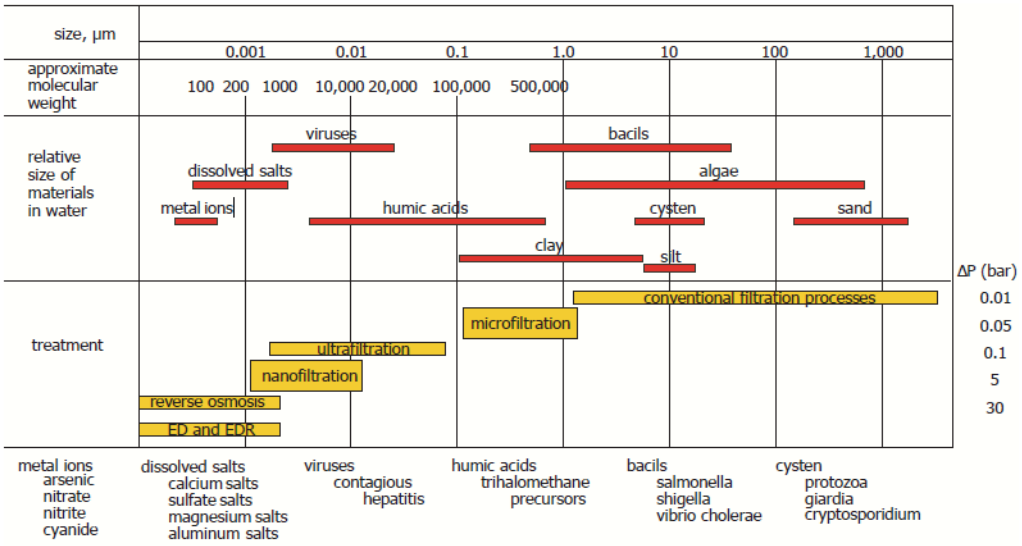

Figure 59: Overview of different filtration processes and sizes of compounds removed (Treatment n.d.)

4.2.3.2 ICP-MS

Inductively coupled plasma mass spectrometry (ICP-MS) is a type mass spectrometry to detect metals at low concentration. Comparing with other inorganic element detecting method, ICP-MS has greater speed, precision, and sensitivity. The results of ICP-MS are shown as follows.

Table 5 demonstrate Fe and Ca concentration of drinking water in two conditions. Fe concentration for both situations are lower than the detection line (less than 0.1mg/L) and the Ca concentration for two conditions are almost the same, about 1mmol/L.

Table 5: ion concentrations of feed water

ion / Location	[Fe]	[Ca]
	mg/L	mg/L
Apartment	<0.1	36.7
Lab	<0.1	35.5

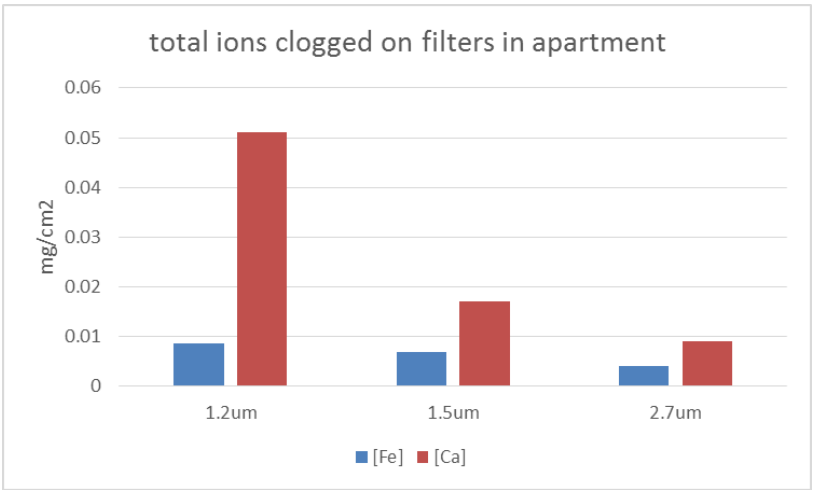

Figure 60: total ions clogged on filters operated under apartment condition

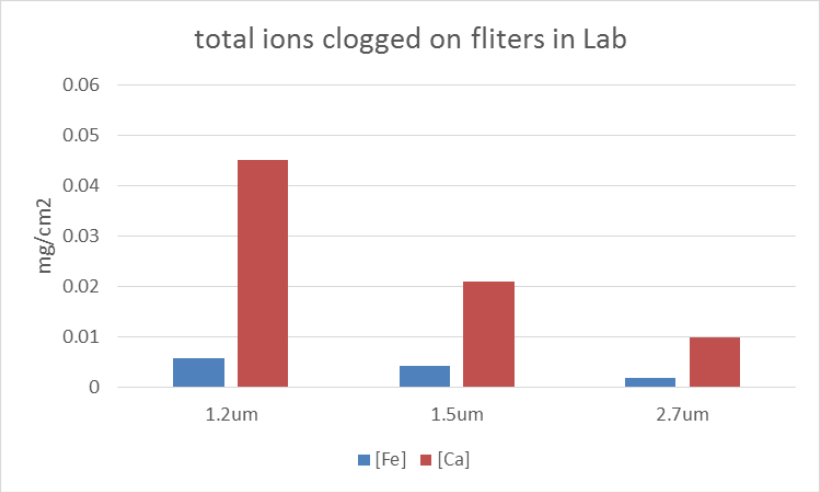

Figure 61: total ions clogged on filters operated under Lab condition

Previous two figures illustrate total clogged ions on filters under two conditions (data are shown in Appendix 3). The whole clogged chemical matters on filters are very low when taking 20 hours operation period into consideration. The main reason is the filter pore size are much larger than ions dimension thus most of the ions will go through filters smoothly. Based on the above two figures, total clogged calcium are almost the same for same filters operated in different situations. The main reason is that the Ca influent concentration is the same in two conditions (see Table 5). However, for Fe, the distinction among various filters operated in different operation situations is noticeable. The total clogged Fe in apartment condition is higher than the counterpart in Lab condition, which shows more Fe clogged in apartment situation. This finding supports the result from Figure 39, in which the filters from apartment situations look darker than filters operated in Lab conditions.

Based on the previous finding, we can assume Fe concentration from apartment inflow is higher than influent from Lab even though there is no direct supporting data.

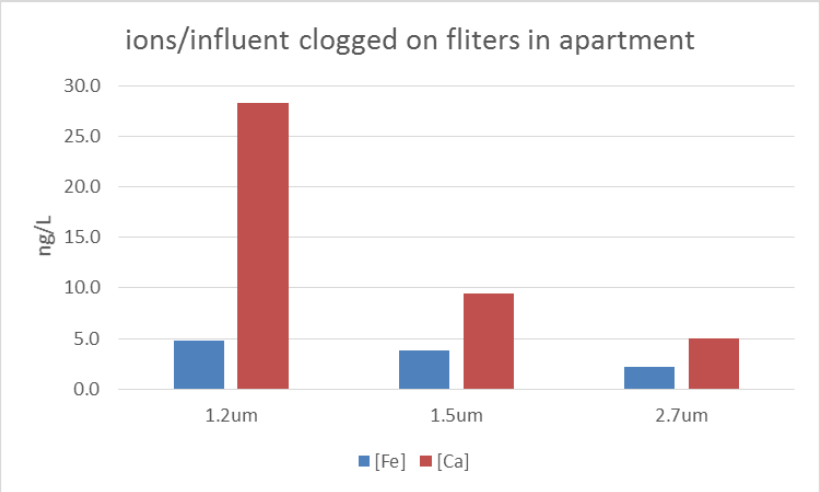

Figure 62: clogged ions/ influent concentration for filters operated under apartment condition

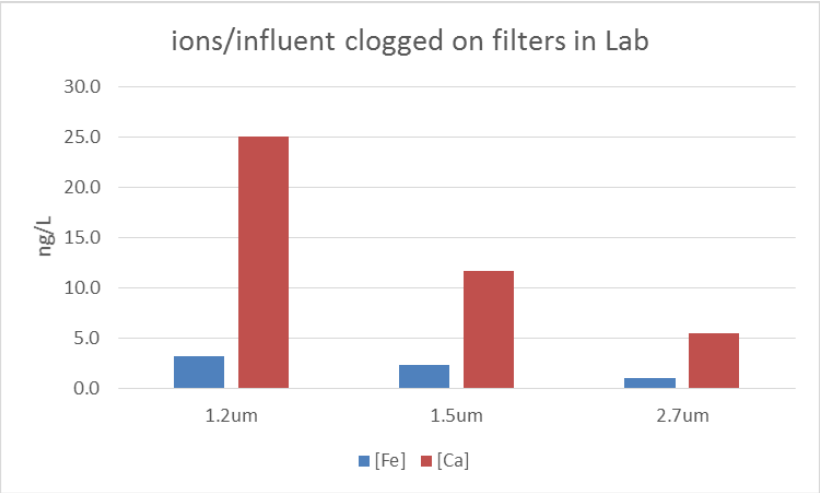

Figure 63: clogged ions/ influent concentration for filters operated under Lab condition

It can be seen that some ions clogged on filters for 1-liter influent. As shown in figures, the maximum clogging value (28.3ng/L) is calcium for 1.2um filter operated in apartment condition. The calcium removal rate for this filter is very low (less than 1 of million). The Fe removal rate cannot be calculated because the initial Fe influent concentration is unknown.

In general, chemical clogging matters are much less than physical and biological clogging because of the small ion size(M. Oldani A. Miquel and G.J. Schock, 1992). A possible result obtained from the chemical analysis is Fe concentration from different taps may vary due to the differences in the distribution network and water retention time. For instance, the Fe concentration of apartment drinking water is higher than the drinking water from Lab.

4.3 CCP result and discussion

4.3.1 Physical part

4.3.1.1 Introduction

The physical analysis in CCP is almost the same as FCP part, which including pressure drop measuring, high-resolution digital microscope observation and particle counting. Pressure drop measuring is the most important part for result analysis because it directly shows the relationship between pressure drop increasing along with the operation time and thus gives a visible evidence for fouling issues. Meanwhile, high-resolution digital microscope observation provides clear pictures for PVC and feed spacer after the operation. Furthermore, particle counter can measure the particle number and size for PVC and feed spacer and based on this data we can know more about fouling issues.

4.3.1.2 Pressure drop increasing

Pressure drop increasing was used to represent the fouling issue in CCP analysis. Because like the FCP experiment, the inflow is directly from the Lab tap water thus the pressure and flux are both inconstant. Therefore, each time to measure the pressure drop increase, the influent will be adjusted to 60L/h manually by calibrating the tap valve. Meanwhile, as described in Section 2.2.3, the more reliable result will be obtained by measuring the CCP in constant influent filtration. Since the flux is constant during the pressure drop measuring period, thus this pressure drop increasing can represent fouling issues during the operation period. Pressure drop increasing curve is shown in the following the figure.

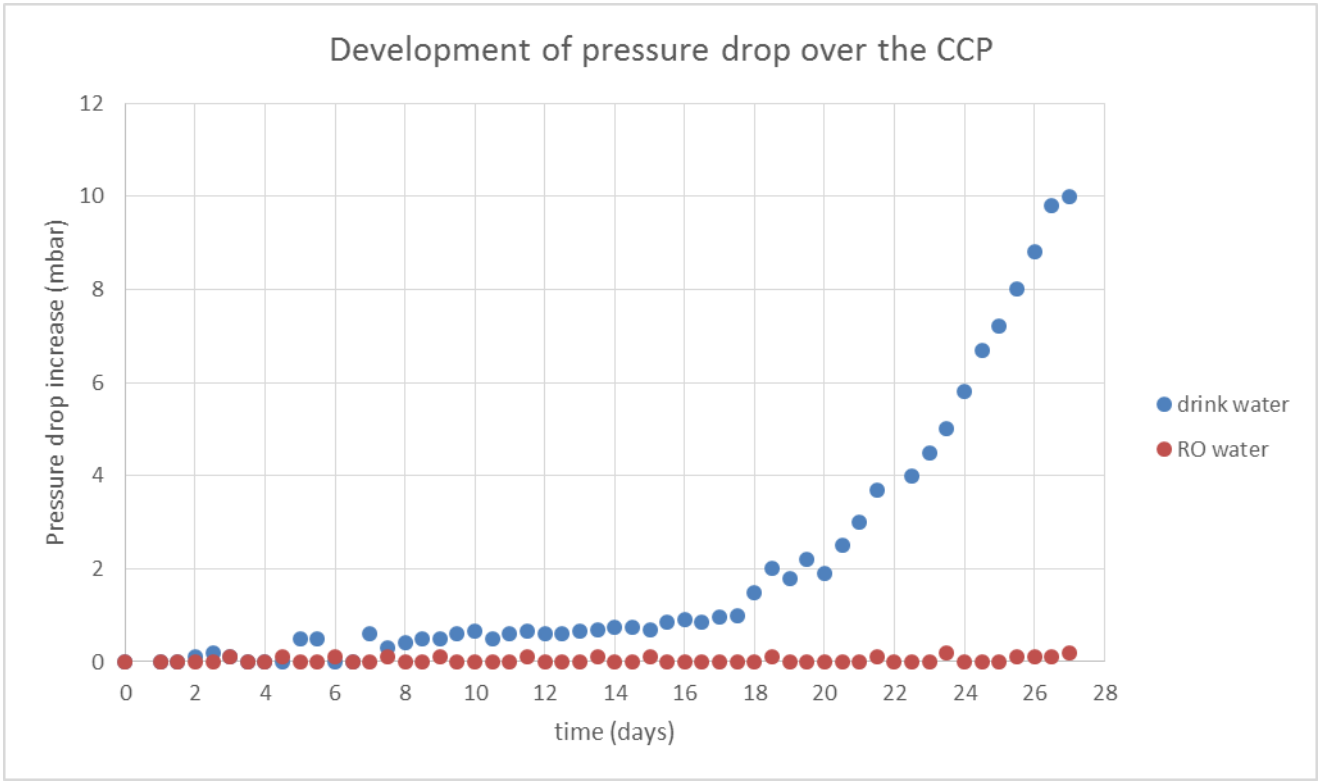

Figure 64: Development of pressure drop over the CCP (data from RO water part is from Vrouwenvelder (Vrouwenvelder et al. 2009)*)*

Results of two different feed water, drinking water and RO water, were shown in the previous figure. Drinking water graph is the result of the Lab experiment. RO water relatively data is from Vrouwenvelder (Vrouwenvelder et al. 2009; Dreszer et al. 2014). No experiment with RO water was done in this research because there is no constant RO water supplied in Lab.

When the feedwater was drinking water, there was no apparent pressure drop increasing for the first seven days. Noticeable pressure drop was growing started from the 8th day. The pressure drop increased exponentially from 18th day and reached the maximum approximately 10mbar on the 28th day. The experiment was stopped on the 28th day because the maximum pressure drop increasing measuring limit for CCP monitor is 10mbar thus no more pressure drop increasing could be measured after the 28th day. However, when changing the feedwater into RO water, which contains 0mg/l organic matters, there was no visible pressure drop increase for the whole operation period.

Result differences between two feedwater are colossal, and this difference is logical and expected. Since RO water is pure water, there is no matter will be retained and microorganism growth during the operation period thus there is no pressure drop increase. For drinking water, the pressure drop increasing is contributed by particle clogging and biofilm growth. This result is also obtained by previous researchers(Oulahal-Lagsir et al. 2000).

Since the initial idea and part of the equipment of CCP are from Membrane fouling Simulator (MFS), it is logical to compare the results of two experiments. Based on the results from J.S. Vrouwenvelder(Vrouwenvelder et al. 2007) and CCP, the pressure drop increasing growing trends are almost the same, which indicating the accuracy and reliable of CCP result. However, there is still a clear difference between two results, when the feedwater for two experiments is both tap water, in MFS result, no visible growing for the first 15 operation days while the apparent growing for CCP begins from the 8th day. Possible explanation for this difference is the feed water flow of MFS is 16L/h while in CCP, the influent is 60L/h. Higher influent indicate more particle and clogging may occur in CCP experiment for the same operation period. Also, the feed water for MFS was drinking water which pretreated with cartridge filters to remove all the suspended solids(Brauns et al. 2002). However, in CCP experiment drinking water from Lab was directly used as feedwater and these Suspended solids in feed water will be accurate the fouling process in CCP research. In general, above two different factors in two experiments may cause the final result difference.

4.3.1.3 High digital microscope

High-resolution digital microscope gives clear pictures of the feed spacer. By comparing the feed spacer differences before and after the operation, we can clear see the obvious fouling issues.

Feed spacer used in this experiment is the standard feed spacer for membrane fouling simulation (see Figure 65). After 18 days operation, the visuals of feed spacer are shown in Figure 66 and Figure 67. As shown in these two figures, biofilms are attached on spacers and these biofilms contribute to the pressure drop increasing.

If we compare the microscope pictures between FCP and CCP, we can notice that the amount of particles retained in FCP is much larger than the counterpart one in CCP. It is logical because in FCP experiment, inflow will filtrate the filter and all the particles smaller than the pore sizes will be retained. However, while in CCP, inflow passes through two PVC slides by crossflow thus most of the particles and biofilm will leave the equipment together with outflow, and the retained particulate matter and biofilms would be much less. This filtration method difference also contributes the much longer expected operation period of CCP compared with FCP.

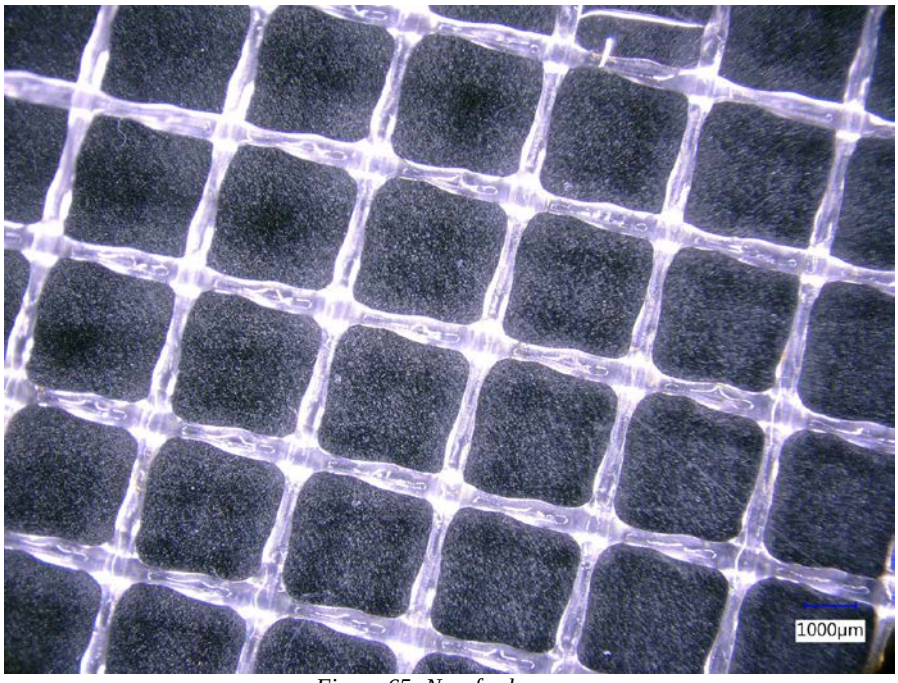

Figure 65: New feed spacer

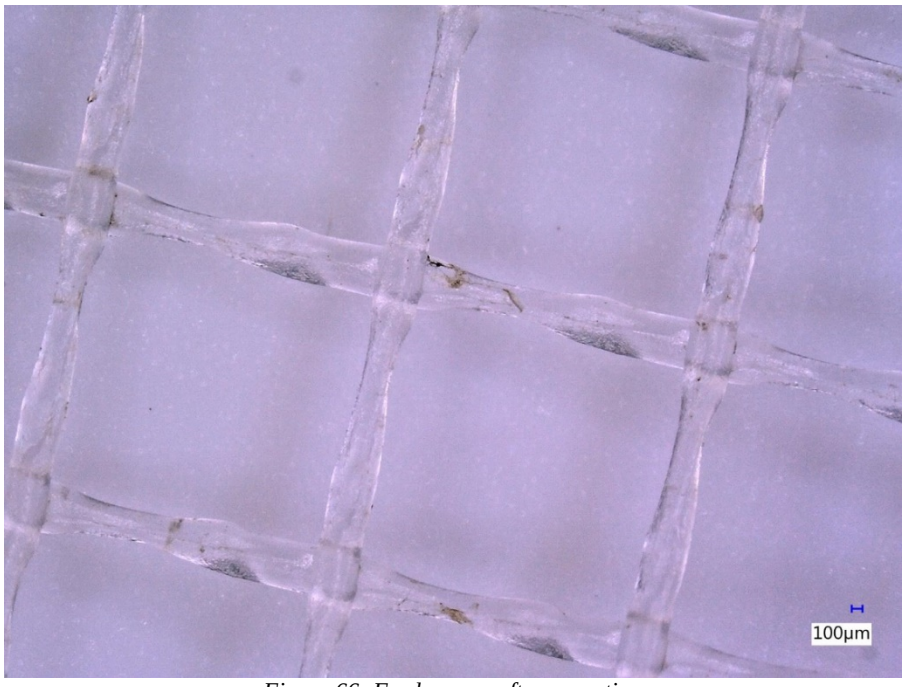

Figure 66: Feed spacer after operation

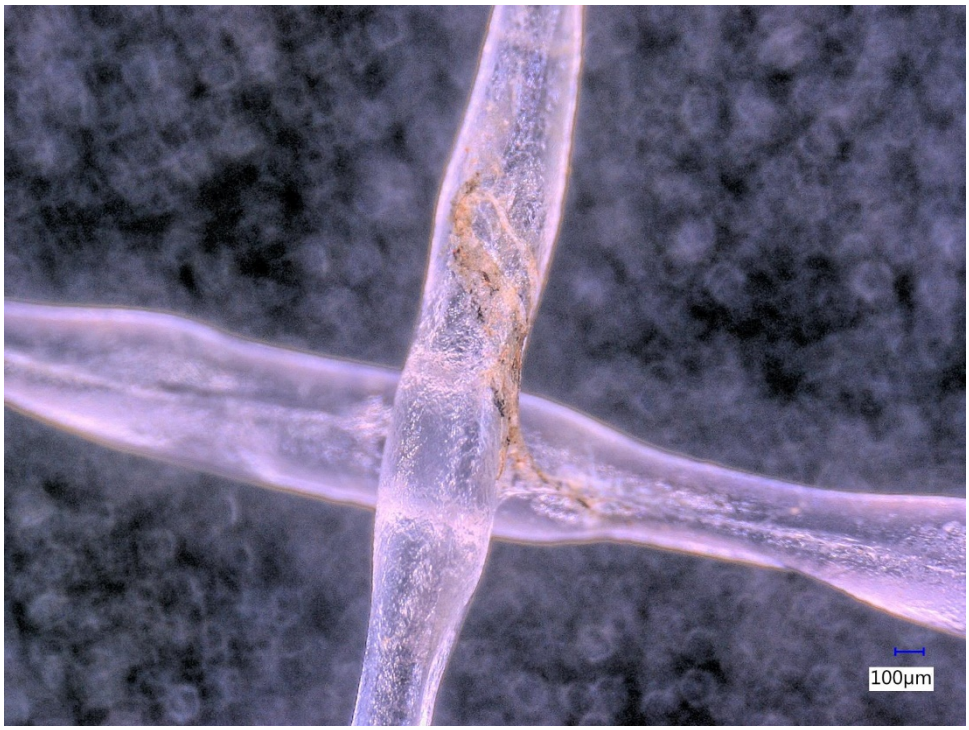

Figure 67: visual details of feed spacer after operation

4.3.1.4 Particle counting

Particle counting is used to determine particle size and number. The number and size distribution of particle indicate the particle fouling issues. Unlike FCP experiment both microscope and particle counter were adopted, in CCP research, only particle counter was used here. The reason is that microscope can only measure the visual biofilm and particles but in CCP most of the fouling is biofilm and biofilm are gather together as a whole in the picture (see Figure 67) thus microscope cannot detect the particle number. The effective measuring method is used the particle counter because before the measuring most the particles and gathered biofilm were trembled and divided into small parts. The result of particle counter is shown in Figure 68.

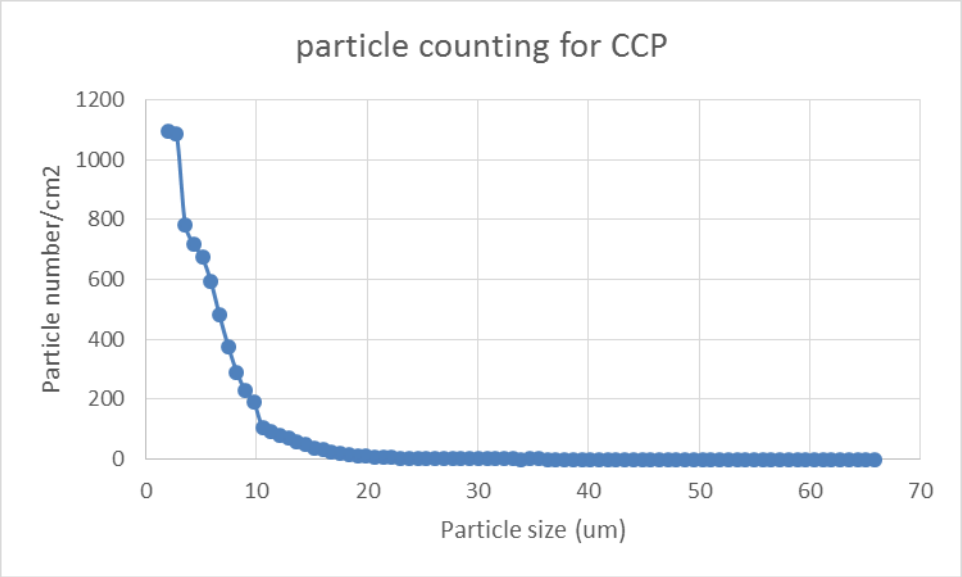

Figure 68: Particle counting for CCP experiment

As can be seen from the previous figure, maximum particle number is around 1100, which is only about 10% of the counterpart one in FCP experiment (see Figure 51). It is logical because as discussed above in microscope section, most of the particles would be retained by filters in FCP while only very few particles will clog in CCP.

4.3.2 Biological part

4.3.2.1 Introduction

The biological part analysis in CCP process is to present biofouling issue. ATP concentration is the primary parameter to indicate the biofouling for the crossflow clogging potential. In CCP process, the ATP measuring parameter is the amount of ATP on $1cm^2$ feed spacer. Because the initial idea and the equipment of CCP come from MFS, the ATP result in CCP will be compared with the counterpart one in MFS literature.

4.3.2.2 ATP measuring

The ATP result of CCP was shown in Table 6. Even though only one experiment was did due to the extended operation period of CCP, ATP measuring was taken three times to make results accurate and reliable. Furthermore, the result of MFS was also shown in this table.

Table 6: ATP result from CCP and MFS (MFS result is from Vrouwenvelder [8])

drinking water	CCP pg/cm2	MFS pg/cm2
round 1	747	-
round 2	727	-
round 3	764	-
average	746	440

The average $cATP/cm^2$ in CCP is 746 pg while the counterpart one for 2.7um filter FCP is around 20,000pg. The huge difference is because of the different flow through methods.

Unlike FCP and CCP, the ATP results of CCP and MFS are comparable because most of the processes and equipment for this two experiments are the same. As shown in above table, the ATP concentration in CCP is $746pg/cm^2$, which is 70% higher than the ATP concentration in MFS. As far as I am concerned, two reasons may cause this difference. The first is the operation period. The operation time of CCP is 18 days, longer than 12 days in MFS. The second explanation is the feed water. The feedwater for CCP is direct drinking water from the Lab while for MFS; the feed water is drinking water treated by two-step cartridge filters. Longer operation period and more biofilm concentration feed water may cause more biomass attached to feed spacer in CCP experiment.

4.3.3 Chemical part

4.3.3.1 Introduction

The aim of chemical part analysis for CCP is to figure out the inorganic matters retained on feed spacer. Based on the constitution of drinking water, the expected inorganic elements are iron and calcium.

4.3.3.2 ICP-MS

ICP-MS Result for CCP is shown in the following table, iron and calcium concentration in feed spacer are slight, which indicates in crossflow process, and the amount of clogged inorganic matters such as Fe and Ca are very little. This result suggests that in CCP test, inorganic matters play an insignificant role in total fouling issues.

Table 7: ICP-MS result for CCP

	[Fe]	[Ca]
	mg/cm2	mg/cm2
feed spacer	0.0006	0.0154

4.4 Comparison of FCP and CCP

A comparison between two different methods, FCP and CCP, was shown in this chapter for a better understanding of the Smart Water Meter. The comparison was made from three parts, physical, biological and chemical. Detail comparison is shown as follows.

4.4.1 Physical part

4.4.1.1 Pressure drop/resistance increase

Pressure drop/ resistance increase is the most important parameter both for FCP and CCP experiments. Based on the pressure drop/resistance increase rate, we can roughly know the fouling issues. In FCP operation, resistance was adopted as a parameter to represent fouling issues while in CCP test pressure drop was used as a signal for fouling. Even though parameters selected in two experiments were different, we can still compare the increasing curve of two indexes.

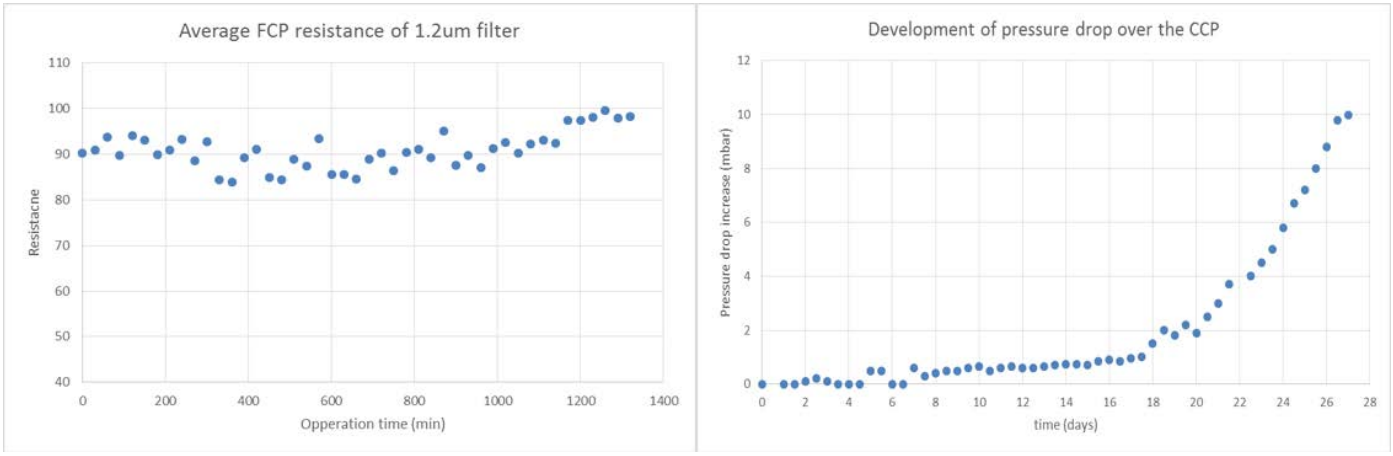

Figure 69: pressure drop/resistance increase curve of FCP (1.2um filter in Lab condition) and CCP (Lab condition)

The resistance and pressure drop increase curve of FCP and CCP was presented in Figure 69. Because there are lots of filters operated in different conditions in FCP experiment, the result chosen here was the 1.2um filter, which has the smallest pore size and the operation state is Lab drinking water, the same as the CCP experiment. As shown in this Figure, in FCP, the resistance increase rate is 10% in 20h operation period while in CCP, there is no visible pressure drop increase in the first seven days.

Based on the previous results, we can notice that the resistance/pressure drop increase rate of FCP is much higher than the counterpart one of the CCP. The main reason is the different filtration mechanisms of two

experiments. For FCP, the mechanism is the dead-end filtration, which means most of the particles and microorganisms larger than the respective pore size will be retained on filter thus the resistance increase rate is high. However, for CCP experiment, the mechanism is crossflow, which indicates most of the particles will leave the feed spacer together with the outflow and thus the corresponding pressure drop growth rate is much lower.

4.4.1.2 Particle counting

Particle concentration of filters and feed spacers after operation represent the amount of particles accumulated during the operation period. By comparing the particle concentration difference between two experiments, we could know the particle retaining efficiency of the two processes and the contribution of particle clogging for fouling issues when taking the resistance/pressure drop increase rate into consideration.

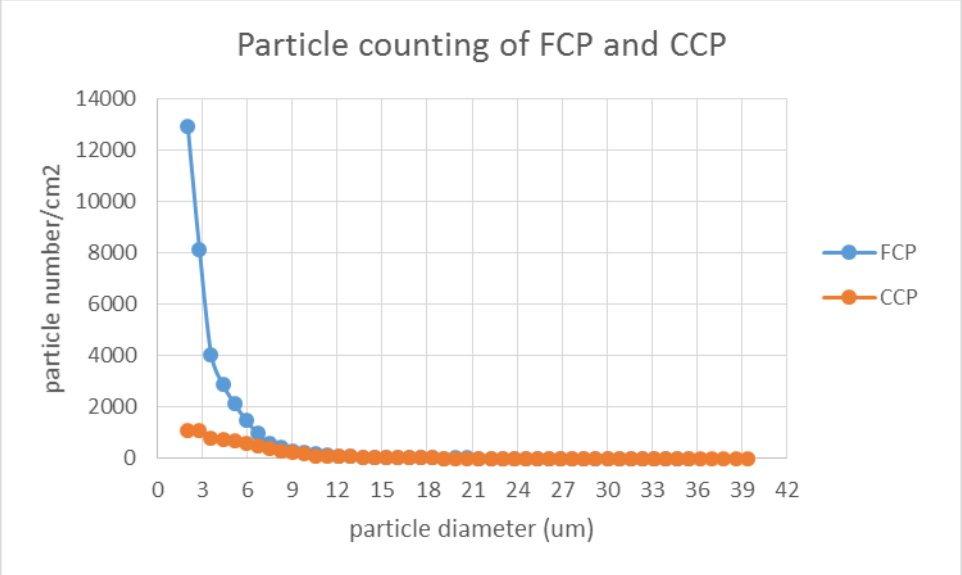

Figure 70: Particle counting for FCP (1.2um filter in Lab condition) and CCP (Lab condition)

As presented in Figure 70, particle concentration of FCP (less than 3um) is almost 10 times higher than the counterpart one on CCP. This result is expected and this result can explain part of the previous result of resistance/pressure drop difference in two experiments; more particles clogged in FCP contributes to a higher pressure drop.

4.4.1.3 Microscope observation

Microscope observations of two experiments have significant variations. Numerous clogged particles can be find directly from FCP pictures (see Figure 39) while in CCP experiment, only a few attached biofilm can be observed (see Figure 66 and 67). Based on microscope images, we can draw an assumption that in FCP particle clogging is the main contributor to resistance increase while in CCP biofilm growth is the leading factor for pressure drop increasing.

4.4.1.4 Operation duration

Different factors influenced operation periods of these two experiments. For FCP, the operation period was controlled by the effective operation duration of filters. In three different filters, 1.2um filter has the shortest expected operation time and the maximum operation time of 1.2um filter is around 20hours (0.83day) according to numerous trails. Therefore, chosen standard service time for three filters in FCP to make the operation period of three filters are the same and the results can be comparable.

For CCP, the operation duration was controlled by the monitor sensor limitation. On 28th operation day, the pressure drop reached 10mbar, which is the maximum pressure drop could be detected by this sensor. Furthermore, most of the MFS operation duration is less than according to Vrouwenvelder.(Vrouwenvelder et al. 2009) Therefore, the process time for CCP was 28dasys.

Table 8: operation time for FCP and CCP

	Operation time
	day
FCP	0.83
CCP	28

4.4.2 Biological part

4.4.2.1 ATP measuring

ATP comparison between FCP and CCP was already explained in Section 4.3.2 thus will not be repeated here.

4.4.3 Chemical part

4.4.3.1 ICP-MS

The result of inorganic matters in FCP and CCP is shown Table 9. As can be seen from this table, the Fe concentration in FCP experiments are all much larger than the counterpart one in CCP experiment. However, for Calcium concentration, the CCP and FCP results are at the same level. This huge inorganic matter retention difference is difficult to be explained. The possible explanation is when taking the CCP feed spacer as sample, some feedwater together with feed spacer into sample and this part of feedwater (drinking water) contribute to the relativity high calcium concentration of the feed spacer.

Table 9 Fe and Ca concentration comparison

	filter	[Fe]	[Ca]
		mg/cm2	mg/cm2
FCP	1.2um	0.0087	0.051
	1.5um	0.0069	0.017
	2.7um	0.004	0.009
CCP	feed spacer	0.0006	0.0154

4.5 Possible influent factors

In this study, all experiments were taken according to the instructions of the either the protocols from drinking water company Oasen or the standard methods from the relevant literature to avoid any possible artificial interference to the experimental results. However, there are still several results showing extreme values, which were considered as unusual and difficult to compare. Reasons behind these inregular results could be due to inappropriate methods, equipment or system errors. Some of the possibilities of these errors will be discussed in this chapter.

4.5.1 Laboratory's sample detection range

In ICP-MS chemical analysis part, some of the Fe concentration were reported lower than the laboratory's detection range thus recorded as 'lower than' a specific value. From the research aspect of view, these data should be presented as specific as possible so that the scientific conclusion can be made based on them.

In future research in the drinking water distribution system, when extreme low (or high) concentration of some parameters are expected, a pretreatment process (either a concentration process for the very little amount or dilute process for very high amount) should be implemented to make the sample in detection range.

4.5.2 The selection of filters

In FCP experiment, since lots of experiments were taken and not all experiments have same efficient operation times, to let results from different filters be comparable, 1400min was chosen to be a operation standard time for all filters and the reasons for operation time variation was shown as follows.

As describe in Section 3.2.2, even though the filter holder was used in FCP experiments, filters will still break after certain operation time. 1.2um filter is the easiest broken filter among these three filters because the pressure

drop and resistance for 1.2um filter is the highest. During the experiment, the actual effective operation period for 1.2um filter range from 8 hours to 20 hours randomly.

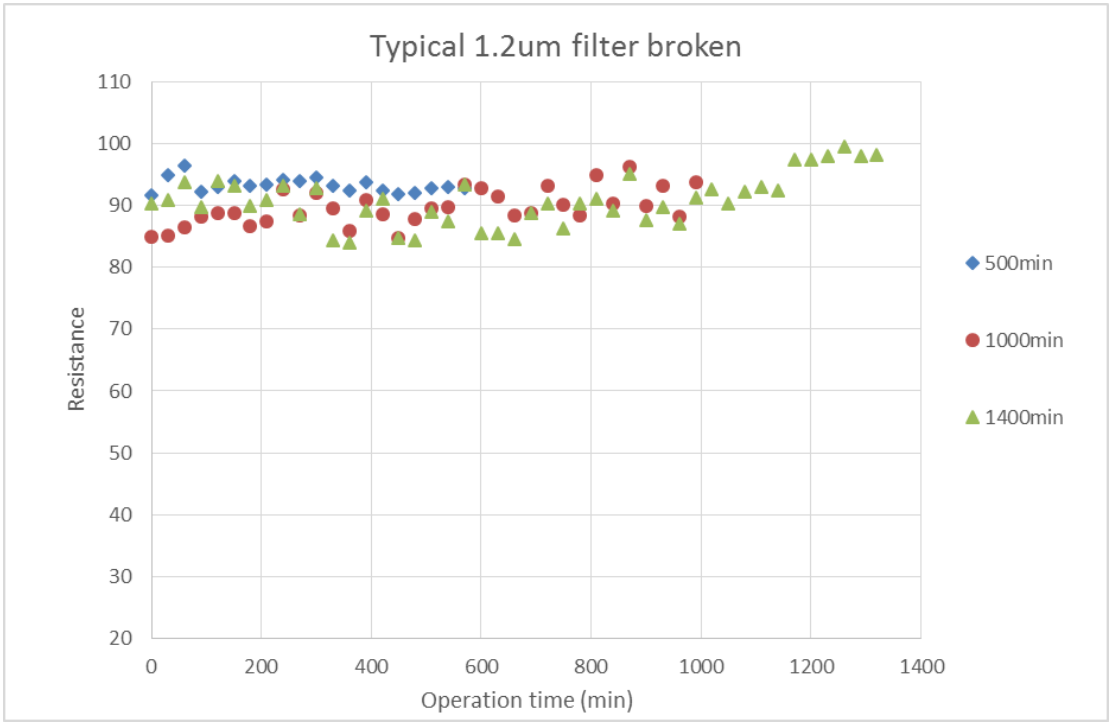

Figure 71: Typical 1.2um filter broken time

As shown in the previous figure, three typical filter broke times were chosen to represent the 1.2um filter operation situation. In general, the effective operation times for 1.2um filter can be divided into three parts, below 500min, around 1000min and 1400min. Possibility for each part is almost the same. The reason for this operation time variation is still unknown. Possible explanation is that particle clogging rate for the short-term filter is higher thus filter is easier to break. Although the resistance is increasing rates in Figure 71 supports this hypothesis, the rate difference of three situations is so small thus the explanation is still under discussion. More researches need to be done for further investigation.

To let the resistance results of different pore size filters be comparable, the operation effective period should be the same. Therefore, 1.2um filter maximum effective operation time, 1400min, was chosen to be the standard operation period for all filters and only the experiment rounds which operation period reach 1400min will be taken for further analysis and discussion.

4.5.3 Sample measuring and frequency

In this research, the pressure drop was measured by monitor every 5 seconds as described in Chapter 3.2.1. The results obtained from this set of equipment are believed as accurate enough for this research.

4.5.4 Reliability of data

As illustrated in Chapter 3.1, the reliability of the data should be checked to verify if the obtained data are capable of making a scientific conclusion, especially to ATP measuring which has a high standard deviation. To make results more accurate, most experiments were taken three parallels. The coefficient of variation of ATP measuring is around 5% which is acceptable. Detail information was shown in Appendix 2.

4.5.5 Research design and implementation

Several other factors during research development and implementation also influence the experiment results. These factors are discussed as follows;

- ICP-MS is an appropriate parameter to describe the level of inorganic matters attached to feed spacer. However, it also shows incapability when used for measuring and comparing some inorganic matters at low concentration. Because the calcium and iron concentration attached on feed spacer is little, and any comparison based on ICP-MS will fluctuate within this range. This fluctuation will make the

comparison difficult and for scientific purpose, equipment with higher precision should be chosen for further analysis.

- Three filters with different pore size were selected in FCP experiment. However, apart from pore size differences, there are still other differences such as porosity and thickness difference for these three filters (see Section 3.2.2), which let the experiment results fluctuation and thus, increase the difficulty of comparison. Because of the manufacturing process for different pore size filter is different even in the same company, it is impossible to obtain filters only have pore size difference. Therefore, their porosity and thickness differences need to be taken into consideration in result analysis.

5 Conclusions & Recommendations

Summarizing the results, conclusions have been drawn towards whether the Smart Water Meter is a suitable equipment to monitor fouling issues and what matters contribute to fouling. In general, the research has led to better understanding the fundamental mechanism of fouling issues in Smart Water Meter from physical, biological and chemical points of view. Because this chapter also led to more questions, this chapter will first deal with the conclusions of this thesis followed by recommendations for further research.

5.1 Conclusions

- Smart Water Meter can act as equipment to detect the biofouling issue during the distribution system.
- The clogging mechanisms of FCP and CCP in Smart Water Meter are different. Particle clogging is the most important contributor for FCP while Biofouling plays a significant role in CCP.
- FCP is more suitable to monitor the particles such as detached biofilm while CCP can detect the microorganism regrowth.
- Filters with different pore size have different clogging rate in FCP process: smaller the pore size; the higher clogging rate will be.
- FCP and CCP in Smart Water Meter have different monitoring periods, for FCP, the expected monitoring period is 20 hours while for CCP the expected operation period is four weeks.
- No relationship can be found between inorganic matters and clogging issues for both FCP and CCP experiments in this research.
- Drinking water quality from consumers' tap is greatly influenced by the distribution process. Both the biofilm and hydraulic retention time will impact the water quality from consumer's tap.

5.2 Recommendations

The research on biofilm from filters is based on the method from literature: ultrasonic trembling and ATP measurement. However, this is not a Standard method and whether this method will influence the microorganism from samples was unknown. For any further research in this field, a well-organized and reliable method should be discussed and confirmed firstly. Thus the results from different researchers can be comparable.

In this research, it has been proved that the pressure drop in Smart Water Meter, especially for FCP, is relativity too high and the residual pressure may not maintain the consumers' requirements. Therefore, in subsequent research, Smart Water Meter can be installed in extra pipelines, which are not connected to customers. In that case, these Smart Water Meters can monitor water quality in various distribution areas without affect consumers' daily uses.

Nowadays, only pressure drop and flux are monitored by the Smart Water Meter. Other parameters such as turbidity, TDS and pH can also be measured in the foreseeable future. Meanwhile, the Smart Water Meter can be integrated into District Metered Area (DMA) and upload the real time water quality parameters online.

6 Reference

Anon, Klimaat en klimaatverandering Klimaat = “ Het gemiddelde weer in een bepaald gebied over langere tijd van o . a . de Klimaatverandering = verandering in gemiddelden en / of de kans op extremen Meetfouten • Natuurlijke variabiliteit + trends • Bewerken / a.

Baker, J.S. & Dudley, L.Y., 1998. Biofouling in membrane systems — A review. *Desalination*, 118(1-3), pp.81–89.

De Barros, S.T.D. et al., 2003. Study of fouling mechanism in pineapple juice clarification by ultrafiltration. *Journal of Membrane Science*, 215(1-2), pp.213–224.

Beech, I.B. & Sunner, J., 2004. Biocorrosion: Towards understanding interactions between biofilms and metals. *Current Opinion in Biotechnology*, 15(3), pp.181–186.

Boerlage, S.F.E. et al., 2004. Development of the MFI-UF in constant flux filtration. *Desalination*, 161(2), pp.103–113.

Boerlage, S.F.E. et al., 1998. Monitoring particulate fouling in membrane systems. *Desalination*, 118(1-3), pp.131–142.

Boerlage, S.F.E. et al., 1997. Prediction of flux decline in membrane systems due to particulate fouling. *Desalination*, 113(2-3), pp.231–233.

Boerlage, S.F.E. et al., 2002. The modified fouling index using ultrafiltration membranes (MFI-UF): Characterisation, filtration mechanisms and proposed reference membrane. *Journal of Membrane Science*, 197(1-2), pp.1–21.

Brauns, E. et al., 2002. A new method of measuring and presenting the membrane fouling potential. *Desalination*, 150(1), pp.31–43.

Bucs, S.S. et al., 2014. Impact of organic nutrient load on biomass accumulation, feed channel pressure drop increase and permeate flux decline in membrane systems. *Water Research*, 67(0), pp.227–242. Available at: http://dx.doi.org/10.1016/j.watres.2014.09.005.

Camper, A.K., 2004. Involvement of humic substances in regrowth. *International Journal of Food Microbiology*, 92(3), pp.355–364.

Choi, J.S. et al., 2009. A systematic approach to determine the fouling index for a RO/NF membrane process. *Desalination*, 238(1-3), pp.117–127. Available at: http://dx.doi.org/10.1016/j.desal.2008.01.042.

Committee On Public Water Supply Distribution Systems: Assessing And Reducing Risks, N.R.C., 2006. *Drinking Water Distribution Systems: Assessing and Reducing Risks*,

Company, P., 1980. Desalination. 32 (1980) 137-148 ® Elsevier Scientific. , 32, pp.137–148.

Dreszer, C. et al., 2013. Hydraulic resistance of biofilms. *Journal of Membrane Science*, 429, pp.436–447. Available at: http://dx.doi.org/10.1016/j.memsci.2012.11.030.

Dreszer, C. et al., 2014. Impact of biofilm accumulation on transmembrane and feed channel pressure drop: Effects of crossflow velocity, feed spacer and biodegradable nutrient. *Water Research*, 50(0), pp.200–211. Available at: http://dx.doi.org/10.1016/j.watres.2013.11.024.

Field, R., 2010. Fundamentals of Fouling. *Membrane Technology*, 4, pp.1–23.

Filippini, a, Taffs, R.E. & Sitkovsky, M. V, 1990. Extracellular ATP in T-lymphocyte activation: possible role in effector functions. *Proceedings of the National Academy of Sciences of the United States of America*, 87(21), pp.8267–8271.

Gibson, P., Schreuder-Gibson, H. & Rivin, D., 2001. Transport properties of porous membranes based on electrospun nanofibers. *Colloids and Surfaces A: Physicochemical and Engineering Aspects*, 187-188, pp.469–481.

Hammes, F. et al., 2010. Measurement and interpretation of microbial adenosine tri-phosphate (ATP) in aquatic environments. *Water Research*, 44(13), pp.3915–3923. Available at: http://dx.doi.org/10.1016/j.watres.2010.04.015.

Hell, S.W. & Wichman, J., 1994. Breaking the diffraction resolution limit by stimulated emission: stimulated-emission-depletion fluorescence microscopy. *Optics Letters*, 19(11), pp.780 – 782.-++++++++++++-++-+

Hermia, J., 1982. Constant Pressure Blocking Filtration Laws – Application to Power-law Non-Newtonian Fluids. *Trans IChemE*, 60(3), p.183.

Liu, G., Lut, M.C., et al., 2013. A comparison of additional treatment processes to limit particle accumulation and microbial growth during drinking water distribution. *Water Research*, 47(8), pp.2719–2728. Available at: http://dx.doi.org/10.1016/j.watres.2013.02.035.

Liu, G. et al., 2016. Comparison of Particle-Associated Bacteria from a Drinking Water Treatment Plant and Distribution Reservoirs with Different Water Sources. *Scientific Reports*, 6(February), p.20367. Available at: http://www.nature.com/articles/srep20367.

Liu, G., Ling, F.Q., et al., 2013. Quantification and identification of particle-associated bacteria in unchlorinated

drinking water from three treatment plants by cultivation-independent methods. *Water Research*, 47(10), pp.3523–3533. Available at: http://dx.doi.org/10.1016/j.watres.2013.03.058.

Liu, G., Verberk, J.Q.J.C. & Van Dijk, J.C., 2013. Bacteriology of drinking water distribution systems: An integral and multidimensional review. *Applied Microbiology and Biotechnology*, 97(21), pp.9265–9276.

M. Oldani A. Miquel and G.J. Schock, E.K., 1992. On the nitrate and monovalent cation selectivity of ion exchange membranes used in drinking water purification. *J. Membr. Sci.*, pp.265–275.

Modified, Q.O. & Kit, Q.T., 2010. Test Kit Instructions. , 33(0), pp.1–6.

Van der Oost, R., Beyer, J. & Vermeulen, N.P.E., 2003. Fish bioaccumulation and biomarkers in environmental risk assessment: A review. *Environmental Toxicology and Pharmacology*, 13(2), pp.57–149.

Oulahal-Lagsir, N. et al., 2000. Ultrasonic methodology coupled to ATP bioluminescence for the non-invasive detection of fouling in food processing equipment--validation and application to a dairy factory. *Journal of Applied Microbiology*, 89(3), pp.433–41.

Park, C. et al., 2006. Variation and prediction of membrane fouling index under various feed water characteristics. *Journal of Membrane Science*, 284(1-2), pp.248–254.

Payment, P. et al., 1997. A prospective epidemiological study of gastrointestinal health effects due to the consumption of drinking water. *International Journal of Environmental Health Research*, 7(1), pp.5–31.

Radu, A.I. et al., 2010. Modeling the effect of biofilm formation on reverse osmosis performance: Flux, feed channel press+----------+-ure drop and solute passage. *Journal of Membrane Science*, 365(1-2), pp.1–15. Available at: http://dx.doi.org/10.1016/j.memsci.2010.07.036.

Regan, J.M. et al., 2002. Ammonia- and Nitrite-Oxidizing Bacterial Communities in a Pilot-Scale Chloraminated Drinking Water Distribution System Ammonia- and Nitrite-Oxidizing Bacterial Communities in a Pilot-Scale Chloraminated Drinking Water Distribution System. , 68(1), pp.73–81.

Rheinheimer, S.J.E. and D.E., 2004. drinking water denitrification using a membrane bioreactor. *Water Research*, pp.3225–3232.

Scott, K., 1998. Handbook of Industrial Membranes. *Handbook of Industrial Membranes*, pp.373–429. Available at: http://www.sciencedirect.com/science/article/pii/B9781856172332500106.

Siddiqui, A. et al., 2016. Development and characterization of 3D-printed feed spacers for spiral wound membrane systems. *Water Research*, 91, pp.55–67.

Treatment, W., Micro- and ultrafiltration.

Vrouwenvelder, H.S. et al., 1998. Biofouling of membranes for drinking water production. *Desalination*, 118(1-3), pp.157–166.

Vrouwenvelder, J.S. et al., 2009. Pressure drop increase by biofilm accumulation in spiral wound RO and NF membrane systems: role of substrate concentration, flow velocity, substrate load and flow direction. *Biofouling*, 25(6), pp.543–555.

Vrouwenvelder, J.S. et al., 2007. The Membrane Fouling Simulator as a new tool for biofouling control of spiral-wound membranes. *Desalination*, 204(1-3 SPEC. ISS.), pp.170–174.

Vrouwenvelder, J.S. et al., 2006. The Membrane Fouling Simulator: A practical tool for fouling prediction and control. *Journal of Membrane Science*, 281, pp.316–324.

Wang, Y. et al., 2007. Quantification of the filterability of freshwater bacteria through 0.45, 0.22, and 0.1 ??m pore size filters and shape-dependent enrichment of filterable bacterial communities. *Environmental Science and Technology*, 41(20), pp.7080–7086.

Yiantsios, S.G. & Karabelas, A.J., 1998. The effect of colloid stability on membrane fouling. *Desalination*, 118(1-3), pp.143–152.

7 Appendix

7.1 Appendix 1 particle counting results for Filters operated in different conditions.

Lab condition						Apartment condition					
2.7um filter		1.5um filter		1.2um filter		2.7um filter		1.5um filter		1.2um filter	
max dia.	counts	max dia.	counts	max dia.	counts	max dia.	counts	max dia.	counts	max dia.	counts
um	-	um	-	um	-	um	-	um	-	um	-
0.4	353	0.4	301	0.4	921	0.4	336	0.4	301	0.4	1830
0.6	332	0.6	167	0.6	501	0.6	235	0.6	167	0.6	825
0.8	128	0.8	87	0.9	249	0.9	118	0.8	87	0.9	572
0.9	154	0.9	138	1	427	1	65	0.9	138	1	473
1.2	43	1.2	41	1.2	96	1.2	34	1.2	41	1.2	119
1.3	89	1.3	79	1.3	42	1.3	4	1.3	79	1.3	66
1.5	31	1.5	36	1.4	196	1.4	43	1.5	36	1.4	227
1.7	38	1.7	27	1.5	142	1.5	50	1.7	27	1.5	115
1.8	11	1.8	6	1.7	24	1.7	3	1.8	6	1.7	35
1.9	18	1.9	15	1.8	116	1.8	38	1.9	15	1.8	117
2.1	12	2.1	14	1.9	92	1.9	46	2.1	14	1.9	77
2.2	14	2.2	7	2.1	63	2.1	26	2.2	7	2.1	49
2.3	10	2.3	8	2.2	50	2.2	19	2.3	8	2.2	42
2.4	5	2.4	6	2.3	57	2.3	33	2.4	6	2.3	40
2.5	6	2.5	21	2.4	24	2.4	8	2.5	21	2.4	13
2.6	6	2.6	3	2.5	58	2.5	41	2.6	3	2.5	42
2.7	15	2.7	23	2.6	17	2.6	8	2.7	23	2.6	29
2.8	5	2.8	6	2.7	82	2.7	42	2.8	6	2.7	38
3	9	3	8	2.9	43	2.9	31	3	8	2.9	22
3.1	13	3.1	15	3	30	3	10	3.1	15	3	26
3.2	7	3.2	8	3.1	58	3.1	35	3.2	8	3.1	27
3.3	4	3.3	11	3.3	28	3.3	19	3.3	11	3.3	15
3.4	12	3.4	7	3.4	24	3.4	7	3.4	7	3.4	12
3.5	4	3.5	7	3.5	50	3.5	31	3.5	7	3.5	28
3.6	10	3.6	14	3.6	8	3.6	1	3.6	14	3.6	9
3.8	4	3.8	11	3.7	47	3.7	26	3.8	11	3.7	16
3.9	3	3.9	9	3.8	16	3.8	13	3.9	9	3.8	10
4	4	4	12	3.9	9	3.9	3	4	12	3.9	6
4.2	6	4.2	20	4	31	4	21	4.2	20	4	15
4.3	3	4.3	5	4.1	15	4.1	8	4.3	5	4.1	13
4.4	8	4.4	5	4.2	13	4.2	12	4.4	5	4.2	9
4.6	6	4.5	2	4.3	19	4.3	10	4.5	2	4.3	8
4.7	4	4.6	6	4.4	30	4.4	9	4.6	6	4.4	13
4.8	4	4.7	3	4.5	10	4.5	13	4.7	3	4.5	4
4.9	2	4.8	6	4.6	17	4.6	17	4.8	6	4.6	21
5	2	4.9	1	4.7	9	4.7	3	4.9	1	4.7	2
5.1	9	5	3	4.8	20	4.8	10	5	3	4.8	7

5.2	3	5.1	10	4.9	21	4.9	13	5.1	10	4.9	13
5.3	2	5.2	6	5	10	5	12	5.2	6	5	7
5.4	4	5.3	2	5.1	3	5.2	16	5.3	2	5.2	14
5.5	4	5.4	1	5.2	27	5.3	3	5.4	1	5.3	1
5.6	1	5.5	2	5.3	2	5.4	9	5.5	2	5.4	3
5.7	2	5.6	2	5.4	10	5.5	5	5.6	2	5.5	7
5.8	2	5.8	4	5.5	5	5.6	8	5.8	4	5.6	10
5.9	3	5.9	2	5.6	20	5.7	3	5.9	2	5.7	2
6	2	6	4	5.7	1	5.8	15	6	4	5.8	10
6.1	2	6.1	3	5.8	12	6	5	6.1	3	6	4
6.2	3	6.2	4	6	9	6.1	10	6.2	4	6.1	8
6.3	1	6.3	2	6.1	15	6.2	6	6.3	2	6.2	4
6.4	2	6.6	4	6.2	5	6.3	3	6.6	4	6.3	3
6.5	3	6.7	5	6.3	2	6.4	8	6.7	5	6.4	6
6.6	3	6.8	3	6.4	12	6.5	3	6.8	3	6.5	8
6.9	1	6.9	2	6.5	5	6.6	5	6.9	2	6.6	4
7	1	7	2	6.7	14	6.7	4	7	2	6.7	7
7.2	3	7.2	5	6.8	3	6.8	4	7.2	5	6.8	2
7.4	2	7.3	2	6.9	8	6.9	5	7.3	2	6.9	2
7.5	2	7.4	1	7	8	7	2	7.4	1	7	8
7.6	4	7.6	4	7.1	2	7.1	8	7.6	4	7.1	5
7.7	2	7.7	2	7.2	3	7.2	4	7.7	2	7.2	2
7.8	3	7.8	2	7.3	9	7.3	3	7.8	2	7.3	6
7.9	4	7.9	1	7.4	1	7.4	4	7.9	1	7.4	1
8.1	5	8	1	7.5	5	7.5	3	8	1	7.5	3
8.2	1	8.1	1	7.6	6	7.6	5	8.1	1	7.6	5
8.4	2	8.3	1	7.7	5	7.7	9	8.3	1	7.7	6
8.5	2	8.4	2	7.8	1	7.8	2	8.4	2	7.8	2
8.6	4	8.5	1	7.9	3	7.9	6	8.5	1	7.9	9
8.7	1	8.6	4	8	2	8.1	4	8.6	4	8.1	1
8.8	3	8.7	3	8.1	8	8.2	3	8.7	3	8.2	3
8.9	1	8.8	1	8.2	6	8.3	12	8.8	1	8.3	3
9	2	8.9	2	8.3	8	8.4	2	8.9	2	8.5	3
9.1	1	9	3	8.4	3	8.5	4	9	3	8.6	4
9.2	3	9.1	1	8.5	9	8.6	4	9.1	1	8.7	2
9.3	3	9.3	1	8.7	2	8.7	1	9.3	1	8.8	2
9.5	2	9.6	1	8.8	3	8.8	10	9.6	1	8.9	2
9.6	2	9.7	2	8.9	1	9	1	9.7	2	9	3
9.7	2	10.2	4	9	2	9.1	6	10.2	4	9.1	3
9.9	1	10.3	2	9.1	9	9.2	6	10.3	2	9.2	3
10.1	2	10.5	2	9.2	3	9.3	3	10.5	2	9.3	2
10.2	1	10.6	3	9.3	1	9.4	3	10.6	3	9.4	2
10.4	1	10.7	1	9.4	3	9.5	5	10.7	1	9.5	5
10.5	1	10.8	1	9.5	7	9.6	1	10.8	1	9.6	2
10.6	1	11	1	9.6	2	9.7	2	11	1	9.7	1
10.7	1	11.1	2	9.7	2	9.8	2	11.1	2	9.8	2

10.8	2	11.2	2	9.9	3	9.9	1	11.2	2	9.9	4
10.9	2	11.4	1	10	3	10	4	11.4	1	10	2
11	4	11.6	1	10.1	4	10.1	2	11.6	1	10.1	1
11.2	2	11.9	1	10.2	5	10.2	1	11.9	1	10.2	1
11.3	1	12	1	10.3	3	10.3	2	12	1	10.3	1
11.4	2	12.1	1	10.4	2	10.4	2	12.1	1	10.4	5
11.5	3	12.3	1	10.5	2	10.5	1	12.3	1	10.5	1
11.6	1	12.7	1	10.6	3	10.6	3	12.7	1	10.6	4
11.7	1	12.9	2	10.7	2	10.7	3	12.9	2	10.8	1
12	1	13	1	11	2	10.8	4	13	1	10.9	2
12.2	1	13.1	1	11.1	1	10.9	4	13.1	1	11	2
12.3	2	13.2	1	11.3	2	11	2	13.2	1	11.1	3
12.4	2	13.4	2	11.4	2	11.1	2	13.4	2	11.2	1
12.5	2	13.5	1	11.6	3	11.2	3	13.5	1	11.3	4
12.6	2	14.1	1	11.7	3	11.3	4	14.1	1	11.5	3
12.7	1	14.3	1	11.8	1	11.4	1	14.3	1	11.6	1
13	1	14.4	3	11.9	2	11.5	2	14.4	3	11.7	5
13.1	1	14.5	1	12	3	11.6	1	14.5	1	11.8	3
13.4	2	14.6	2	12.1	1	11.8	1	14.6	2	11.9	3
13.6	2	15	1	12.2	3	11.9	3	15	1	12	2
13.7	2	15.6	1	12.3	1	12	5	15.6	1	12.1	1
13.8	2	15.7	1	12.4	3	12.1	2	15.7	1	12.3	1
14	2	16.2	1	12.5	3	12.2	2	16.2	1	12.6	1
14.2	3	16.3	1	12.7	1	12.3	1	16.3	1	12.7	1
14.3	2	16.5	1	12.8	2	12.4	2	16.5	1	12.8	2
14.4	1	16.6	1	13	2	12.5	2	16.6	1	12.9	4
14.5	1	16.8	1	13.1	1	12.6	2	16.8	1	13	1
14.6	2	17.1	1	13.3	3	12.7	2	17.1	1	13.1	4
14.7	1	17.3	1	13.4	2	12.8	4	17.3	1	13.2	2
14.8	1	17.4	1	13.5	2	12.9	1	17.4	1	13.3	1
15	1	17.8	1	13.6	1	13	1	17.8	1	13.4	2
15.2	2	17.9	2	13.7	1	13.1	3	17.9	2	13.5	1
15.3	3	18.1	1	14	1	13.2	1	18.1	1	13.6	1
15.5	1	18.4	2	14.1	2	13.3	2	18.4	2	13.8	1
15.6	2	18.6	1	14.3	2	13.5	5	18.6	1	14	3
15.7	1	18.8	1	14.4	1	13.8	1	18.8	1	14.1	1
15.9	1	18.9	2	14.5	1	14	2	18.9	2	14.2	4
16.2	1	19.1	2	14.6	2	14.1	1	19.1	2	14.3	3
16.5	1	19.2	2	14.8	1	14.3	2	19.2	2	14.6	1
16.6	1	19.9	1	14.9	1	14.5	2	19.9	1	14.7	3
16.8	4	20	1	15	4	14.8	1	20	1	14.8	2
16.9	4	20.5	2	15.1	1	15	4	20.5	2	15	3
17.1	2	20.9	1	15.3	1	15.1	1	20.9	1	15.2	3
17.3	2	21	1	15.4	1	15.2	3	21	1	15.4	2
17.4	1	21.1	1	15.5	3	15.4	3	21.1	1	15.5	4
17.5	2	21.2	1	15.6	1	15.5	3	21.2	1	15.6	1

17.7	1	21.6	1	15.7	1	15.6	1	21.6	1	15.8	2
17.8	2	22.8	1	15.8	2	15.7	2	22.8	1	15.9	2
18.5	1	23.1	1	15.9	1	16	1	23.1	1	16	2
18.6	2	23.3	1	16	1	16.2	3	23.3	1	16.1	1
18.7	3	24	1	16.3	1	16.6	2	24	1	16.2	1
19.1	1	24.2	1	16.4	1	16.7	2	24.2	1	16.4	3
19.2	1	24.4	1	16.7	1	17	2	24.4	1	16.5	1
19.5	2	25.7	1	16.8	2	17.1	1	25.7	1	16.6	1
19.7	2	26	2	17	2	17.3	1	26	2	16.8	1
19.8	1	27.4	1	17.1	2	17.5	2	27.4	1	17.1	1
19.9	1	28.4	1	17.2	3	17.7	4	28.4	1	17.2	1
20.3	2	28.5	1	17.4	1	18.1	1	28.5	1	17.3	3
20.5	1	30.2	1	17.5	1	18.2	2	30.2	1	17.5	1
20.8	1	30.9	1	17.6	1	18.3	1	30.9	1	17.6	1
21.2	1	31.2	2	17.7	2	18.6	1	31.2	2	17.9	1
21.6	1	31.5	1	17.8	1	18.7	1	31.5	1	18.2	4
21.7	1	31.7	1	18.1	1	18.9	1	31.7	1	18.3	2
22.2	1	34.3	1	18.5	1	19.1	3	34.3	1	18.5	1
22.7	2	34.5	1	19.1	1	19.2	2	34.5	1	18.6	1
23.2	1	37.7	1	19.2	2	19.4	4	37.7	1	18.9	4
23.3	1	38.5	1	19.4	2	19.7	1	38.5	1	19	1
23.4	1	39	1	19.5	1	19.8	1	39	1	19.3	1
23.7	1	43.8	1	20.6	1	20.2	1	43.8	1	19.4	1
24.4	1	45.3	1	20.8	1	20.4	1	45.3	1	19.6	1
24.7	1	47.5	1	21	1	20.6	3	47.5	1	19.7	1
24.8	1	71.2	1	21.6	1	21	1	71.2	1	19.8	1
25.3	1	74.2	1	22	1	21.2	1	74.2	1	20	2
26.2	1	83	1	22.1	1	21.3	1	83	1	20.1	1
27.1	1	-	-	22.4	1	21.4	1	-	-	20.4	2
27.2	1	-	-	22.9	1	21.6	1	-	-	20.5	1
27.7	1	-	-	23.2	2	21.8	1	-	-	20.7	1
28.9	1	-	-	23.3	1	22.1	2	-	-	20.9	2
30.7	1	-	-	23.5	1	22.5	1	-	-	21	2
32.5	1	-	-	23.9	2	23.1	1	-	-	21.1	2
32.8	1	-	-	24	1	24	1	-	-	21.3	3
33	1	-	-	24.6	2	24.2	2	-	-	21.4	1
33.9	1	-	-	25.3	1	24.6	1	-	-	21.9	1
34.6	1	-	-	25.6	1	24.8	1	-	-	22.2	1
36.1	1	-	-	25.7	2	25.1	1	-	-	22.5	1
36.5	1	-	-	26.3	1	25.2	1	-	-	22.7	1
36.8	1	-	-	26.4	1	25.3	1	-	-	23.2	2
60	1	-	-	26.5	1	25.6	1	-	-	23.5	1
-	-	-	-	26.9	1	26.3	1	-	-	23.8	2
-	-	-	-	28.2	1	26.7	1	-	-	24	1
-	-	-	-	28.4	1	26.9	1	-	-	24.2	1
-	-	-	-	28.5	1	27.3	1	-	-	25.1	1

-	-	-	-	28.6	1	27.7	1	-	-	25.2	1
-	-	-	-	29	1	28.6	1	-	-	25.8	1
-	-	-	-	29.2	2	29.3	1	-	-	26.2	1
-	-	-	-	29.4	1	30	1	-	-	26.3	1
-	-	-	-	30.7	3	30.1	1	-	-	26.6	1
-	-	-	-	30.8	1	30.5	2	-	-	26.9	2
-	-	-	-	31.3	1	37.6	1	-	-	27.1	1
-	-	-	-	31.8	1	42	2	-	-	28.1	1
-	-	-	-	33.7	1	-	-	-	-	28.2	1
-	-	-	-	33.9	1	-	-	-	-	28.3	1
-	-	-	-	34.3	1	-	-	-	-	29	1
-	-	-	-	34.4	1	-	-	-	-	29.2	1
-	-	-	-	35.2	1	-	-	-	-	29.4	1
-	-	-	-	35.7	1	-	-	-	-	29.6	1
-	-	-	-	37.2	1	-	-	-	-	29.7	1
-	-	-	-	38	1	-	-	-	-	30.2	1
-	-	-	-	38.9	1	-	-	-	-	30.6	2
-	-	-	-	39	1	-	-	-	-	31	1
-	-	-	-	39.3	1	-	-	-	-	31.8	2
-	-	-	-	39.5	1	-	-	-	-	31.9	1
-	-	-	-	40.1	1	-	-	-	-	32.3	1
-	-	-	-	40.9	1	-	-	-	-	32.7	1
-	-	-	-	41.8	1	-	-	-	-	33	1
-	-	-	-	43	1	-	-	-	-	34	1
-	-	-	-	43.8	1	-	-	-	-	34.9	1
-	-	-	-	45	1	-	-	-	-	35.4	1
-	-	-	-	48.2	1	-	-	-	-	35.5	1
-	-	-	-	50	1	-	-	-	-	35.6	1
-	-	-	-	50.3	1	-	-	-	-	36.7	2
-	-	-	-	50.7	1	-	-	-	-	37.4	2
-	-	-	-	50.9	1	-	-	-	-	37.6	1
						-	-	-	-	37.8	1

7.2 Appendix 2 ATP measuring results for filters in FCP experiment

Lab condition	total ATP	total ATP	total ATP	total ATP	total ATP	σ/μ
No.	1	2	3	4	average	
	pg	pg	pg	pg	pg	
1.2um	49639	48228	47322	51235	49106	3%
1.5um	37997	35314	37235	38915	37365	4%
2.7um	21724	20852	22722	21406	21676	4%

Lab condition	cATP/flux	cATP/flux	cATP/flux	cATP/flux	cATP/flux	σ/μ
No.	1	2	3	4	average	
	pg/L	pg/L	pg/L	pg/L	pg/L	
1.2um	30.0	27.0	33.0	29.0	29.8	8%
1.5um	21.0	20.0	18.0	22.0	20.3	8%
2.7um	8.0	6.5	7.0	8.2	7.4	11%

Apartment	total ATP	total ATP	total ATP	total ATP	total ATP	σ/μ
No.	1	2	3	4	average	
	pg	pg	pg	pg	pg	
1.2um	32688	28229	29367	34295	31145	9%
1.5um	27444	24924	24807	26131	25827	5%
2.7um	21429	22619	18932	19979	20740	8%

Apartment	cATP/flux	cATP/flux	cATP/flux	cATP/flux	cATP/flux	σ/μ
No.	1	2	3	4	average	
	pg/L	pg/L	pg/L	pg/L	pg/L	
1.2um	25.0	22.0	23.0	22.0	23.0	6%
1.5um	17.0	15.0	15.0	19.0	16.5	12%
2.7um	7.0	6.5	7.2	7.8	7.1	8%

7.3 Appendix 3 ICP-MS results for filters

Apartment	[Fe]	[Ca]	[Fe]/flux	[Ca]/flux
	mg/cm2	mg/cm2	ng/L	ng/L
1.2um	0.0087	0.051	4.8	28.3
1.5um	0.0069	0.017	3.8	9.4
2.7um	0.004	0.009	2.2	5.0

Lab	[Fe]	[Ca]	[Fe]/flux	[Ca]/flux
	mg/cm2	mg/cm2	ng/L	ng/L
1.2um	0.0059	0.045	3.3	25.0
1.5um	0.0043	0.021	2.4	11.7
2.7um	0.002	0.01	1.1	5.6